

بِسْمِ اللَّهِ الرَّحْمَنِ الرَّحِيمِ

*Bismillah-ir-Rehman-ir-Raheem*

*(In The Name of Allah, the Most Gracious and*

*the Most Merciful)*

*This thesis is dedicated to my beloved parents*

*Mr. S. Zariful Hassan Naqvi and Mrs. Aziz Zehra*

*Mr. S. Muhammad Ali Naqvi and Mrs. Jamshaid Haidry*



# **Characterization of Ciliate Mitochondrial Function**

**School of Biological Sciences  
Faculty of Science and Engineering  
Flinders University of South Australia  
December 2016**

## International Conferences

- Poster presented in ComBio International Conference, Lorne, Victoria, Feb 2012  
*Isolation of ATP synthase from an Alveolate*
- Presented a poster in ComBio International Conference, Christchurch, New Zealand  
*Identification of Mitochondria in Alveolates – Dec 2009*

## Local Conferences

- Poster presented in Australian Society for Medical Research (ASMR), Sept. 2012  
about *Identification of ATP synthase in T. thermophila; A possible target to treat Alveolate Infections*
- Presented research work at Postgrad Annual Conference, Flinders University, South Australia, June, 2011 and June 2012.
- Guest Speaker: Delivered a Lecture at University of South Australia, March 2012  
about *Alveolate mitochondria; A possible target to treat Malaria.*
- Poster presentation: Presented a poster in Australian Society for Medical Research (ASMR) , May, 2010 about *Mitochondrial ATP synthase in Alveolates*

# Table of Contents

Conferences .....	iii
Abstract.....	viii
Declaration.....	x
Acknowledgements .....	xi
<b>Chapter 1 Introduction.....</b>	<b>1</b>
<b>1.1) Mitochondria - Structure and Function.....</b>	<b>1</b>
<b>1.2) Endosymbiosis and genome reduction .....</b>	<b>2</b>
<b>1.3) A typical Electron Transport Chain.....</b>	<b>3</b>
<b>1.4) The ATP Synthase (Complex V).....</b>	<b>5</b>
1.4.1) Structure of ATP synthase.....	6
1.4.2) Function of ATP Synthesis .....	8
<b>1.5) Introduction to Alveolates .....</b>	<b>8</b>
1.5.1) Ciliates .....	10
1.5.2) Dinoflagellates .....	11
1.5.3) Apicomplexa.....	12
<b>1.6) Respiratory function of the Alveolata.....</b>	<b>13</b>
<b>1.7) Alveolate mitochondrial genomes.....</b>	<b>16</b>
<b>1.8) Aims of Project.....</b>	<b>18</b>
<b>Chapter 2 Materials and Methods .....</b>	<b>19</b>
<b>2.1) Materials.....</b>	<b>19</b>
<b>2.2) Culturing <i>Tetrahymena thermophila</i> .....</b>	<b>19</b>
<b>2.3) Mitochondrial isolation .....</b>	<b>20</b>
2.3.1) Isolation of crude mitochondria.....	20
2.3.2) Isolation of purified mitochondria using Percoll gradient technique .....	21

<b>2.4) Protein estimation techniques .....</b>	<b>22</b>
<b>2.5) Transmission Electron Microscopy .....</b>	<b>23</b>
2.5.1) <i>In-situ</i> Immuno-gold labelling .....	23
2.5.2) Negative Staining .....	25
<b>2.6) Enzyme assays.....</b>	<b>26</b>
2.6.1) Malate Dehydrogenase .....	26
2.6.2) Cytochrome oxidase (Complex-IV).....	27
2.6.3) Oxygen consumption assays .....	27
<b>2.7) Bioluminescent ATP assay/ Luciferase assay.....</b>	<b>28</b>
<b>2.8) Molecular Biology Techniques .....</b>	<b>28</b>
2.8.1) Preparation of competent <i>E. coli</i> .....	28
2.8.2) Heat shock transformation of <i>E. coli</i> .....	29
2.8.3) Plasmid purification and quantification.....	29
2.8.4) Restriction enzyme digests .....	30
2.8.5) DNA gel electrophoresis.....	30
<b>2.9) Expression of Inhibitor Protein in <i>E. coli</i> .....</b>	<b>31</b>
2.9.1) Starter culture .....	31
2.9.2) Propagation of <i>E. coli</i> in the fermenter.....	32
<b>2.10) Purification of IF<sub>1-60</sub>-His .....</b>	<b>32</b>
2.10.1) Cell lysis.....	32
2.10.2) Nickel affinity purification of IF <sub>1-60</sub> -His .....	33
<b>2.11) ATP synthase pull down techniques .....</b>	<b>35</b>
2.11.1) IF <sub>1-60</sub> -His pull down of ATP synthase.....	35
2.11.2) Antibody pull down of ATP synthase by using CN-Br Sepharose beads .....	37
2.11.3) Methanol precipitation of purified protein .....	38
2.11.4) Sodium dodecyl sulphate polyacrylamide gel electrophoresis (SDS-PAGE) .....	39
2.11.6) Protein detection by western blotting.....	39

2.11.7) Coomassie staining of protein bands .....	40
<b>2.12) Mass spectrometry techniques .....</b>	<b>41</b>
2.12.1) Excision of bands from SDS-PAGE gel for trypsin digest.....	41
2.12.2) In-Gel preparation for Trypsin Digest .....	41
2.12.3) Trypsin Digest of Gel bands.....	42
2.12.4) Peptide removal from Polyacrylamide Matrix Gels .....	42
2.12.5) Peptide clean-up for mass spectrometry using Zip Tips .....	43
2.12.6) MALDI-ToF mass spectrometry.....	43
<b>2.13) Mass spectra analysis .....</b>	<b>44</b>
 <b>Chapter 3</b>	
<b>Isolation and identification of <i>Tetrahymena thermophila</i> mitochondria .....</b>	<b>45</b>
<b>3.1) Introduction .....</b>	<b>45</b>
<b>3.2) Results .....</b>	<b>48</b>
3.2.1) Microscopic observation of <i>T. thermophila</i> .....	48
3.2.2) Enzyme assays.....	59
<b>3.3) Discussion .....</b>	<b>65</b>
<b>3.4) Conclusion .....</b>	<b>68</b>
 <b>Chapter 4</b>	
<b>Characterization of respiration and ATP synthesis in <i>T. thermophila</i> mitochondria ..</b>	<b>70</b>
<b>4.1) Introduction .....</b>	<b>70</b>
<b>4.2) Results .....</b>	<b>73</b>
4.2.1) Effect of various substrates on oxygen consumption.....	73
4.2.2) Effect of ADP on oxygen consumption in the presence of different substrates.....	73
4.2.3) Observation of typical respiratory state 3 and state 4 transitions in the presence of succinate and ADP.....	75

4.2.4) Experiments in the presence and absence of phosphate using crude mitochondria .....	77
4.2.5) Effect of inhibitors and uncoupler on oxygen consumption.....	83
4.2.6) Experiments using purified mitochondria from <i>T. thermophila</i> .....	84
4.2.7) Measurement of ATP in crude mitochondria of <i>T. thermophila</i> in the presence and absence of phosphatase inhibitor cocktail (sodium fluoride, sodium orthovanadate, tetrasodium pyrophosphate) .....	88
<b>4.3) Discussion .....</b>	<b>91</b>
<b>4.4) Conclusion .....</b>	<b>94</b>
 <b>Chapter 5</b>	
 <b>Identification of mitochondrial ATP synthase subunits of <i>T. thermophila</i>.....</b>	<b>95</b>
 5.1) Introduction .....	95
5.2) Results .....	102
5.2.1) Production and purification of the inhibitor protein IF <sub>1-60</sub> -His.....	102
5.2.2) <i>T. thermophila</i> ATP synthase pull down techniques.....	103
5.2.3) Mass Spectrometry protein analysis via MALDI-TOF .....	113
5.2.4) Identification of subunit a .....	121
5.2.5) Identification of subunit b.....	127
<b>5.3) Discussion .....</b>	<b>132</b>
<b>5.4) Conclusion .....</b>	<b>136</b>
 <b>Chapter 6 Final Conclusion .....</b>	<b>137</b>
 <b>References .....</b>	<b>145</b>
 <b>Appendix 1 .....</b>	<b>153</b>

# Abstract

The electron transport chain and oxidative phosphorylation are two major phenomena which occur in mitochondria simultaneously. These processes are facilitated by the protein complexes of the electron transport chain, located in the inner membrane of mitochondria in eukaryotes. Among these complexes, ATP synthase is an enzyme of a crucial importance. A typical eukaryote ATP synthase consist of an F<sub>1</sub> domain and an F<sub>o</sub> domain. The F<sub>1</sub> domain consists of five subunits including  $\alpha$ ,  $\beta$ ,  $\gamma$ ,  $\delta$  and  $\epsilon$ . The F<sub>o</sub> domain consists of a, b, c, d, OSCP and F<sub>6</sub>. This enzyme couples oxidation of respiratory substrates to ATP synthesis in the mitochondria. The core subunits of the ATP synthase were thought to be well conserved across all forms of life. However, the availability of genome data has revealed that organisms belonging to the alveolate super phylum which includes *Plasmodium*, dinoflagellate algae and ciliates (including *Tetrahymena thermophila*) do not have genes homologous to those in other organisms that code for subunits that are critical for the function of the F<sub>o</sub> domain. One of the apparently missing subunit is 'a' which plays a crucial role in the proton translocation during the process of ATP synthesis in mitochondria. It was hypothesized that as alveolates appear to have a functional ATP synthase, they must have some alternative subunits, with low homology to other species that fulfill the same function. This study involves the purification and identification of mitochondria in *T. thermophila*, investigation of the respiratory pathways and ATP synthesis, purification of ATP synthase and identification of its component subunits. In this study electron micrograph images showed the presence of mitochondria in *T. thermophila* and purified fractions. Biochemical and oxygen consumption assays confirmed that these purified mitochondria were intact, coupled, and able to synthesize ATP. The ATP synthase was affinity purified using a recombinant expressed ATP synthase inhibitor protein and an

anti-beta subunit antibody. The purifications were carried out with mitochondria which were not treated with and without the chemical crosslinker DTBP. ATP synthase subunits were resolved by SDS-PAGE and the bands were excised and analyzed by MALDI-ToF mass spectrometry. Altogether 56 different proteins, including all the annotated ATP synthase subunits, were isolated and identified through MS. After an extensive range of bioinformatics analysis, one protein (A2-32, XP\_001010660.1) was identified as a putative **a** subunit of ATP synthase of *T. thermophila* mitochondria. A2-32 is a membrane-bound protein with a molecular weight of 37 kDa, which is targeted to the mitochondria. Another protein (G25-1, XP\_001015517.2) was identified as a putative **b** subunit, this protein had a molecular weight of 39 kDa, with a hydrophobic N-terminus and hydrophilic C-Terminus. In this study, none of the putative ATP synthase proteins suggested by Nina *et al* (2010) were identified. Also the putative *Plasmodium* subunit **a** (XP\_001347344) identified by the bioinformatics study of Mogi and Kita (2009) did not show any homology to the proteins identified here. Hence this study has successfully identified a mitochondrially-targeted **a** subunit protein, which is of expected size and contains key conserved residues necessary for the passage of protons during ATP synthase.

# Declaration

I certify that this thesis does not incorporate without acknowledgment any material previously submitted for a degree or diploma in any university; and that to the best of my knowledge and belief it does not contain any material previously published or written by another person except where due reference is made in the text.

Mrs. Anjum Zehra Naqvi

December 2016

# Acknowledgements

All Praise Belongs to Allah and unlimited thanks to the Lord of the Worlds, and May Peace and Blessings be upon the Greatest and Trustworthy Prophet (P.B.U.H.) and His Pure Progeny, His Chosen Companions, and upon all Divine Messengers.

This journey of PhD was a challenge for me throughout. I am very thankful to Allah for blessing me with such a great research team whom I called my Australian Family. I am very thankful to Dr. Catherine Abbott for accepting me under her supervision and for continuous support throughout my PhD. Lots of thanks to the Head of the research team Dr. Ian Menz. Ian's support and confidence in the beginning of my research helped me a lot in understanding research methodology. He spent hours of his precious time in explaining to me every little thing related to my work. I am very grateful to you for encouraging me in hard times. You are a great source of inspiration for me in my life.

I am also very much thankful to a great personality of my life and my research career, Dr. Ellen Nisbet. I didn't see angels in this world until I met you. You made my Ph.D possible for me. I have no words to thank to you Ellen. You will remain a role model for me as a great teacher, a supervisor and especially a great human being.

I would like to thank Dr. Vivek Vijayraghavan. His consistent behavior proved to be very helpful during my thesis writing. Unlimited thanks to another angel of my lab team, my brother Dr. James Herbert. No words can thank you enough, James. You gave me your extra time while you were extremely busy with your tasks. Especially I would like to thank you for the work of Mass spectrometry and Bioinformatics analyses at the end. Also heartiest thanks to Mike, whom I used to say my sister, the way he cares for me, a friend who has helped me continuously until I finished my FPLC work. Being an international student, I shared many good and bad moments with James and Mike, many silent cries and laughter, sharing little foods and having coffee during times of extreme tension.

I am very grateful to Eiman Saleh for your help, guidance and love in my first year of PhD. Many thanks to my Japanese brother Yuya Samura for his little jokes and martial arts fun which made our working environment such a pleasant place. Also I would like to thank my little friend Imogen White, for sharing a good time and teaching me little things related to my research. Michael Petronolis is another great person of my lab. Though you joined us late, a short time with you gave me lots of pleasure.

I would like to thank specially Professor Tracy Bryan of the University of Sydney for providing me the culture of *Tetrahymena thermophila*. Special thanks to Professor Chris Howe from Cambridge University for providing me with a valuable insight and figuring

out the issues in my work. Also so much thanks to Dr. Kathleen Soole, Dr. Peter Anderson and Dr. Crystal Sweetman for providing me their lab facilities and technical guidance in my work. I am very grateful to Jason Young and Maurizio Ronci at Flinders Analytical lab for providing me their expertise in MALDI-TOF Mass Spectrometry.

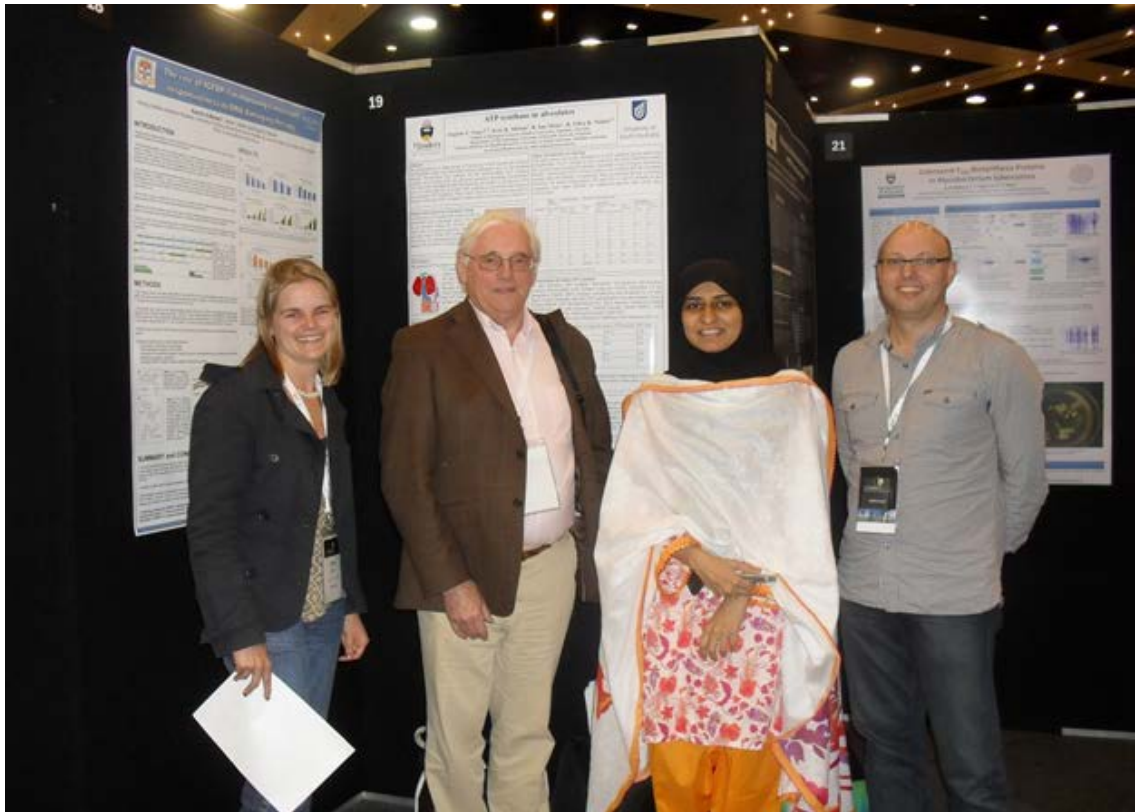
I am very grateful to Dr. Sohail Naqvi, former Executive Director of Higher Education commission, Pakistan for his special support in providing me funds to undertake this research. Heartiest thanks to my dearest Prof. Dr. Hajra Khatoon, former Chairperson of Microbiology department, University of Karachi for her great support to obtain the scholarship allowing me to travel to Australia. Many thanks to my colleagues from Microbiology department, Prof. Perveen Tariq, Mrs. Shahnaz Mansoor, Dr. Tanveer Abbas and Dr. Asma Saeed for their extraordinary moral support to achieve my aims.

Heartiest thanks to Ms. Jane Horgan of ISSU and Mr. Geoff Boyce of Oasis for their continuous moral support throughout my research. Special thanks to Mr. Dominic Reppucci who always made sure all the machineries in my use were in working condition which made it possible to complete my experiments in time.

I am very much thankful to Allah for blessing me with such a nice parents and family members who made this PhD easier to achieve. Special thanks to my gorgeous and wonderful parents and my husband's parents whose unlimited prayers and love made this PhD possible, specially my Mum. I believe whatever I am today is because of my mum's endless struggles, support, prayers and love (Unfortunately my lovely mum passed away before the award of my PhD. May Allah rest her soul in peace, Amin). My father Mr. Zariful Hassan Naqvi, although not alive but his teachings in my childhood remains a spiritual sustenance for me in his absence. Also sincerest thanks to all of my lovely siblings who kept in touch with me to show their subsistence and love until the end. Especial thanks to my fabulous sister Bano whom I praise and respect like she is my mother too. I am very obliged to you as you were the one who made sure that our mum is safe and healthy which allowed me focus on my research. Also special thanks to Tabbasum, Annie and Hassan, your generous moral and financial provisions were the continuous sources of encouragement for me throughout. Heartiest thanks to my great brothers Haider, Azeem, Zeeshan, Imran and to my lovely sisters Syeda, Noroze, Shan, Tasneem, Uzma, Fakhra, Durr-e-shahwar and Tatheer. I love you all.

Finally, I would like to thank my love, my life, my friend and my husband Mr. Syed Kamran Haider Naqvi for his endless emotional support, patience, devotions, care and love during my thesis writing.

To all those who helped me in this tough journey of my PhD, I would pray to Allah that He may bless you with the best of His rewards in this world and in another world, Amin.



Dr. Ellen Nisbet, Sir John Walker (Noble Prize), Ms. Anjum Naqvi and Dr. Ian Menz, ComBio, New Zealand, 2009.

# Chapter 1 Introduction

## 1.1) Mitochondria - Structure and Function

Mitochondria play a key role in the energy metabolism of eukaryotic cells. The organelle serves as an energy production centre for the cell, as well as playing an important role in programmed cell death or apoptosis (Desagher, 2000). In addition, mitochondria perform vital functions in biosynthetic pathways. For example mitochondria synthesize many key components which are required by the mitochondrial electron transport chain (ETC). These include co-enzyme Q (Ubiquinone); iron-sulphur clusters which are the prosthetic group for many proteins, substrates of the tricarboxylic acid cycle and heme; a prosthetic group in cytochromes. However, perhaps the most important function of mitochondria is the synthesis of adenosine triphosphate (ATP).

All mitochondria possess a double- membrane structure and contain import pathways which allow proteins, small molecules and ions to enter from the cytosol. The two membranes are separated by an intermembrane space. The inner membrane forms several convoluted structures which are known as cristae (Figure 1.1). The cristae possess all of the important enzyme complexes including an F-type ATP synthase, the complex for proton translocation and ATP production. This complex is responsible for the majority of ATP production in the cell.

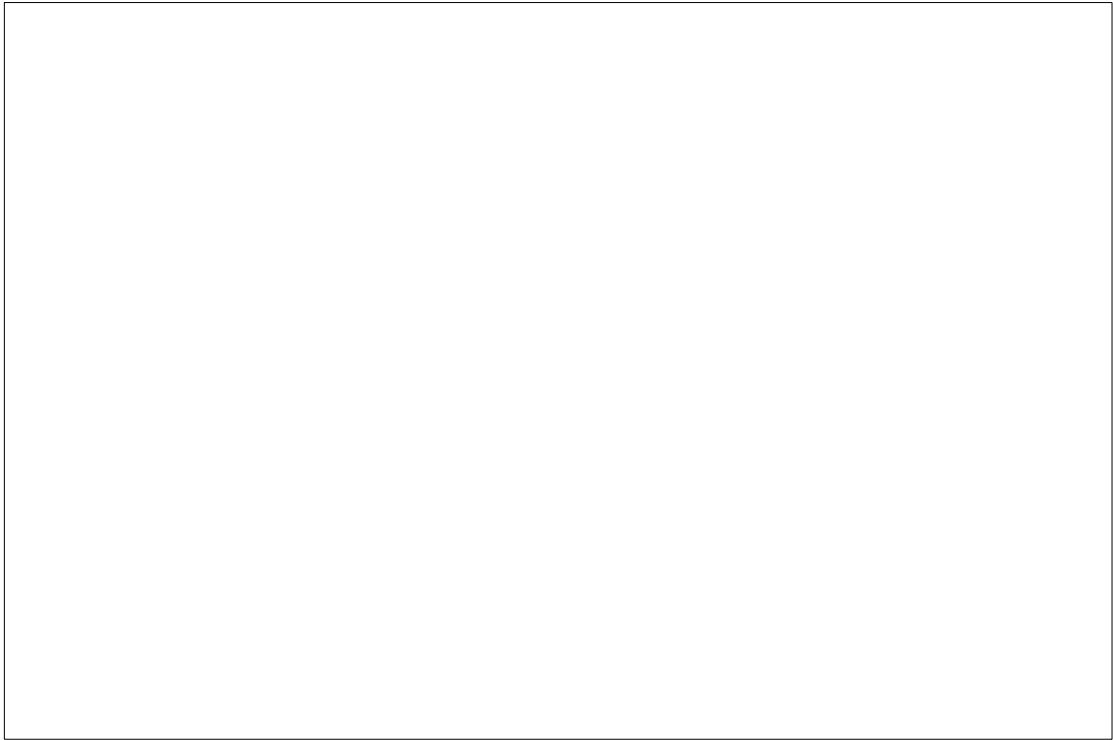


**Figure 1.1** Mitochondria. Key features of mitochondria, including the presence of ATP synthase (from Lodish *et al*, Molecular Biology of the Cell, 2006).

The matrix is the site for many biochemical reactions including the tricarboxylic acid (Krebs) cycle which fuels the process of adenosine triphosphate (ATP) synthesis. Mitochondria are also the site for oxidative phosphorylation which synthesizes adenosine triphosphate via ATP synthase. These ATP molecules are then used by the cell for all energy requiring processes including cell division, growth, movement, production and transportation of essential molecules, enzymes and hormones.

## **1.2) Endosymbiosis and genome reduction**

The evolutionary history of eukaryotes showed that all mitochondria evolved from the primary endosymbiosis of alpha-protobacterium by a non-photosynthetic host cell, which was probably an archaeon cell (Martin, 2015). This bacterium-archaeon relationship acquired a mutual association with each other. Gradually, genes were

moved from the bacterium to the host genome, and non-essential genes were lost from the bacterium (Gray, 2012). Later, due to the dependence on the host-derived nutrients, the bacterium gradually reduced in size and became an energy-producing organelle for the eukaryotic host. This organelle is now known as a mitochondrion. In some cases the symbiont's genome was lost completely, giving rise to hydrogenosomes and mitosomes (Martin, 1998; Martin, 2015).

### **1. 3) A typical Electron Transport Chain**

The components that form the electron transport chain are located in the cristae in each mitochondrion. They are responsible for the transfer of electrons and the creation of a proton gradient across the inner-membrane which provides the energy to produce ATP from ADP and inorganic phosphate via ATP synthase. This energy is primarily generated during respiration (Boyer, 1997). The main enzymes of electron transport chain are NADH-ubiquinone oxidoreductase (Complex I), Succinate-ubiquinone oxidoreductase (Complex II), Cytochrome *bcl* oxidoreductase (Complex III), Cytochrome oxidase (Complex IV) and ATP synthase (Complex V) (Figure 1.2). The NADH dehydrogenase is the largest enzyme (Brandt, 2006). NADH possesses high-energy electrons and is produced as a result of oxidation of carbon compounds in the tricarboxylic acid cycle. The NADH dehydrogenase initiates the electron transfer reaction by donating a pair of electrons to the electron transport chain. During this electron transfer, four H<sup>+</sup> ions are vectorially transferred from the inner side of the matrix to the outside of the matrix into inter-membrane space. The electrons are received by ubiquinone converting it to Ubiquinol QH<sub>2</sub> (reduced form of ubiquinone). Ubiquinone acts as a mobile electron carrier. Ubiquinone is also reduced by the electron transfer through succinate dehydrogenase during the conversion of succinate into

fumarate. Ubiquinol transfers electrons to the cytochrome  $bc_1$  complex. This in turn reduces cytochrome  $c$  which is then oxidized by cytochrome oxidase (complex IV) where the electrons in the presence of  $H^+$  reduce  $O_2$  to water. The translocation of  $H^+$  during this transfer of electron at complex I, complex III and complex IV generates an electrochemical proton gradient across the inner membrane. This proton-motive force drives protons back into the matrix via the  $F_0$  domain of ATP synthase and at the same time ADP is phosphorylated via the  $F_1$  domain to produce ATP (von Ballmoos *et al*, 2009).

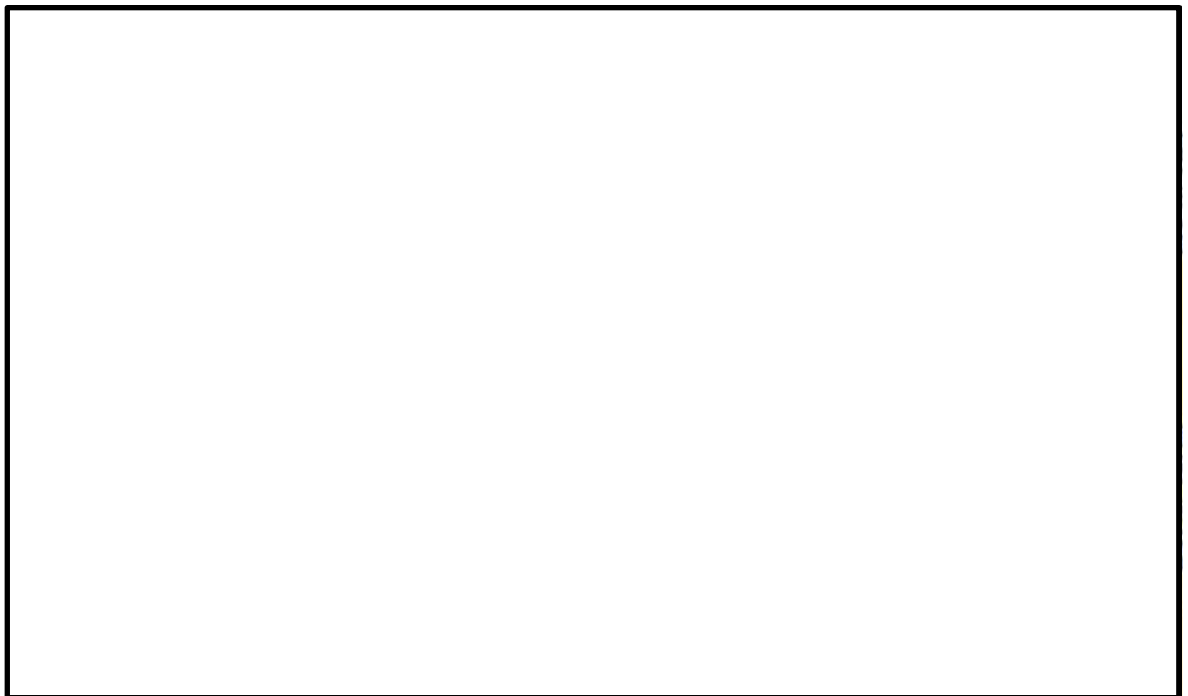


**Figure 1.2 Electron Transport Chain.** A basic Electron Transport Chain representing five membrane-embedded enzyme complexes. The subunit composition and architecture indicated is a composite from a variety of different organisms for which structures have been determined (from Lehninger, Principles of Biochemistry, 4th ed., 2008).

## 1.4) The ATP Synthase (Complex V)

ATP synthase is the final complex in the mitochondrial respiratory electron transport chain. F-type ATP synthases are commonly found in mitochondria, the thylakoid membranes of chloroplast and in the plasma membrane of bacteria. Bacteria have the simplest F-type ATP synthase consisting of eight different polypeptides, while ATP synthase found in eukaryotes are more complex. For example, the F-type ATP synthase found in bovine mitochondria is composed of 13 different polypeptides (Walker, 1987). In contrast, an analysis of the genome sequence from the ciliate *Tetrahymena thermophila* reveals that it possesses only six polypeptides that are homologous to F-type ATP synthase subunits found in other organisms (Table 1).

**Table 1** Subunit composition and equivalence of F<sub>1</sub>F<sub>0</sub> ATP synthase among prokaryotes, eukaryotes and ciliates

Domains	Prokaryotes	Eukaryotes- bovine	Eukaryotes- ciliates
F <sub>1</sub>	α	α	α
	B	β	β
	γ	γ	γ
	δ	OSCP	OSCP
	ε	δ	-
	-	ε	-
F <sub>0</sub>	A	a	-
	B	b	-
	C	c	c
	-	d	d
	-	e	
	-	f	-
	-	g	
	-	h/F6	
		i/j	
	-	8/A6L	

Interestingly, subunits a and b of ATP synthase which play a crucial role in ATP synthesis were not identified (Eisen *et al*, 2006). Even without these subunits, *Tetrahymena* possess significant ATP synthase activity in its mitochondria, suggesting that the complex is functional (Conklin and Chou, 1972).

### **1.4.1) Structure of ATP synthase**

The ATP synthase consists of two domains known as F<sub>1</sub> and F<sub>0</sub>. The F<sub>0</sub> domain is found embedded in the inner membrane of the mitochondrion while the F<sub>1</sub> region extends into the matrix space. The complex has been shown to form dimers where the two monomers of ATP synthase are joined through a protein bridge on both the intermembrane space and matrix side of the complex (Fernando *et al*, 2005). The crystallographic studies by Walker and colleagues showed that F<sub>1</sub> domain consists of nine subunits of five different types with the stoichiometry  $\alpha_3, \beta_3, \gamma, \delta, \epsilon$  (Walker, 2013). The catalytic sites responsible for ATP synthesis are located at the interface between  $\alpha$  the  $\beta$  subunit. During the catalytic cycle the conformation of each active site changes due to its changing relationship to the rotating  $\gamma$  subunit. Therefore, at any point in time the active sites will adopt three different conformations representing different points in the catalytic cycle. The F<sub>0</sub> domain consists of the oligomycin-sensitive conferring protein (OSCP), which binds the inhibitor oligomycin (Ko *et al*, 2003), subunit a and then subunit b and c at different stoichiometry depending on the species. Studies on yeast mitochondria showed ten c subunits, which have a  $\alpha$ -helical hairpin structure, arranged in a ring (Stock *et al*, 1999). This domain provides a channel for H<sup>+</sup> to be transferred from the intermembrane space to the matrix. In yeast mitochondria, these subunits are arranged in such a way that the c subunit connects (on its vertical axis) with the  $\epsilon$  and  $\gamma$  subunits of F<sub>1</sub> which act as a rotator, forming a central

stalk (Stock *et al.*, 1999). This central stalk supports the attachment of  $\alpha$  and  $\beta$  subunits, which are arranged in an alternate fashion surrounding the central stalk of the  $\gamma$  subunit. The two domains of ATP synthase are supported by a peripheral stalk, which in *E. coli* involves two b subunits and the  $\delta$  subunit which connects to the side of one of the  $\beta$  subunits. In this way, the  $F_0$  domain performs the role of a hook to which  $F_1$  domain is fixed. The  $F_1$  domain is responsible for the phosphorylation of ADP to ATP in the presence of inorganic phosphate (C. von Ballmoos *et al.*, 2009)

There are various minor differences between prokaryotic and eukaryotic subunits (Figure 1.3) (Table 1). Although some subunit names are different, they encode essentially the same protein (e.g. OSCP in eukaryotes,  $\delta$  in prokaryotes). Eukaryotes have additionally a number of accessory proteins and a more complex peripheral stalk (Walker, 2006) including F6 and d. It should be noted that some eukaryotes (e.g. *Chlamydomonas* and related species) contain very different stalk proteins (Miranda-Astudillo, 2014): these are discussed later in the thesis.

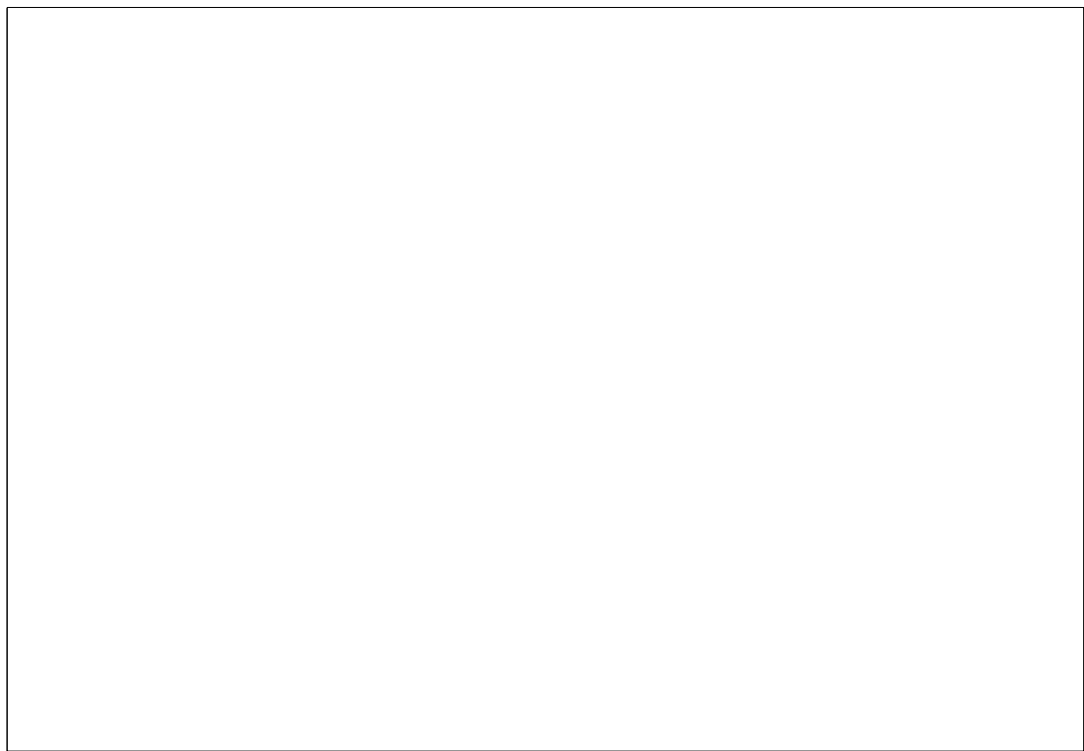


**Figure 1.3 Model of ATP Synthase.** (A) in prokaryotes (after Fillingame *et al.*, 2003)  
(B) Eukaryotes (after Walker and Dickson, 2006)

## 1.4.2) Function of ATP Synthesis

The ATP synthase functions concurrently with the electron transport chain. The rotary motor of  $F_0$  subunit functions when an electromotive potential is built up by the vectorial transfer of  $H^+$  into the intermembrane space. Due to the accumulation of  $H^+$  in the intermembrane space, an electrochemical potential is created. In contrast, the matrix space becomes more negatively charged. This imbalance is harnessed by the  $F_0$  domain which allows the passage of  $H^+$  from the mitochondrial intermembrane space to the matrix to maintain the equilibrium state. Therefore, the rotary motor (consisting of the c subunits of  $F_0$  and  $\gamma$  and  $\epsilon$  subunit of the  $F_1$  domain) couples the proton translocation with ATP synthesis at the catalytic sites formed between the  $\alpha$  and  $\beta$  subunits (Gibbons *et al*, 2000). As the asymmetric  $\gamma$  subunit rotates, inside the assembly of alternately arranged  $\alpha$  and  $\beta$  subunits, the conformation of each catalytic site changes. In this way during each full  $360^\circ$  rotation of  $\gamma$  subunit, the three different catalytic sites undergo conformational changes associated with a complete catalytic cycle and produce three molecules of ATP from ADP and  $P_i$ . The process of ATP synthesis is reversible in the absence of a proton gradient in the intermembrane space.

## 1.5) Introduction to Alveolates

Alveolates are included in one of the major groups of eukaryotes known as Chromalveolata (Adl *et al*, 2005). The alveolates are named after the small sac-like structures found immediately under the cell membrane which are known as alveoli. Alveoli contain a small group of proteins known as alveolins (Gould, 2008), and the presence of alveoli is the defining feature of all alveolate species. The members of the alveolate group possess extremely diverse modes of nutrition including photoautotrophs, intracellular parasites and predators. Nearly all contain mitochondria

with tubular cristae (Walker, 2011). The alveolate group contains many medically and economically important organisms which display tremendous diversity in their structure and function. The three main groups are the apicomplexans, ciliates and dinoflagellate algae, as shown in Figure 1.4 (Cavelier-Smith, 2003)

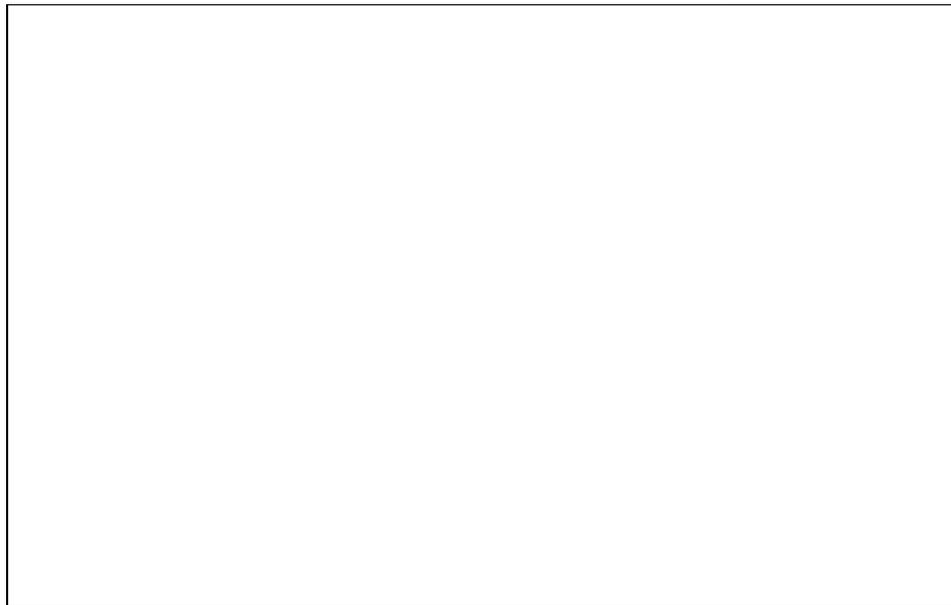


**Figure 1.4 Alveolates.** Scanning electron micrographs of (left to right) a ciliate, a dinoflagellate and an apicomplexa. (From: Tree of life, Leander, 2009)

Alveolates contain three major groups, the ciliates, the dinoflagellates and the apicomplexa (both photosynthetic and non-photosynthetic), as shown in Figure 1.5.

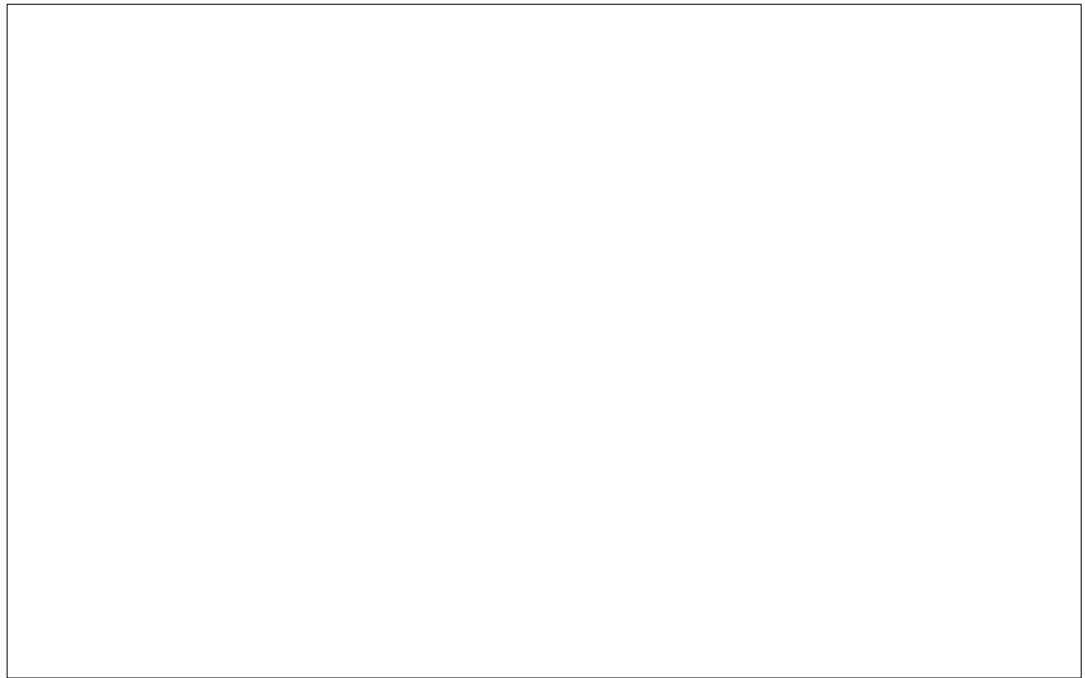


**Figure 1.5 The relationship between Alveolates.** Adapted from Butterfield *et al*, 2012.

### **1.5.1) Ciliates**

Ciliates are one of the most important groups of protists (Yi Z *et al*, 2008) and consist of several classes and subclasses. All ciliates contain numerous hair-like appendages known as cilia, which allow significant movement (Walker, 2011). They perform multiple functions such as feeding, swimming, attachment, crawling and sensation. Although single celled, some ciliates are large, and can be up to 2 mm in length. Ciliates usually exist in water but some species are also found in soil. Many ciliates are free-living (e.g. *Tetrahymena*, *Paramecium*) and most feed on bacteria, fungi, eukaryotic algae or other ciliates. Such species have an oral groove (mouth) for feeding while some of them are mouthless obtaining their food by absorption. The use of specialized tentacles is also common in a few ciliate species (e.g. *Suctorina*). Ciliates have a cytoproct (anus) through which waste material is excreted by the process of exocytosis.

A few species are endosymbionts or live as opportunistic or obligate parasites. These include the sole human ciliate pathogen *Balantidium coli*, which have a reservoir in pigs (Pomajbíková *et al*, 2013) and causes diarrhea. A few ciliates species are anaerobic, such as *Nyctotherus ovalis* which lives in the hindgut of cockroaches (de Graaf, 2011). These species have recently become anaerobic, having lost key mitochondrial enzyme complexes, presumably due to the change in life cycle (Boxma *et al*, 2005).

### **1.5.1.1) Tetrahymena thermophila**

*Tetrahymena thermophila* is a free-living ciliate and was initially known as *T. pyriformis* type-I (Nanney, 2000). Due to the rapid growth of this organism on a variety of synthetic and semisynthetic media with a minimum doubling time of two hours under lab conditions, it is frequently used as a model organism to study the cell cycle, growth and nutrition in eukaryotes (Wheatley, 1994; Collins, 2005). For example, the role of telomeres in cell division was first discovered in *Tetrahymena thermophila* (Greider and Blackburn, 1985).

### **1.5.2) Dinoflagellates**

Dinoflagellates are a large group of flagellated protists. They are usually photosynthetic and found in marine and fresh water habitats depending upon salinity, depth and temperature. About 50% of dinoflagellates obtain their energy from photosynthesis, and therefore contain a chloroplast (Taylor, 1987). Unlike the nuclei of other eukaryotes, dinoflagellate nuclei lack conventional histones and nucleosomes (Gornik, 2012). Instead, novel proteins, called DVNP have been recruited as dinoflagellate histones, possibly from a virus (Gornik, 2012). The nuclear chromosomes remain in a condensed

form during mitosis. Dinoflagellates possess typically eukaryotic organelles such as food vacuoles, golgi apparatus, starch grains, and mitochondria (Steidinger *et al*, 1996).

### **1.5.3) Apicomplexa**

Apicomplexan protozoa were first observed by Antony van Leuwenhoek in the gall bladder of a rabbit in 1674. This phylum contains many human and animal pathogens (Walker, 2011) such as *Toxoplasma* which causes Toxoplasmosis and *Plasmodium* which is the causative agent of malaria (Bremant, 2001). Compared with other alveolates and single-celled organisms, many apicomplexans have a highly complex life cycle which consists of both sexual and asexual modes of reproduction, which may occur in more than one host. Apicomplexa do not possess any locomotory organs apart from gametes which have flagella. The unique feature of most apicomplexans species is that they contain an organelle known as an apicoplast, which is a remnant chloroplast acquired via secondary endosymbiosis (Waller, 1998; Foth, 2003). Over time, the apicoplast lost its photosynthetic ability (Foth and McFadden, 2003), although some photosynthetic apicomplexa do still exist (e.g. *Chromera* and *Vitrella*) (Weatherby, 2013)). The apicoplast is essential, and is required for parasite survival (Marechal *et al*, 2001). Yeh and DeRisi (2011) demonstrated that the loss of apicoplast in antibiotic-treated parasites resulted in failure to process or localize organelle proteins. The apicoplast carries out type II fatty acid synthesis, isoprenoid synthesis and portions of the heme biosynthesis pathway (Goodman and Mcfadden, 2007; Krungkrai, 2004; reviewed in Lim, 2010). The apicoplast and mitochondrion are usually found in physical association with each other in the asexual stage of parasite life cycle (van Dooren *et al*, 2005).

## 1.6) Respiratory function of the Alveolata

It has been known for many years that the ciliate *Tetrahymena* contains a functional, respiring mitochondrion (Kilpatrick, 1977). Surprisingly little has been published on the biochemistry of ciliate mitochondria. It is known that respiration is inhibited by cyanide and rotenone, albeit at significantly higher concentrations than in mammalian cells (Kilpatrick, 1977). More recently, Prikhodko (2009) showed that the uncoupler FCCP was functional, suggesting the presence of a classical electron-transport chain linked to ATP synthase. Various other papers have been published, though mostly on parasitic ciliates such as *Philasterides dicentrarchi* (a parasite of the turbot fish), which contains an alternative oxidase (Mallo *et al*, 2013), while some anaerobic ciliates contain hydrogenosomes, remnant mitochondria which produce hydrogen (Hjort, 2010).

Analysis of the ciliate *T. thermophila* genome showed the presence of genes encoding proteins for the mitochondrial electron transport chain. However, genes encoding significant proteins in the ATP synthase complex are missing (Table 2). These include subunits  $\epsilon$ . and the important subunit *a* from the F<sub>0</sub> domain which performs proton translocation (Nina *et al*, 2010; Eisen, 2006). Other subunits including *a*, *b*, *d* and F<sub>6</sub> proteins are also missing. These genes are not encoded on the genome, and have not been found in a proteomic analysis (Smith, 2007). It could be that the proteins are present, but are so divergent that standard bioinformatics searches were not able to identify the gene: for example Smith *et al* (2007) identified the oligomycin-sensitive conferring protein (OSCP) from the F<sub>0</sub> portion of ATP synthase, which was not identified in the genome sequence. However, the nuclear encoded gene for the c subunit was not identified in the proteome (Smith, 2007), and nor were the other subunits.

Nina *et al* (2011) isolated ATP synthase complexes from ciliate mitochondria in an attempt to identify some of these missing subunits. Using blue-native PAGE, they were

able to identify the mitochondrially-encoded protein Ymf66 as part of the ATP synthase complex, which was suggested to function instead of the missing **a** subunit. Although further proteins were also identified, none were similar to the remaining missing proteins (Nina, 2011).

An analysis of dinoflagellate EST data for the presence of transcripts encoding ATP synthase proteins identified subunits  $\alpha$ ,  $\beta$ ,  $\gamma$ ,  $\delta$  and  $\epsilon$  of F<sub>1</sub> domain as well as the subunit **c** and OSCP of F<sub>0</sub> domain (Butterfield *et al*, 2012). The key subunits of F<sub>0</sub> domain which are responsible for holding the stator in the structure of ATP synthase were found to be missing. These subunits are the same as those that have not been identified in ciliates (Table 2).

The apicomplexan *Plasmodium falciparum* genome encodes an ATP synthase with well conserved F<sub>1</sub> domain of ATP synthase along with membrane-bound **c** subunit and OSCP (Gardner *et al*, 2002). It too appears to lack many F<sub>0</sub> subunits including **a** and **b** (Gardner *et al*, 2002). A subsequent extensive study of both the mitochondrial and nuclear genome of the apicomplexan *Plasmodium* reveals that unlike typical eukaryotic organisms, the parasite does not contain all genes necessary for proteins involved in a typical electron transport chain and ATP synthesis (Balabaskaran Nina, 2011). Two candidate proteins have been identified using bioinformatics approach for the **a** and **b** subunits (Mogi and Kita, 2009), although these have not yet been confirmed experimentally.

Early investigations assumed that the parasite primarily depends on its glycolytic metabolism to fulfil its energy requirements during the blood stage of the life cycle (Painter, 2007) as the genome lacked the genes encoding F<sub>0</sub>F<sub>1</sub> ATP synthase. Therefore the mitochondria were not considered as an energy source for the parasitic survival (Fry, 1990). However, it has since been found that mitochondria in *Plasmodium* act as

electron source for de novo pyrimidine biosynthetic pathway through dihydroorotate dehydrogenase, and thus a functional electron transport chain is required (Sherman, 1998).

Despite the missing genes, it has been shown the ATP synthase complex is functional (Uyemura, 2004; Painter, 2007), although the sexual stage of parasite has greater activity in the TCA cycle, electron transport chain, and ATP synthase (Ke *et al*, 2015; MacRae *et al*, 2013; Sturm *et al*, 2015) . Very recent research has shown that mitochondrial ATP synthase is not necessary during the blood stage of infection (Sturm, 2015). The proposed model for *Plasmodium* mitochondrial function is shown in Figure 1.6.

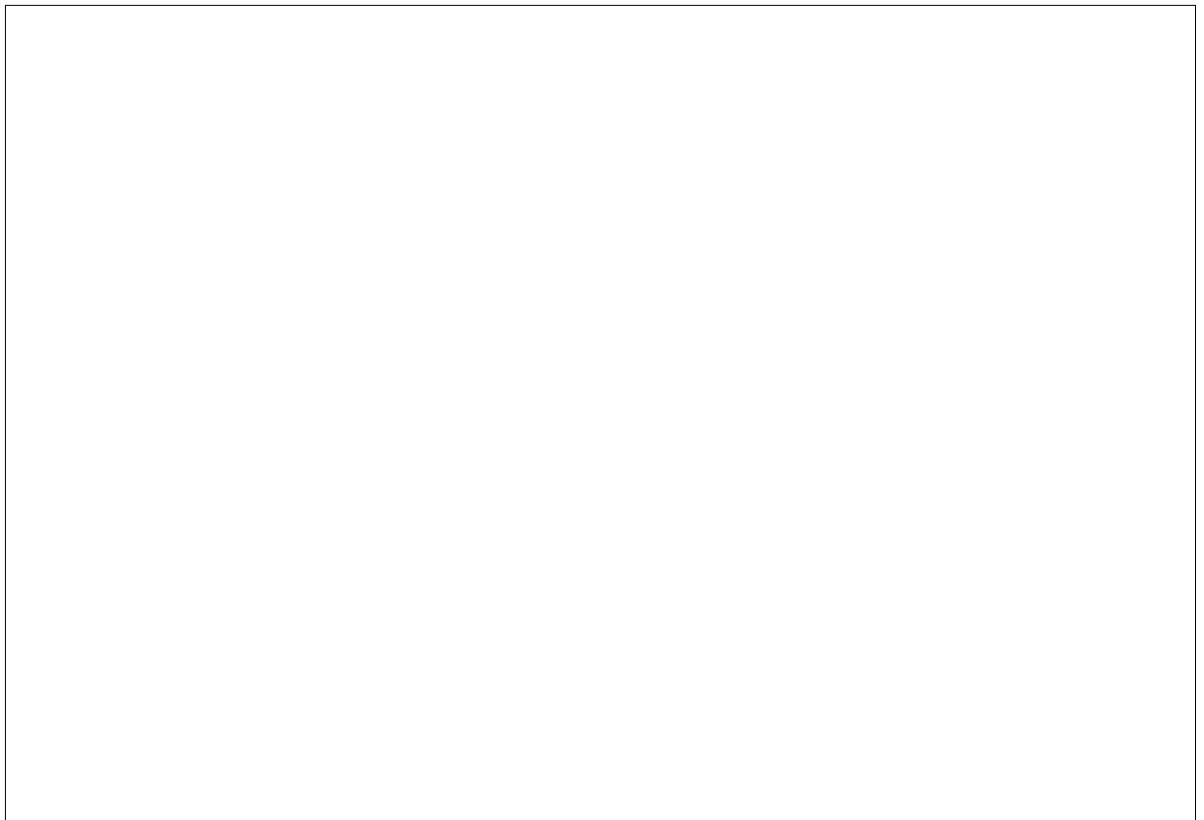


**Figure 1.6 A putative model for electron transport through the inner membrane of the mitochondria of *Plasmodium falciparum* (van Dooren *et al*, 2006)**

Thus, a similar set of genes encoding key subunits for ATP synthase were not found in all alveolate species studies to date. It could be that these genes are present, but extremely divergent, or that alveolate mitochondria may contain some alternative proteins which are functionally equivalent in order to maintain a functional ATP synthase.

**Table 2 Summary of key ATP synthase subunits in Alveolates**

Domain	Subunit	Ciliates	Dinoflagellates	Apicomplexa
F <sub>1</sub>	$\alpha$	+	+	+
	$\beta$	+	+	+
	$\gamma$	+	+	+
	$\delta$	-	+	+
	$\epsilon$	-	+	+
F <sub>0</sub>	a	-	-	-
	b	-	-	-
	c	+	+	+
	d	+	-	-
	OSCP	+	+	+
	f <sub>6</sub>	-	-	-

## 1.7) Alveolate mitochondrial genomes

Mitochondria from *Tetrahymena pyriformis* strain *GL* were first isolated by Kobayashi (1965). Ciliates have a linear mitochondrial genome, similar to that found in other eukaryotic species. Burger (2000) published the first complete ciliate mitochondrial genome sequence, using the model organism *T. pyriformis* closely followed by Brunk *et al* (2003) with *T. thermophila*. The *T. thermophila* mitochondrial genome encodes 44 proteins (Brunk *et al*, 2003) out of which 25 have known functions. Proteomic analyses of the ciliate mitochondria were able to identify proteins from 19 of the 25 annotated

mitochondrial DNA (mtDNA)-encoded proteins, including subunits of complex I, complex III (Cob) and complex IV (Cox1,2) (Smith *et al*, 2007). Subsequent studies of multiple ciliate mitochondrial genomes reveal that all are linear, between 40 and 47 kb in length, all containing around 50 genes or so. Many genes encode novel proteins, some of which are species-specific (Barth 2011).

In contrast, the dinoflagellate mitochondrial genome is fragmented, into multiple, 30kb + linear molecules, and encodes just three genes *cox1*, *cox3* and *cob* (Nash *et al*, 2007; Waller, 2009). The current estimate (based on a transcriptome analysis) suggests that the whole genome is over 300 kb. The three genes encode cytochrome oxidase subunit 1, cytochrome oxidase subunit 3 and cytochrome b, all subunits of the mitochondrial electron transport chain (Shoguchi *et al*, 2015). These are the same three genes as found on the 6kb apicomplexa mitochondrial genome (Feagin *et al*, 1991; Feagin, 1992), and all remaining protein-coding genes have been transferred to the nuclear genome (Gardner, 2002).

## 1.8) Aims of Project

This project is focused on the detailed investigations of *T. thermophila* mitochondria. The study aimed to characterize the respiratory pathways and oxidative phosphorylation, as well as isolating and identifying the key subunits of ATP synthase in *T.thermophila*, in order to better understand the function of the mitochondria across the alveolates. The mains aims were:

- To develop methods to isolate and purify *T. thermophila* mitochondria
- To characterize the ciliate mitochondrial electron transport chain
- To analyse ciliate ATP synthase activity to determine if the complex is functional.
- To isolate and purify the ciliate ATP synthase complex.
- To identification any alternative proteins which may fulfil the functional role of the key missing subunits of ATP synthase.

## Chapter 2      Materials and Methods

### 2.1) Materials

*Tetrahymena thermophila* strain CU428 was provided by Assoc. Professor Tracy Bryan (Children's Medical Research Institute, Westmead Sydney, Australia). *Arabidopsis thaliana* mitochondria were kindly provided by Dr. Kathleen Soole (Flinders University, Australia). Polyclonal antibody raised against *Arabidopsis thaliana* mitochondrial ATP synthase beta subunit was purchased from Agrisera, Sweden. The plasmid construct pRUN-IF<sub>1-60</sub>-His was kindly supplied by Sir John Walker (MRC Mitochondrial Biology Unit, Cambridge, UK). Skimmed milk powder was purchased from a local store (Diploma, Victoria, Australia). Ampicillin was obtained from F. Hoffmann-La Roche Ltd. (Basel, Switzerland). Percoll was supplied by GE Health Care (Chicago, USA). Protease peptone medium, bacteriological agar and yeast extract were purchased from Oxoid, Basingstoke, UK. Dimethyl 3,3'-dithiobispropionimidateHCL (DTBP) was purchased from Pierce Thermo Fisher (Melbourne, Australia). All chemicals were of chemical grade and mostly supplied by the Sigma Chemical Company (Sydney, Australia) or Promega (Fitchburg, Wisconsin, United States).

### 2.2) Culturing *Tetrahymena thermophila*

*T. thermophila* culturing procedures were adapted from Bryan *et al.* (1998). A stock culture of *T. thermophila* was maintained by subculturing 1 mL cells in 100 mL Minimal growth medium every fifteen days. Minimal growth medium comprised 2 % (w/v) protease peptone which was autoclaved at 121 °C before the addition of filter

sterilised FeCl<sub>3</sub> to a final concentration of 10 µM. After inoculation, the culture was maintained at 25 °C without shaking.

For cell counts 100 µL of *T. thermophila* culture was treated with 10 µL of formaldehyde to kill the cells before 10 µL was loaded in a haemocytometer and observed using compound light microscopy. Cells were then counted in 9 squares to obtain average number of cells per square. This number was then multiplied by 1x10<sup>4</sup> to obtain the total number of cells per mL of culture.

In order to obtain *T. thermophila* for use in biochemical analyses, a starter culture was initially grown. For this, skimmed milk medium was made in 500 mL Erlenmeyer flasks (6.6 g/L skimmed milk powder and 5.7 g/L of yeast extract in 200 mL distilled water, autoclaved at 121 °C for one hour). After cooling to room temperature, 10 µM FeCl<sub>3</sub> was added. Stock culture (5 to 10 mL) was used to inoculate skimmed milk media. Cultures were incubated at 32 °C for 16 hours with constant shaking at 100 rpm.

For bulk culture *T. thermophila* were grown in 5-10 L of skimmed milk media. After inoculation, the culture was grown at 32 °C for 16 hours (log phase, approx. 10<sup>5</sup>cells/mL) with constant shaking at 100 rpm.

## **2.3) Mitochondrial isolation**

### **2.3.1) Isolation of crude mitochondria**

Log phase *Tetrahymena* cells were harvested by centrifugation (3000g for 10 minutes at 4 °C). The pellet was resuspended in isolation buffer (250 mM sucrose, 0.2 % BSA, 10 mM MOPS, 1 mM EDTA, adjusted to pH 7.2 with 5 M potassium hydroxide). The cell suspension was twice passed through a hand held homogenizer followed by one passage

through the Emulsiflex-C5 Avestin homogenizer with a pressure range between 14-28 MPa. The lysed cells were centrifuged at 1000g for 10 minutes at 4 °C, and the supernatant collected. The supernatant was further centrifuged at 12,500g for 20 minutes at 4 °C. The resulting pellet (crude mitochondria) was resuspended in resuspension buffer (10 mM MOPS, 250 mM sucrose, adjusted to pH 7.2 with 5 M potassium hydroxide). The crude mitochondria were washed by centrifugation at 12,500g for 20 minutes at 4 °C. Finally, the crude mitochondria were resuspended in resuspension buffer (mentioned above) and divided into aliquots of 1 mL in 1.5 mL Eppendorf tubes. Extracted mitochondria were either used immediately or further purified by Percoll gradient centrifugation (see below). In either case, the final protein concentration was measured by a Bradford assay or BCA protein estimation (section 4). Where indicated the resuspended crude mitochondria were resuspended in resuspension buffer supplemented with phosphatase inhibitor cocktail (10 mM NaF, 1 mM Na-orthovanadate, 1 mM Tetrasodium Pyrophosphate). Crude mitochondria aliquots were stored at -80 °C. This method was adapted from Turner *et al* (1971) and Smith *et al* (2007).

### **2.3.2) Isolation of purified mitochondria using Percoll gradient technique**

Purified mitochondria were obtained from crude mitochondria (section 2.3.1) using a Percoll discontinuous gradient centrifugation protocol (Menz *et al*, 1992). The gradient consisted of 15 mL 10 % (v/v) Percoll, 10 mL 20 % (v/v) Percoll, 10 mL 30 % (v/v) Percoll and 5 mL 40 % (v/v) Percoll, in resuspension buffer. The crude mitochondrial pellet (2 mL/ gradient) was layered carefully on top of the gradient tube using a 5 mL syringe with a needle. The needle was fixed such that it lent against the wall of the tube,

(on ice). Once the crude mitochondria were settled on the top of the gradient, the tube was transferred to a Beckman Coulter ultracentrifuge in a SW-32 Ti swing rotor and centrifuged at 55000 g for 40 minutes at 4 °C. Four mitochondrial Percoll % fractions were obtained which were extracted with a pasteur pipette. Each mitochondrial fraction was washed twice with resuspension buffer (above) by centrifuging at 12,500g for 20 minutes at 4 °C. The four final pellets were resuspended in 1mL of resuspension buffer and divided into 200 µL aliquots. The protein concentration of each Percoll % fraction was measured using a Bradford assay before storage at -80°C.

## **2.4) Protein estimation techniques**

Bovine serum albumin (BSA, Sigma) was dissolved in water preparing solution to create protein standards. The standards consisted of 11 tubes which range between 0-1.0 mg/mL BSA. 25 µl of each standard were mixed with 250 µl of Bradford reagent (Sigma) and incubated at room temperature for 1 hour. The absorbance of each standard was read at 334 nm, and a standard curve was drawn. Samples were prepared in the same way and concentrations estimated from the standard curve.

Protein quantitation was also determined using Pierce® BCA Protein Assay Kit (#23227, Thermo Scientific, IL, USA). The procedure was followed as per the manufacturer's instructions using BSA as the standard. All absorbance measurements were completed using a Starstedt® 96 well plate (Nümbrecht, Germany) on an Omega® spectrophotometer (BMG LABTECH GmbH, Ortenberg, Germany) with an incubation period of 30 minutes at 37 °C following manufacturer's instructions.

## **2.5) Transmission Electron Microscopy**

### **2.5.1) *In-situ* Immuno-gold labelling**

Previously isolated crude mitochondria (1 mL) were centrifuged at 1700g in a microfuge (Eppendorf, MiniSpin Plus). The pellet (0.5 mL) was incubated for one hour with 0.5 mL fixative which contained 4 % (v/v) paraformaldehyde, 10 % (v/v) glutaraldehyde, 4 % (v/v) sucrose in phosphate buffered saline (0.7 g anhydrous Na<sub>2</sub>HPO<sub>4</sub>, 0.16 g KH<sub>2</sub>PO<sub>4</sub>, 8.5 g NaCl, pH 7.2) (Tonkin, 2004). The mitochondria were collected by rotating on an orbital rotator at 10 rpm for 10 minutes. The resulting pellet was washed three times by mixing with 1 mL of washing buffer (4 % (w/v) sucrose in phosphate buffer). The pellet was left for a few seconds to settle, and the supernatant removed. The pellet was then dehydrated by washing three times with 1ml 70 % (v/v) ethanol. The pellet was then washed three times with each of 90 % (v/v), 95 % (v/v) and 100 % (v/v) ethanol in the same way. A 1:1 ratio of LR white resin (LR White C024 (ProSciTech, Australia)) and 100 % ethanol were mixed to give a total volume of 1 mL. This mixture was added into the mitochondrial pellet and shaken on an orbital shaker at 10 rpm overnight. The following day, the contents of the microfuge tube were allowed to settle, the supernatant was removed and 1 mL of 100 % LR White resin was added. It was then incubated on an orbital shaker at 10 rpm for 8 hours at room temperature. After 8 hours the pellet was again allowed to settle for few minutes and the supernatant was removed. This step was repeated twice in the same way using 100 % LR white resin. After removal of the final supernatant, a further 1mL of 100% resin was added to the sample, mixed thoroughly and allowed to settle. The excess resin was removed.

A gelatin capsule (in two parts) was used to embed the sample (ProSciTech, Kirwan, QLD, Australia). The larger part was then filled with 100 % resin and then the sample was poured in. The capsule was further filled with 100 % resin to ensure that the sample was completely covered by the resin. The two parts of the capsule were closed together tightly. In order to polymerize the resin, the capsule was incubated at 50 °C for 24 hours.

After 24 hours, the polymerized resin was taken out using sterile forceps and placed onto a Microtome. Sectioning was carried out using an ultra-microtome (LEICA Ultra-cut S) with FCS Cryo-attachment. Sections were cut at a thickness of 85-95 µm using a gold knife. Sections were then mounted on to Nickel grids.

Two sections of nickel grids were used where one section served as a negative control and the other section was the 'test sample'. Each grid was placed upside down on a 20 µL drop of 0.1M glycine. The samples were incubated for 20 minutes at room temperature. Each section was removed from glycine and was then blot/dried by touching the edges of the section with a piece of Whatman filter paper. Each grid was then washed in 20 µL Blocking buffer (1 % (w/v) Bovine serum albumin in 50 mL of phosphate buffered saline) to stop non-specific binding of protein. The grids were again blotted onto filter paper. Then the primary antibody (rabbit polyclonal antibody raised against the ATP synthase beta subunit from *Arabidopsis thaliana* (AgriSera, Vännäs, Sweden)) was prepared in a 1:100 dilution in phosphate buffered saline solution. One grid was then incubated with the antibody for 2 hours at room temperature or at 4 °C overnight. The second grid was used as a negative control which was not treated with primary antibody. The grids were then washed 6 times with 20 µL of blocking buffer for five minutes. After the final wash, sections were blotted on a filter paper. The secondary antibody (gold-labelled anti-rabbit raised in goats) was prepared in 1:100

dilution using PBS. A drop (20  $\mu$ L) of this secondary antibody (1:100 in PBS) was added to each grid and incubated for 1.5 hours at room temperature.

Each grid was washed six times in 20  $\mu$ L PBS for 5 minutes. The grid sections were then washed sequentially 4 times with 20  $\mu$ L of MilliQ water. After the final wash, each grid section was blotted onto filter paper.

For staining, the grids were washed in 500  $\mu$ L of 4 % saturated uranyl acetate for 5 minutes. Finally the nickel grid sections were washed three times by dipping each grid in to Milli-Q water. The grids were finally placed on Whatman filter paper to dry.

The stained sections were observed under an Electron Microscope (EM Phillips CM 100 TEM) using different magnifications. Images were captured and saved.

## **2.5.2) Negative Staining**

Isolated crude or purified mitochondria were pelleted by centrifugation. The pellet (0.5 mL) was incubated overnight with the first fixative which contained 4 % (v/v) paraformaldehyde, 1.25 % (v/v) glutaraldehyde, 4 % (v/v) sucrose in phosphate buffered saline (pH 7.2) (Tonkin, 2004). The mitochondria were pelleted on an orbital rotator at 10 rpm for 10 minutes and the resulting pellet was washed three times with 1 mL of washing buffer comprising of 4 % (w/v) sucrose in phosphate buffer for 10 minutes. Post-fixation was carried out by the addition of 2 % (w/v) Osmium tetroxide ( $\text{OsO}_4$ ) for one hour on an orbital rotator. The pellet was then dehydrated by washing with 70 % (v/v) ethanol, 90 % (v/v), 95 % (v/v) and 100 % (v/v) ethanol. After the removal of the supernatant, the pellet was washed in the similar way in 1 mL propylene oxide. The pellet was then embedded in epoxy resin and polymerized at 50  $^{\circ}\text{C}$  overnight. Sectioning was then carried out using an ultra-microtome (LEICA Ultra-cut

S) with FCS Cryo-attachment. Sections were cut at a thickness of 85-95  $\mu\text{m}$  with a gold knife. These sections were then mounted on the copper grid and stained. The copper grid was placed upside down on 500  $\mu\text{L}$  of uranyl acetate for 5 minutes. The grid was then placed on a drop of 4 % lead acetate for 5 minutes. Finally, the copper grid sections were washed three times by dipping the grid in a series of three beakers containing Milli-Q water and dried on Whatman filter paper. The preparation was observed using an EM Phillips CM 100 TEM.

## **2.6) Enzyme assays**

Enzyme assays were carried out by using crude mitochondria or by using one of the four Percoll fractions of *T. thermophila* purified mitochondria obtained by Percoll density gradient ultracentrifugation.

### **2.6.1) Malate Dehydrogenase**

Malate dehydrogenase assays were performed spectrophotometrically on crude or purified mitochondrial samples (5  $\mu\text{L}$ ) in an assay medium containing 0.25 M sucrose, 10 mM TES (N-tris(hydroxymethyl)methyl-2-aminoethane sulfonic acid (pH 7.2)), 10 mM  $\text{MKH}_2\text{PO}_4$ , 5 mM  $\text{MgCl}_2$ , 4 mM oxaloacetate, and 4  $\mu\text{M}$  antimycin A. The reaction was initiated with the addition of 0.2 mM NADH. The reaction was allowed to proceed for 3 minutes at 25  $^\circ\text{C}$  and the malate dehydrogenase activity was determined by measuring the oxidation of NADH at 340nm, using the extinction coefficient of  $6.22 \times 10^3 \text{ M cm}^{-1}$ . To determine the intactness of mitochondria the malate dehydrogenase activity in the presence or absence of 0.04% (v/v) Triton-X was compared.

## **2.6.2) Cytochrome oxidase (Complex-IV)**

Cytochrome oxidase activity in mitochondrial samples was determined by oxygen consumption assays (section 2.6.3) in a reaction medium (250 mM sucrose, 10 mM  $\text{KH}_2\text{PO}_4$ , 10 mM MOPS pH 7.2, 5 mM  $\text{MgCl}_2$  and 0.1 % (w/v) BSA) with 1.25 mM TMPD-ascorbate and 0.5  $\mu\text{M}$  FCCP.

## **2.6.3) Oxygen consumption assays**

Oxygen consumption was measured polarographically with a Rank Oxygen electrode (Cambridge, UK). The reaction medium (1-3 mL) contained 250 mM Sucrose, 10 mM MOPS pH 7.0, 2 mM  $\text{MgCl}_2$ , 0.7 mM EDTA, 20 mM Glucose and 10 mM NaF (Kilpatrick, 1977) and maintained at a constant temperature of 25 °C. To test the effect of phosphate on respiratory rates the reaction media was supplemented with 10 mM  $\text{KH}_2\text{PO}_4$ . The electrodes' zero point was calibrated with sodium dithionite in water and the total dissolved oxygen concentration in the oxygen saturated reaction medium was considered as 240  $\mu\text{M}$ . Following addition of a substrate or an inhibitor the reaction was left to proceed until a linear rate of oxygen consumption was obtained. In situations where the rate of oxygen consumption decreased over time then the maximal rate of oxygen consumption following the addition was used.

The respiratory pathways of *T. thermophila* mitochondria were characterized by measuring oxygen consumption in the presence of a variety of mitochondrial substrates and inhibitors, the stock and final concentrations of substrates and inhibitors used in the assays are listed in Table 2.1. In some experiments 200  $\mu\text{L}$  aliquots were removed from the oxygen electrode for determination of ATP/ADP concentration (Section 2.7). The removed aliquot was then immediately heat denatured at 95 °C for 5 minutes and then kept at -80 °C.

**Table 2.1** Stock concentrations and working concentrations of substrates, inhibitors and uncoupler

Chemical	Concentration of stock solution	Final concentration
Succinate	1 M	10 mM
NADH	0.1 M	0.66 mM
Malate	1 M	3.3 mM
Isocitrate	1 M	6.6 mM
TMPD-Ascorbate	0.25 M	0.83 mM
ADP	10 mM	0.06 mM or 0.1 mM for S3/S4 transitions
FCCP	0.5 $\mu$ M	1.25 nM
Oligomycin	10 mg/mL	0.0167 mg/mL
KCN	0.5 M	0.83 mM

## 2.7) Bioluminescent ATP assay/ Luciferase assay

For determination of ATP and ADP concentration samples (100  $\mu$ L each) collected during respiratory measurements were heated at 95°C for 5 minutes and centrifuged at 14000g using bench top centrifuge for 5 minutes to collect the supernatant. Then 100  $\mu$ L of the supernatant was used for each reaction. The adenosine 5'-triphosphate (ATP) bioluminescent assay kit was used to measure the ATP content according to the manufacturer's instructions (Sigma, Sydney, Australia).

## 2.8) Molecular Biology Techniques

### 2.8.1) Preparation of competent *E. coli*

Heat-shock competent *E. coli* were prepared according to the method of Sambrook *et al*, (1989). *E. coli* strain PMC103 (Doherty *et al*, 1993) was used for plasmid propagation, whilst strain BL21 (DE3) was used for protein expression.. Cells were streaked aseptically on Luria-Bertani (LB) agar plates containing 1 % (w/v) tryptone, 0.5 % (w/v) yeast extract, 0.5 % (w/v) NaCl, and 1.5 % (w/v) bacteriological agar pH 7.5 and

grown overnight at 37°C. A single colony was then used to inoculate a 10 mL LB culture which was grown overnight at 37°C with shaking. A 5 mL aliquot of the overnight culture was used to inoculate 100 mL of LB liquid medium. The culture was then grown at 37°C until the OD<sub>600nm</sub> reached 0.6. The cells were then pelleted by centrifugation at 2355 g for 10 minutes at 4°C and then resuspended in 10 mL of ice cold 0.1 M Calcium Chloride and left on ice for 20 minutes. The cells were pelleted again by centrifugation and resuspended in 0.2 mL of ice cold Calcium Chloride and stored at 4°C for up to a week before use.

### **2.8.2) Heat shock transformation of *E. coli***

Competent *E.coli* was transformed by the heat shock method (Sambrook *et al.* 1989). Plasmid samples (2 µl) were incubated with 100 µl of competent *E. coli* on ice for 20 minutes. The cells were then transferred to 42 °C for 45 seconds before being transferred back to ice for 2 minutes, after which 900 µl of LB medium was added and the cells incubated for 1 hour at 37 °C with shaking. The heat shock cells were then spread plated on LB-agar plates containing the appropriate antibiotic for selection of the plasmid (150 µg/mL ampicillin for pRUN -IF<sub>1-60</sub>-His). The plates were incubated at 37 °C for 24 hours.

### **2.8.3) Plasmid purification and quantification**

The plasmid pRun-IF1-60-His (containing the bovine inhibitor protein fused to a his-tag, Bason, 2011) was used to transform *E. coli* BL21 (DE3). A single transformed colony was used to inoculate 15 mL of sterile LB broth (containing 150 µg/mL Ampicillin for selection of pRUN -IF<sub>1-60</sub>-His) which was incubated at 37 °C overnight with shaking. Plasmid was then purified from this overnight culture using the Wizard® Plus SV Miniprep DNA Purification System according to the manufacturer's instruction

(Promega, WI, USA). The DNA concentration was measured (162 ng/ $\mu$ l) using a NanoDrop-1000 v3.3 spectrophotometer (NanoDrop Technologies, DE, USA).

### **2.8.4) Restriction enzyme digests**

The plasmid preparation was digested with restriction enzymes *NdeI* and *HindIII*. The reaction was carried out in a 1.5 mL Eppendorf tube by mixing 1  $\mu$ g of plasmid DNA (pRUN -IF<sub>1-60</sub>-His) with 1  $\mu$ L *NdeI* (10 Units/ $\mu$ L), 2  $\mu$ L *HindIII* (10 Units/ $\mu$ L) and 2.5  $\mu$ L buffer 4 (New England BioLabs, MA, USA). The reaction was incubated at 37 °C for one hour.

### **2.8.5) DNA gel electrophoresis**

DNA samples were separated on 0.8 - 1.3 % (w/v) agarose gels prepared with 1 x TAE buffer (40 mM Tris-Base, 0.11 % (v/v) glacial acetic acid and 1 mM EDTA pH 8.0) containing 0.5  $\mu$ g/mL ethidium bromide according to Sambrook *et al.* (1989). All samples were mixed with 6x DNA loading dye (2.5 % (v/v) glycerol and 1.6 % (w/v) bromophenol blue) to a final concentration of 1x. Gels were electrophoresed in 1 x TAE buffer at a constant voltage of 80 V for 80 to 130 minutes in a Bio-Rad® Wide Mini-Sub® Cell GT tank (Bio-Rad Laboratories, Hercules, CA, USA). A digital picture was taken using an Eastman KODAK® Digi-Doc Camera (Rochester, NY, USA) with illumination from a BioRad® UV trans illuminator 2000 (Bio-Rad Laboratories, Hercules, CA, USA). For optimum image contrast, colour levels were altered using Adobe® Photoshop 5.5 (Adobe Systems Incorporated, San Jose, CA, USA). The digested DNA sample was run on an agarose gel alongside undigested plasmid, as shown in Figure 2.1.

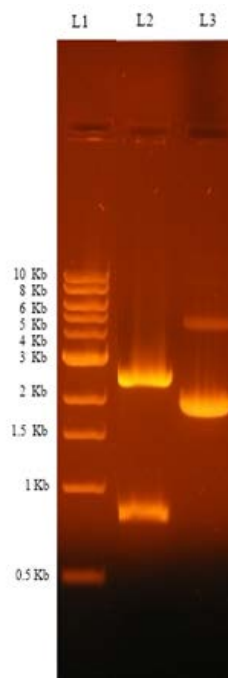


**Figure 2.1 Restriction digest of pRun-IF<sub>1-60</sub>-His purified from *E.coli* BL21 (DE3) cells.** Samples were run on a 2% agarose gel and visualized under UV light. L1; DNA size marker with sizes to the left, L2; *Nde*I and *Hind*III digested plasmid (20 $\mu$ L), L3; undigested plasmid (10 $\mu$ L).

The gel showed that the undigested plasmid control had two bands, one smaller supercoiled band (2.0 kb) and another larger band corresponding to the nicked construct (5.0 kb). The larger band in the digested sample was consistent with the pRun vector at approximately 2500 bp while the smaller band was consistent with the IF<sub>1-60</sub>-His insert (198bp) and 600bp of the vector which shows the band at 800bp. This plasmid was used for all later expressions. 2.9) Expression of Inhibitor Protein in *E. coli*

### 2.9.1) Starter culture

A single colony of *E. coli* cells transformed with pRUN -IF<sub>1-60</sub>-His was used to inoculate 50 mL of LB medium containing 150  $\mu$ g/mL ampicillin. The starter culture was grown at 37 °C with constant shaking at 160 rpm overnight.

## **2.9.2) Propagation of *E. coli* in the fermenter**

About 4 L of sterile LB media containing 0.1 % (w/v) glucose, 150 µg/mL ampicillin and 0.5 mL Antifoam A was inoculated with 50 mL of overnight starter culture (above) in a BioFlo110 Modular Bench top fermenter (New Brunswick Scientific, NJ, USA). The fermenter vessel was previously autoclaved at 121 °C for 40 minutes. The fermenter conditions were maintained at 37 °C, 150 rpm agitation: and air supply of 7 L/min. In order to induce the expression of IF<sub>1-60</sub>-His, 0.286 mg/mL isopropyl β-D-thiogalactopyranoside (IPTG) was added when the optical density at 600 nm reached 0.6 - 0.8. At this stage, the temperature was readjusted to 25°C. 16 hours after the addition of IPTG, cells were harvested by centrifugation at 6,800 g for 10 minutes at 4°C . The pellets were resuspended in 250 mL buffer A containing 20 mM Tris pH 7.4, 10 % (v/v) glycerol, 25 mM imidazole, 0.1 M NaCl. The buffer was filtered and degassed by using vacuum pump filtration unit with Millipore filter (0.2 µm). The suspension was divided into five 50 mL Falcon tubes and stored at -20 °C for future use.

## **2.10) Purification of IF<sub>1-60</sub>-His**

### **2.10.1) Cell lysis**

PMSF at a final concentration of 1 mM was added to 50 mL suspension of *E.coli* BL 21 (DE3) expressing IF<sub>1-60</sub>-His. In order to release the newly expressed inhibitor protein, the cells were lysed by twice passing through a cell crusher at 48-82 MPa-12000 psi. The suspension was filtered to remove any cell debris and stored at -20°C until required. The suspension was ultracentrifuged at 203,000 g at 4 °C for 45 minutes. Without disturbing the pellet, the supernatant was collected carefully with a pipette and filtered using 0.2 µm filter with syringe and collected in a 50 mL Falcon tube. The volume was then made up to 50 mL with Buffer A, pH 7 to 7.5.

### **2.10.2) Nickel affinity purification of IF<sub>1-60</sub>-His**

The purification of IF<sub>1-60</sub>-His was carried out according to a protocol provided by Prof. Sir John Walker (unpublished protocol, personal communication). To purify the inhibitor protein, IF<sub>1-60</sub>-His, a HiTrap™ IMAC HP column (GE Health Care, Buckinghamshire, England) was used in an ÄKTA explorer chromatography system (GE Healthcare, Buckinghamshire, England). The total column volume was 5 mL and the matrix was charged with 0.1 M nickel sulphate at a rate of 0.5 mL per minute between each run cycle. The soluble protein extract was loaded onto the column that was pre-equilibrated with buffer A (20 mM Tris, 25 mM imidazole, 10 % (v/v) glycerol, 0.1 M NaCl, 500 mL water, pH 7.4, filtered and degassed) and then washed with 10 column volumes of buffer A. The bound inhibitor protein was eluted by shifting a step gradient from low to 100% with Buffer B (500 mL buffer A with the addition of 300 mM imidazole). This resulted in the elution of inhibitor protein peak, as shown in Figure 2.2. Those fractions which showed a peak in the A280 absorption (220 mL to 260 mL) were selected and the protein concentration checked with a NanoDrop-1000. The fractions containing protein were combined, and the purified inhibitor protein was desalted and concentrated in a Viva spin-20 (Viva Products) according to the manufacturer's protocol. This process was repeated three times by using buffer A in order to remove the imidazole, the yellowish concentrate represented the purified IF<sub>1-60</sub>-His. After the final wash the concentrate was collected and made up to a total volume of 5 mL in buffer A.

The final protein concentration was found to be 11.87 mg/mL. This purified inhibitor protein was stored at -20 °C until required. SDS-PAGE was used to confirm the presence of purified IF<sub>1-60</sub>-His, as shown in Figure 2.3. Several bands were observed

including some contaminating proteins. However, the dominant band observed at 26KDa, was as expected for the successful purification of IF<sub>1-60</sub>-His (Figure 2.3).

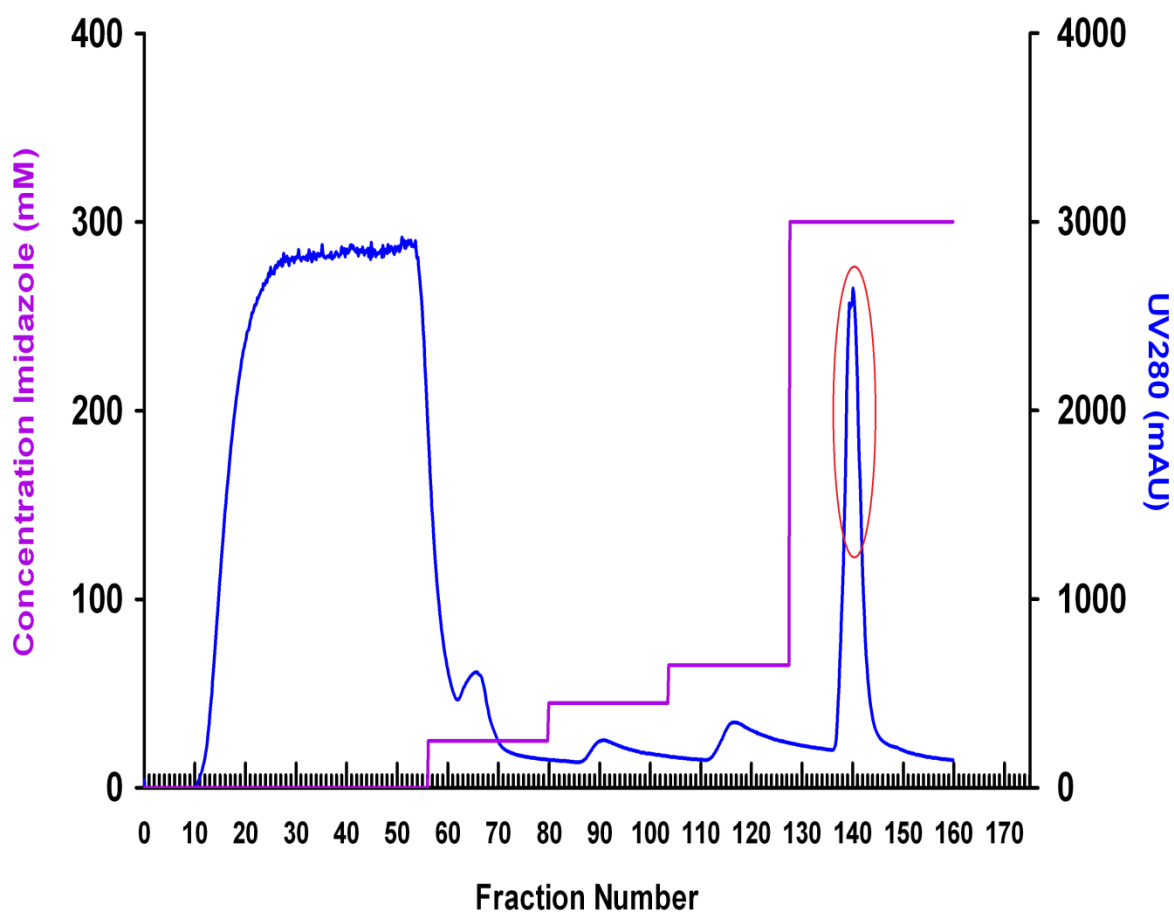


**Figure 2.2** A chromatogram showing the elution profile of IF<sub>1-60</sub>-His with step gradient purification using a nickel affinity HiTrap™ HP IMAC column. Imidazole concentration is represented by the purple line and the step gradient varied from 0 mM and 300 mM imidazole. The inhibitor protein peak is represented by a red circle. The blue line represents the absorbance at 280 nm. The fraction number is represented on x-axis scale.

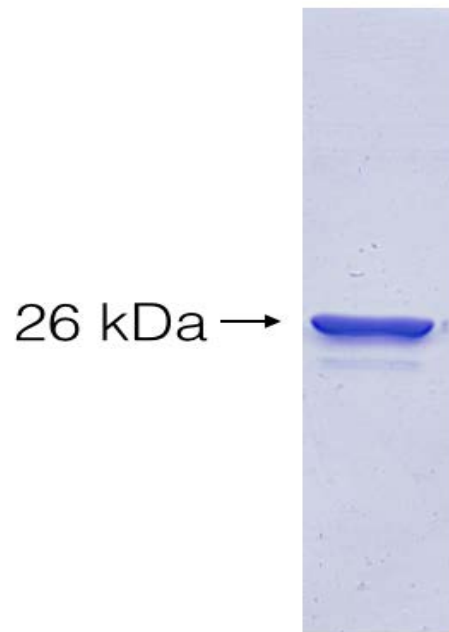


**Figure 2.3** Coomassie stained SDS-PAGE gel showing the purified Inhibitor protein IF<sub>1-60</sub>-His (26KDa). Left annotated molecular marker.

## **2.11) ATP synthase pull down techniques**

### **2.11.1) IF<sub>1-60</sub>-His pull down of ATP synthase**

#### **a) Binding of ATP synthase to IF<sub>1-60</sub>-His**

Previously isolated mitochondria of known protein concentration and volume (approx. 1mL) were washed three times using wash buffer (50 mM disodium hydrogen phosphate, 10 mM sucrose, 0.5 mM EDTA) at 18,000 g for 20 minutes at 4 °C. For experiments conducted in the presence of cross linker, the mitochondria (100 µL) were added with 30 µL of 3 mM DTBP (Dimethyl 3,3'-dithiobispropionimidate.HCL) and incubated at room temperature for one hour prior to these wash steps. Following the washes TG buffer (20 mM Tris, 10 % Glycerol, pH 8.0) was added to the pellet to give a final approximate concentration of 8.5mg/mL of total protein. To lyse the

mitochondrial membrane and to expose any hydrophobic proteins, the sample was then incubated with 1 % (w/v) N-dodecyl- $\beta$ -D-maltoside (DDM) for 20 minutes on ice. Samples were centrifuged at 48,000 g for 10 minutes at 4 °C. The supernatant was removed, and collected in a 10 mL tube. ATP and magnesium sulphate buffer (6 mM ATP, 6 mM MgSO<sub>4</sub>, pH 7.0) was added to the supernatant at a quantity equal to the TG buffer used previously to achieve 300 mM final concentration of the sample.

The mitochondrial protein sample was incubated with the previously isolated IF<sub>1-60</sub>-His at a 1:1 ratio at 37 °C for 5 minutes (with the assumption that 10 % of the total concentration of the initial mitochondrial sample was ATP synthase). After incubation, 830  $\mu$ L of 264 mM Imidazole and 1 mL of 1M NaCl were added and the total volume was made up to 10 mL with distilled water. The sample was then filtered using 0.2  $\mu$ m Minisart® syringe filter (Sartorius Stedium Biotech, Aubagne, France). Finally the pH was measured to ensure that it was approximately pH 7.4.

## **b) Purification of ATP synthase / IF<sub>1-60</sub>-His complex by FPLC**

In this technique an ÄKTA explorer Chromatography System was used. A 5 mL HiTrap™ IMAC HP column (GE Healthcare, Buckinghamshire, England) charged with nickel was equilibrated with buffer A (20 mM Tris, 10 % (v/v) glycerol, 0.1M NaCl, 0.05 % DDM, 1 mM ATP, 25 mM imidazole, 2 mM MgSO<sub>4</sub>) at a rate of 1mL/minute. The 10 mL ATP synthase/ inhibitor protein sample was loaded on to the column. The column was washed with buffer A (at a rate of 1mL/minute from the column was then washed with a 25 mM to 75 mM imidazole gradient in Buffer A. To elute the protein complex, the imidazole concentration was gradually increased to 500 mM. The eluted fractions were collected in 1.5 mL Eppendorf tubes. Those fractions which showed an

absorbance peak at 280 nm were then assayed for protein content by either a Bradford assay or BCA protein estimation (Section 2.4).

## **2.11.2) Antibody pull down of ATP synthase by using CN-Br Sepharose beads**

### **a) Preparation of anti- $\beta$ subunit affinity matrix**

The anti-ATP synthase  $\beta$ -subunit antibody (16  $\mu$ L at 1 $\mu$ g/ $\mu$ L) was coupled to cyanobromide (CN-Br) sepharose beads) according to the manufacturer's instruction. The resulting sepharose media was packed into a 0.5 ml column using the AKTA FPLC. The column was equilibrated with Buffer A (20 mM Tris, 10% (v/v) glycerol, 0.1 M NaCl, 0.05% DDM, 1 mM ATP, 25 mM imidazole, 2 mM MgSO<sub>4</sub>).

### **b) Sample preparation**

A 1ml sample of crude *T. thermophila* mitochondria were suspended in Resuspension buffer (Section 2.3.1) containing 0.02 M Imidazole and 0.05 M NaCl. . The mitochondria were incubated with 1 % (w/v) DDM for 20 minutes at 4 °C, at pH 6 to 6.5. The sample was centrifuged at 7,650 g for 10 minutes at 4°C. The supernatant was filtered using a 0.2  $\mu$ m Millipore filters using a sterile syringe.

## **c) Protein purification by Fast-Pressure liquid Chromatography (FPLC)**

The prepared sample was loaded on to the anti- $\beta$  affinity column and was washed with 10 column volumes of buffer A. Purified ATP synthase was eluted by using high salt concentration (buffer B; 1.5 M imidazole, 1.2 M NaCl, pH 6.5, filtered and degassed). The eluted fractions were collected in 1.5 mL microcentrifuge tubes at a flow rate of 0.3 mL per minute.

### **2.11.3) Methanol precipitation of purified protein**

Methanol precipitation was performed according to the method of Wessel and Flugge (1984), 100 $\mu$ L of protein sample and 400  $\mu$ l methanol were mixed in a 1.5 mL Eppendorf. After vortexing for five seconds, the tube was centrifuged at approx. 1073 g for 10 minutes (Eppendorf, MiniSpin Plus). Chloroform 100  $\mu$ L was added and the sample was vortexed for five seconds and centrifuged again at 1073 g for 10 minutes. Sterile water 300  $\mu$ L was added and the sample was vortexed for five seconds. The sample was centrifuged at 1073 g for one minute. The upper fraction was removed and discarded, and 300  $\mu$ l methanol was added to the lower fraction. The solutions were mixed by inverting the tube 3-4 times, followed by centrifugation 1073 g for five minutes. Finally, the supernatant was removed without disturbing the protein precipitate. The tube was left with the lid open in the laminar flow hood in order to dry the protein pellet. Finally, the dried protein was resuspended in resuspension buffer (as before) and stored at -80 °C until SDS-PAGE was performed.

## **2.11.4) Sodium dodecyl sulphate polyacrylamide gel electrophoresis (SDS-PAGE)**

Tris-Cl buffered SDS-PAGE gradient gels (7 – 20 %) were used to get the isolated protein. SDS-PAGE gradient gels were poured using a 10 stack pre-cast Hoefer apparatus as per the manufacturer's instructions. The 20 % solution consisted of 14 mL 40 % (w/v) acrylamide, 7 mL 1.5 M Tris-HCl (pH 8.8), 280  $\mu$ L 10 % (w/v) SDS and 6.72 mL distilled water. And 7 % solution consisted of 4.9 mL 40 % (w/v) acrylamide, 7 mL 1.5 M Tris-HCl (pH 8.8), 280  $\mu$ L 10 % (w/v) SDS, and 15.82 mL distilled water.

## **2.11.6) Protein detection by western blotting**

### **a) Membrane transfer**

Transfer of proteins from the SDS-PAGE for western blots was carried out using a Bio-Rad Trans-blot® SD Semi-Dry Transfer Cell. Millipore Immobilon-P, 0.45  $\mu$ m, PVDF transfer membranes were used. The membrane, SDS-PAGE gel, and 10 $\times$  gel blotting papers were soaked for 30 mins in Semi-Dry Transfer Buffer (20 % methanol (v/v), 25 mM Tris base, 152 mM glycine, pH 8.0). The transfer was then arranged in the cell in the following order: Anode base, 5  $\times$  Blotting papers, PVDF membrane, SDS-PAGE gel, 5 $\times$  Blotting Papers, Cathode top plate. Transfers were carried out at maximum 22 V and at 0.8 mA/cm<sup>2</sup> (of SDS-PAGE gel) for 1.5 hours.

### **b) Blotting and detection**

Blocking Buffer was prepared from TBST (25 mM Tris-Cl pH 7.4, 140 mM NaCl, 2.7 mM KCl, 0.1 % (v/v) Tween-20). Blocking buffer was prepared by dissolving 50 g/L of skim milk powder in TBST and centrifuging at 4000 $\times$  g for 20 minutes to remove any

undissolved particulate material and stored at 4 °C until use. TBST and Blocking Buffer were prepared fresh and used no later than a week after preparation.

Membranes were blocked overnight at 4 °C in 10 mL of Blocking Buffer with gentle rocking. All subsequent steps were carried out at room temperature with gentle agitation. Membranes were washed five times with 10 mL of TBST for 5 minutes per wash. The membranes were then incubated with 5 mL of TBST containing 1 µL anti-beta subunit antibody (AgriSera, raised in rabbit) for 1 hour at room temperature. The membranes were then washed five times with 10 mL of Blocking Buffer for 5 minutes per wash. Then 5 µL secondary antibody (anti-rabbit antibody conjugated to horse radish peroxidase) in 5 mL TBST was added, and the membranes incubated at room temperature for 1 hour. The membranes were then washed five times with TBST for 5 minutes per wash.

Blotted membranes were treated with Thermo Scientific SuperSignal® West Pico Chemiluminescent Substrate using the manufacturer's instructions. Membranes were exposed to Kodak X-Omat™ K XK-1 Diagnostic Film for 30 minutes unless otherwise stated, and developed using the manufacturer's instructions and solutions.

### **2.11.7) Coomassie staining of protein bands**

Following PAGE, protein gels were stained with Coomassie brilliant blue stain (0.25 % (w/v) Coomassie Brilliant Blue, 45 % (v/v) methanol, 10 % (v/v) glacial acetic acid) for a minimum of 1 hour to overnight and then transferred into destain solution (45 % (v/v) methanol, 10 % (v/v) glacial acetic acid) for a maximum of 2 hours. The gels were scanned with an Epson Perfection V700 Photo Scanner and processed using Adobe® Photoshop CS5

## **2.12) Mass spectrometry techniques**

### **2.12.1) Excision of bands from SDS-PAGE gel for trypsin digest**

Coomassie-stained SDS-PAGE gels were soaked for 3 hours in Milli-Q water. Specific bands were excised (1 mm x 1 mm) with a #11 scalpel and treated with trypsin in preparation for mass spectrometry according to the protocol by Shevchenko *et al*, (2007). Bands were transferred into sterile 1.5 mL microfuge tubes and centrifuged at 2,415 g for 2 minutes in a MiniSpin Plus microcentrifuge (Eppendorf, Hamburg, Germany).

### **2.12.2) In-Gel preparation for Trypsin Digest**

In order to shrink the gel pieces, 500  $\mu$ L acetonitrile (ACN) was added to each samples and incubated for 10 minutes at room temperature. Tubes were centrifuged at 2,415 g for 2 minutes and the supernatant was carefully removed using a fine gel tip. 30  $\mu$ L to 50  $\mu$ L of DTT solution (10 mM DTT, 100 mM ammonium bicarbonate) was added to each sample and incubated for 30 minutes at 56°C. The tubes were cooled to room temperature and incubated with a further 500  $\mu$ L ACN for 10 minutes at room temperature. Samples were centrifuged at 2,415 g for 2 minutes in a microcentrifuge and the supernatant was removed with fine gel tips. About 30  $\mu$ L to 50  $\mu$ L iodoacetamide solution (55 mM iodoacetamide, 100 mM ammonium bicarbonate) was added in order to completely cover each sample and incubated for 20 minutes at room temperature. The samples were then further incubated for 10 minutes with a final aliquot of 500  $\mu$ L ACN before removing all liquid as before.

### **2.12.3) Trypsin Digest of Gel bands**

Each protein sample (i.e. gel band) was covered with 50-80  $\mu\text{L}$  trypsin buffer (13  $\mu\text{g}/\text{mL}$  proteomics grade trypsin from porcine pancreas (Sigma Aldrich, Germany), 10 mM ammonium bicarbonate, 10 % (v/v) acetonitrile. For the maximum saturation of trypsin, samples were incubated at 4  $^{\circ}\text{C}$  for 2 hours, followed by the addition of 20  $\mu\text{L}$  of 100 mM ammonium bicarbonate. Samples were incubated overnight at 37 $^{\circ}\text{C}$ , and allowed to cool to room temperature.

### **2.12.4) Peptide removal from Polyacrylamide Matrix Gels**

Samples were centrifuged at 6,700 g for 2 minutes in a MiniSpin Plus centrifuge (Eppendorf, Hamburg, Germany). To extract the digested peptides from the polyacrylamide matrix, 100  $\mu\text{L}$  of extraction buffer (1.67 % (v/v) formic acid, 66 % (v/v) ACN) was added and incubated for 15 minutes with shaking at 37 $^{\circ}\text{C}$ . The supernatant containing digested peptides was transferred using a fine gel tip to sterile 0.2 mL PCR tubes (which had had the lids removed). To evaporate the supernatant, samples were placed in a HetoVac VR-1 Rotary Evaporator (Heto Lab Equipment, Denmark) under full vacuum for 30 minutes to several hours until a dry peptide residue or minimal volume of peptide solution retained. Samples were resuspended in 15  $\mu\text{L}$  0.1 % (v/v) Trifluoroacetic Acid (TFA).

### **2.12.5) Peptide clean-up for mass spectrometry using Zip Tips**

To prepare the matrix for MS, 20 mg  $\alpha$ -Cyano-4-hydroxycinnamic acid (CHCA) matrix was dissolved in 1 mL of solvent (50 % (v/v) ACN, 0.1 % (v/v) TFA). The matrix was vortexed for 1 minute, and centrifuged at 2,415 g for 1 minute (MiniSpin Plus centrifuge, Eppendorf, Hamburg, Germany). The supernatant was retained for use as the matrix. Millipore C18 zip tip® pipette tips (Millipore, MA, USA) were equilibrated by slowly drawing up 10  $\mu$ L equilibration buffer (50 % (v/v) ACN, 0.1 % (v/v) TFA) then eluting without drawing air. The zip tip was equilibrated 5 times sequentially. The zip tip was washed 5 times with 10  $\mu$ L 0.1 % (v/v) TFA. Binding of sample was carried out by pipetting 10  $\mu$ L of sample slowly up and down 15 times without aerating the tip followed by the wash step. Finally the sample was eluted by slowly pipetting 2  $\mu$ L to 5  $\mu$ L of 40 matrix up and down 10 to 15 times and eluting the matrix onto an MS reading plate (Bruker Daltonics Inc., MA, USA).

### **2.12.6) MALDI-ToF mass spectrometry**

MALDI-ToF MS was performed by Jason Young and Maurizio Ronci at Flinders Analytical (Bedford Park, South Australia). The samples were run on an Autoflex III Smart beam MALDI-ToF MS/MS mass spectrometer (Bruker Daltonics Inc., MA, USA) and operated in linear mode with a nitrogen smart beam II laser.

## 2.13) Mass spectra analysis

All mass spectra were obtained and converted to mzXML file format using the Bio Tools software package (Bruker Daltonics Inc., MA, USA). Mass spectra were visualised using mMass open source mass spectrometry tool (Strohalm *et al.*, 2010). Peaks were selected with mMass (Strohalm *et al.*, 2010) default peak picking setting with the following changes. Peaks were selected from the first visible peak to 4,500 Da, the cycles were increased to 5 to reduce noise, the S/N threshold was set to 2 and peak intensity threshold was set to 40. Peak data was manually calibrated in excel to round integers before being entered into Mascot Peptide Mass Sequencing (Matrix Science, London, UK). Where scores were above approximately 50 with reasonable peptide matches (10-20), the peptide sequences were used to search the NCBI-nr database, with species restricted to the Alveolates. If not feasible matches were identified in the top 5 results, searches were extended to the top 50 results. When no sound matches were found using the NCBI-nr database (with or without limiting to the Alveolates), the data were searched using cRAP, a database including common contaminant such as keratin, BSA and trypsin compiled by the Global Proteome Machine Organization.

# Chapter 3

## Isolation and identification of *Tetrahymena thermophila* mitochondria

### 3.1) Introduction

Mitochondria are important organelles in eukaryotic cells, being the site of respiration. The mitochondrial inner membrane consists of several energy generating protein complex which are together known as Electron Transport Chains (ETC). These chains, together with the ATP synthase complex, carry out a series of biochemical reactions which results in the synthesis of adenosine triphosphate (ATP), known as the energy currency of the cell. These chains are located at the cristae of mitochondria. Cristae are the inner membrane extensions inside the mitochondria. These cristae are easily visible under an electron microscope. Schwab-Stey *et al* (1971) reported the presence of different types of mitochondria in *Tetrahymena pyriformis*, based on electron microscopy investigations. According to them, *T. pyriformis* contained some mitochondria which had an electron dense matrix which they called ‘condensed mitochondria’. Some had an optically void matrix termed as ‘orthodox’, whilst others had medium contrast of the matrix and were termed as ‘Intermediate mitochondria’ (Figure 3.1). The research presented in this chapter describes the identification and isolation of active mitochondria from *Tetrahymena thermophila*.

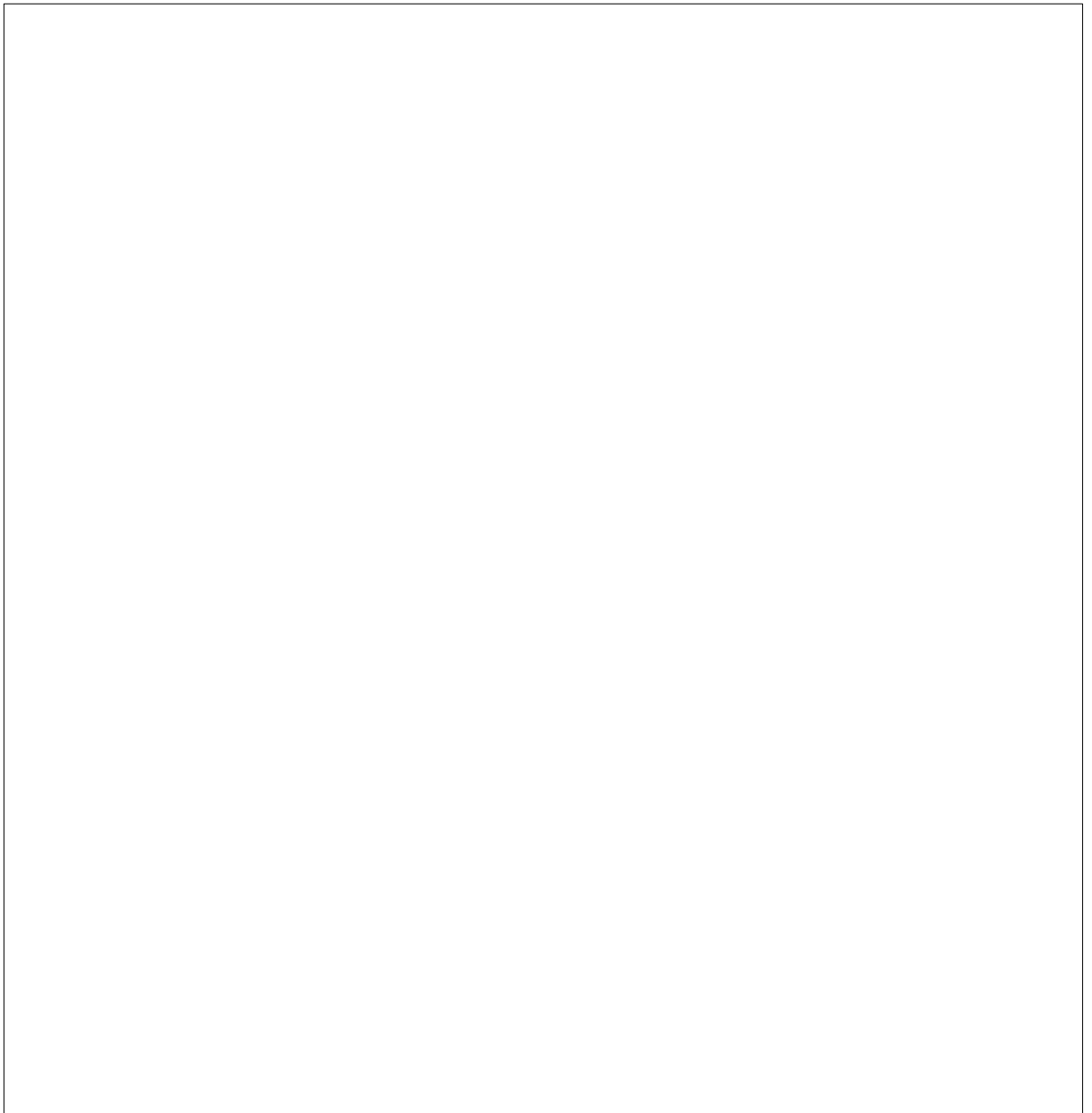


**Figure 3.1** Electron micrographs of three different types of mitochondria in *Tetrahymena pyriformis* (from Schwab-Stey *et al*, 1971). Mitochondria were termed as Condensed (C), Orthodox (O) and Intermediate (I) based on electron density as indicated in enlarged insert panel.

This study used several different techniques. The first was based on light microscopy to observe the viability of the cells and to check for any possible contamination. Mitochondria were then purified by using four different percentages of Percoll. This is known as Percoll-gradient purification method, and results in four purified fractions. Previous research had isolated mitochondria using sucrose gradients (e.g. Smith, 2007; Tsoukatos 1993). While this is a suitable method for isolating intact mitochondria, it does not give rise to biochemically active mitochondria, for which a Percoll gradient isolation is required. A continuous percoll gradient had been applied to *Tetrahymena pyriformis* (Tellis, 2003) resulting in the isolation of purified, active mitochondria. However, no attempt was made to determine the intactness of the mitochondria, and nor was the technique applied to *T. thermophila* (Tellis, 2003). A crude mitochondrial extract using 10% Percoll was utilized in Kobayashi (2005), however again, no attempts were made to determine the intactness of mitochondria, and amount of mitochondria was determined by PCR (i.e. presence of mitochondrial genome).

Following isolation, immuno-gold transmission electron microscopy was carried out to confirm mitochondrial identification. This was carried out by labelling colloidal gold particles with a secondary antibody which is specific to the primary antibody which in turn specifically binds to its target antigen (a subunit of mitochondrial ATP synthase). Therefore the specific binding of gold-labelled antibody gives high electron dense dark spots which are clearly visible under EM. Isolated mitochondria were observed using Transmission Electron Microscopy (TEM).

Finally, the activity of mitochondrial marker enzymes was determined in order to discover which Percoll fraction contained the highest number and purity of mitochondria and which fraction contained the most intact mitochondria. Cytochrome oxidase is an enzyme which is used to identify the presence of mitochondria. This

enzyme (also known as Complex IV) is present in the mitochondrial electron transport chain (ETC). In addition, malate dehydrogenase was used to investigate the intactness of mitochondria. This enzyme plays a crucial role in Tricarboxylic acid cycle. It reversibly catalyses the oxidation of malate to oxaloacetate coupled to the reduction of  $\text{NAD}^+$  to NADH. (In order to stop the NADH formed being oxidised by the ETC, antimycin A was added to the reaction medium. Antimycin A blocks two sites of ubiquinone binding on Complex III. This binding stops the electron flow to Complex IV). The activity of malate dehydrogenase was measured in the presence and absence of the detergent Triton X-100. Triton X-100 disrupts the mitochondrial membranes hence allowing the organelle-bound enzymes to be released, thus allowing the maximum activity of the enzyme to be measured. In the absence of detergent, only the activity of malate dehydrogenase that is not protected by an intact inner mitochondrial membrane is measured.

## **3.2) Results**

### **3.2.1) Microscopic observation of *T. thermophila***

#### **3.2.1.1) Compound Microscopy**

*Tetrahymena thermophila* was easily visible under the light microscope as the cell size is approximately  $60\mu\text{m}$ . A magnification of 10 x showed clear morphology of a single cell of *T. thermophila*. Cells were found to be oval in shape with one end of the cell slightly narrower than the other. *T. thermophila* contains numerous vacuoles in the cytoplasm, and a well-defined cytoskeleton which was surrounded by cilia. Cells were observed to swim in a rotatory motion. In addition, young cells (log phase) appeared to

be quite different from the older cells (stationary phase). Log phase cells were quite circular with very fast movement whereas the stationary phase cells were elongated and flattened with much slower movement.

### **3.2.1.2) *In situ* immunogold Transmission Electron Microscopy**

*In situ* immunogold TEM was performed in order to identify mitochondria in *T. thermophila* by use of a gold-labelled secondary antibody specific to a specific primary antibody which recognises the beta subunit of ATP synthase, a marker enzyme for mitochondria. The significance of this technique is that the cells are 'frozen' in their original condition and polymerized in a resin. The sections were cut and then immunolabelling was carried out, followed by staining. In this way the results obtained are very close to the original positions of the organelles in the cell. There were no electron dense dark spots observed in the negative control images (Figure 3.2) from cells where primary antibody was omitted. In contrast, electron micrographs of immunolabelled cells showed numerous organelles that contained electron dense dark spots, indicating the presence of the ATP synthase enzyme complex, in the cytoplasm of a single cell of *T. thermophila* (Figure 3.3 and 3.4).

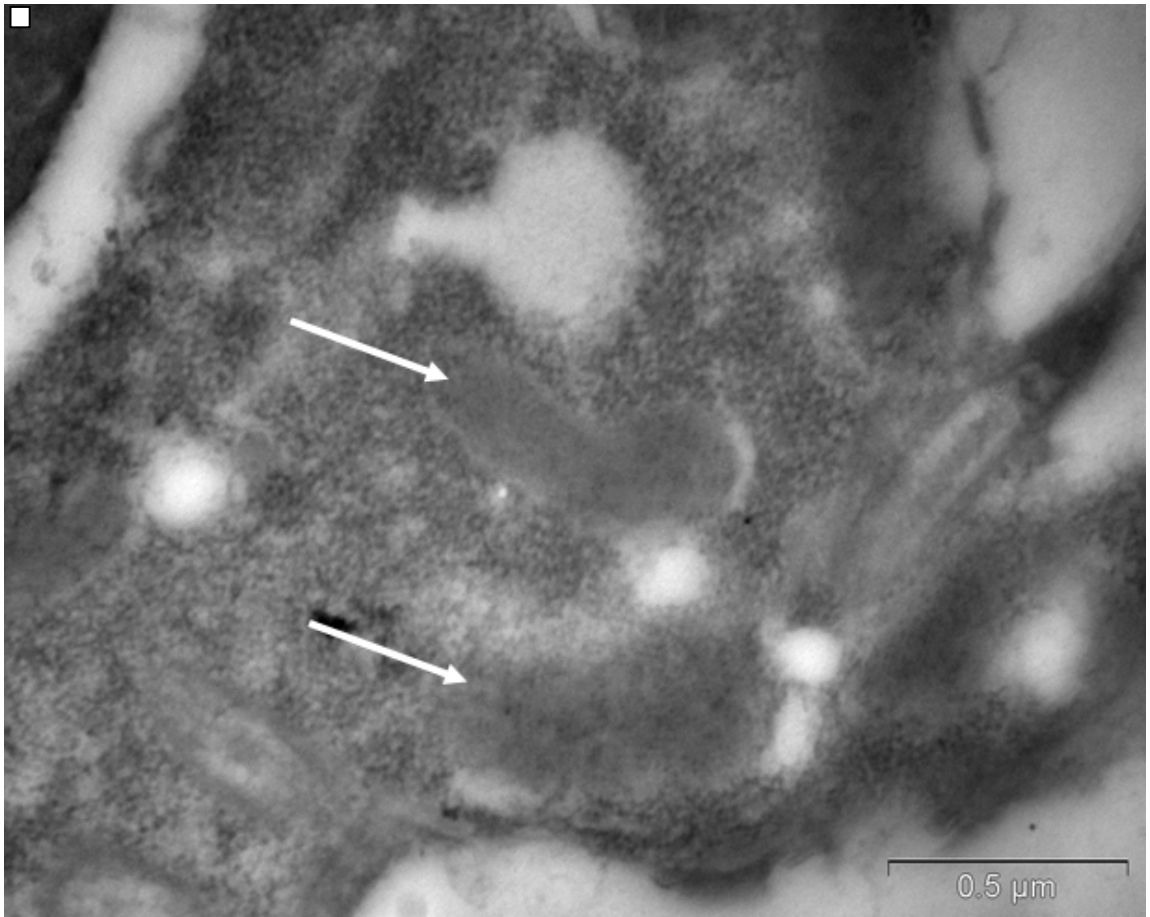


**Figure 3.2 Negative control for *In situ* immunogold TEM images of whole *T. thermophila*.** Picture represents a negative control (without primary antibody) of *T. thermophila* at 34000x magnification. Individual cells are indicated with arrows. Images were collected on a Phillips CM-100 electron microscope as detailed in 2.5.

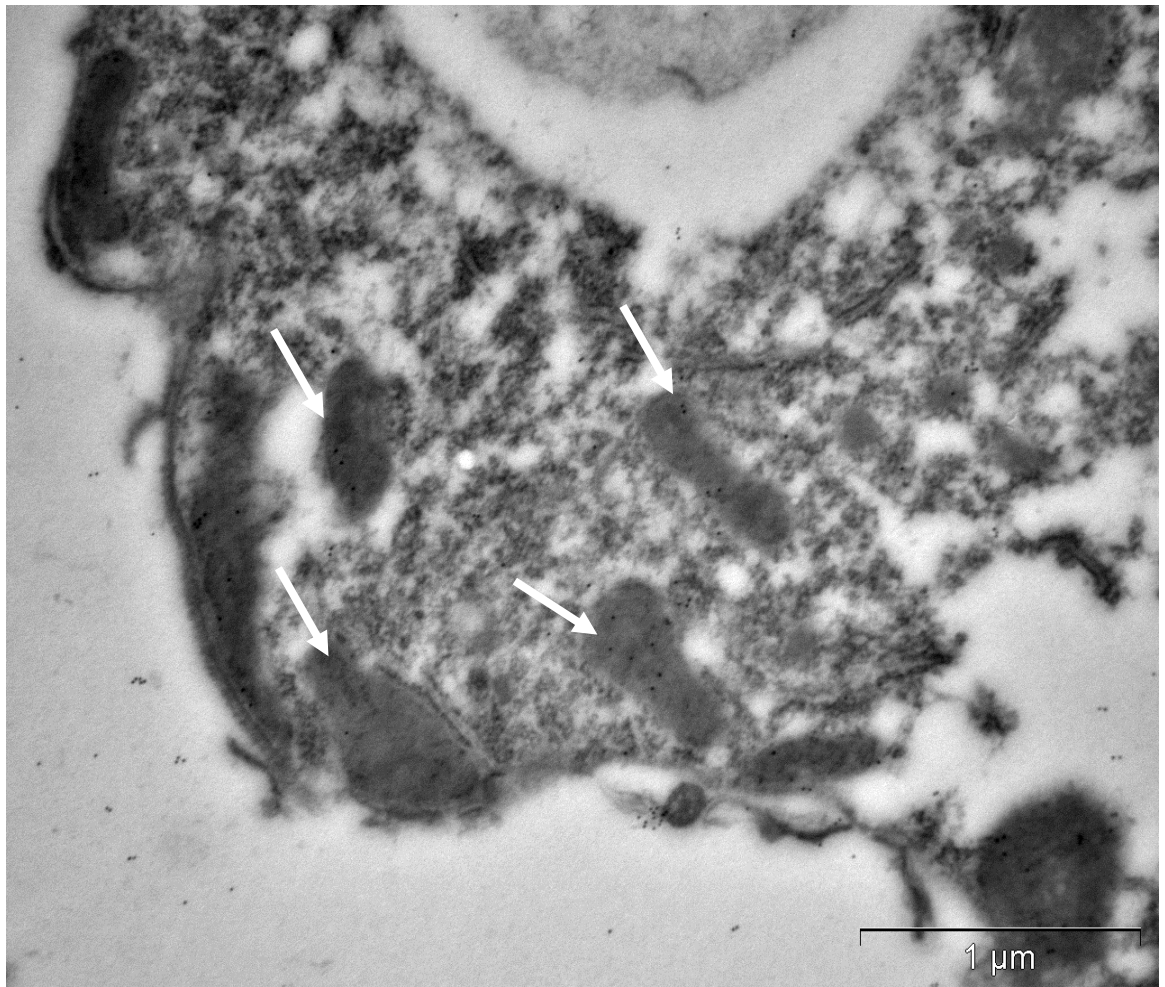


**Figure 3.3** *In situ* immunogold TEM images of whole *T. thermophila* showing labelling of ATP synthase inside mitochondria. Arrows indicate electron dense dark spots showing the specific binding of the gold label to the ATP synthase beta-subunit located in the mitochondria. 17000 x magnification. Images were collected on a Phillips CM-100 electron microscope as detailed in 2.5.

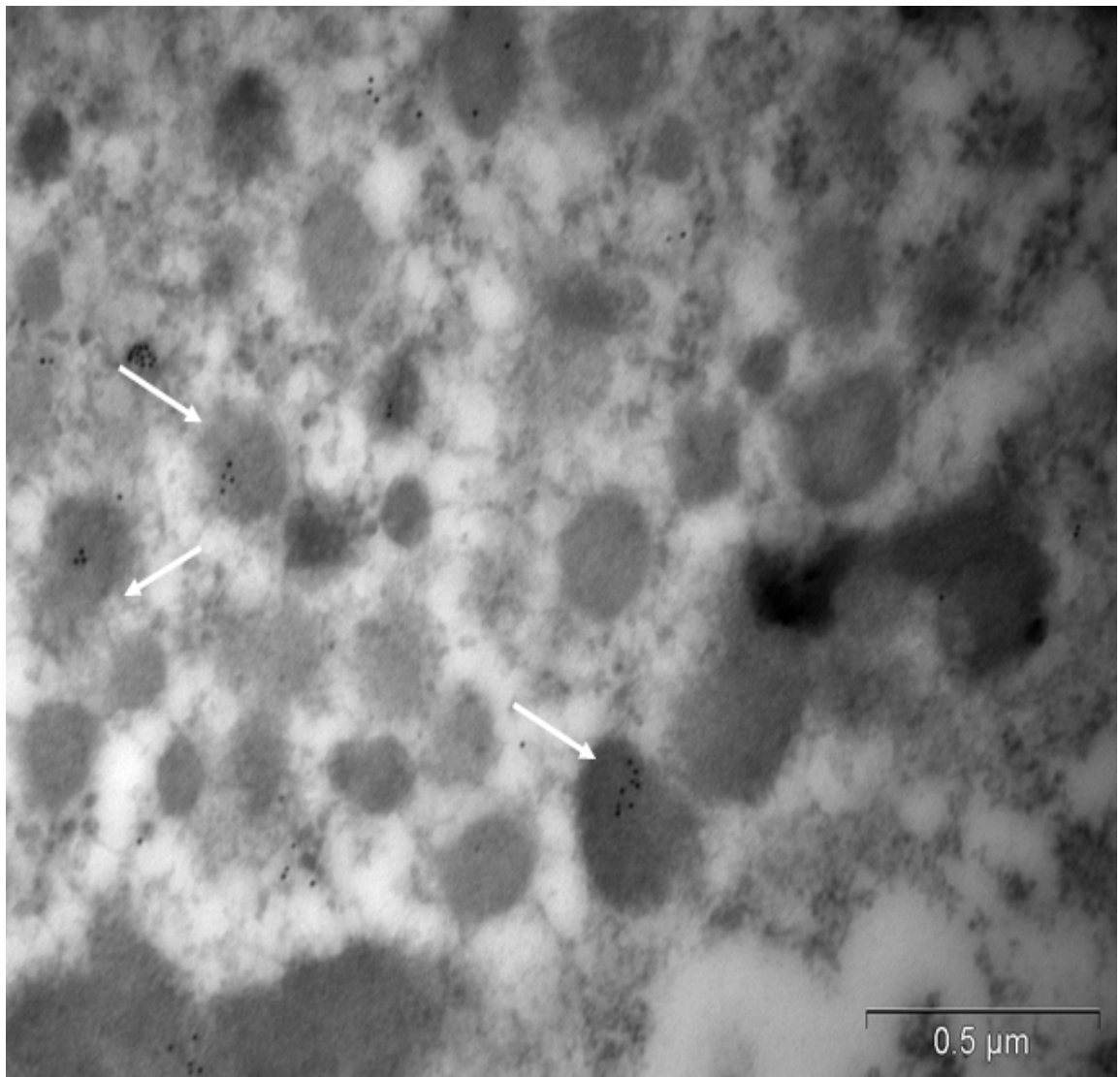


**Figure 3.4** A second view of *in situ* immunogold TEM images of whole *T. thermophila* showing labelling of ATP synthase inside mitochondria. Arrows represent electron dense dark spots showing the specific binding of the gold label to the ATP synthase beta-subunit in the mitochondria. 34000 x magnification. Images were collected on a Phillips CM-100 electron microscope as detailed in 2.5.

### **3.2.1.3) Transmission Electron Microscope analysis of crude and purified mitochondria**

The TEM images of crude mitochondria showed the presence of a variety of different structures (Figure 3.6). In this study, the presence of mitochondria was recognized by the presence of cristae which are unique to mitochondria. For microscopic observations, cristae are widely used as morphological markers of mitochondria. The TEM images therefore demonstrated the presence of mitochondria in the isolated crude fractions of *T. thermophila*. Two different samples of crude mitochondria were used for TEM studies. The *T. thermophila* cells were broken open at pressures of 2000 psi and 5000 psi using the cell crusher in order to determine the optimum conditions for release of mitochondria. The greatest number of intact mitochondria (as opposed to broken mitochondria) was obtained when cells had been broken open at 2000 psi (Figure 3.5a and 3.5 b), compared with those broken at 5000 psi (Figure 3.5c and 3.5d). The presence of massive numbers of cristae in intact organelles indicates the presence of potentially functionally active mitochondria in this *T. thermophila* fraction (Figure 3.5a and 3.5b). When cells were broken at 5000 psi and TEM images were viewed at 10500 x magnification, there were few intact mitochondria which were full of cristae while some were hollow with no cristae found inside the mitochondria (Figure 3.5c and 3.5d).

A step gradient centrifugation using four different percentages of Percoll (10 %, 20 %, 30 % and 40 %) was used to purify *T. thermophila* mitochondria as shown in Figure 3.6. Samples were removed from each layer for analyses, and named after the percentage Percoll. All the fractions were cream in colour. The 10 % Percoll fraction was condensed and smaller in size. The fraction containing 20 % Percoll was the densest and had the greatest amount of protein present. The 30 % layer was bigger in size, but more dilute as compared to the 10 % and 20 % fractions. It also appeared to be granular. The 40 % Percoll fraction was much more dilute and was not as compact as the other fractions.

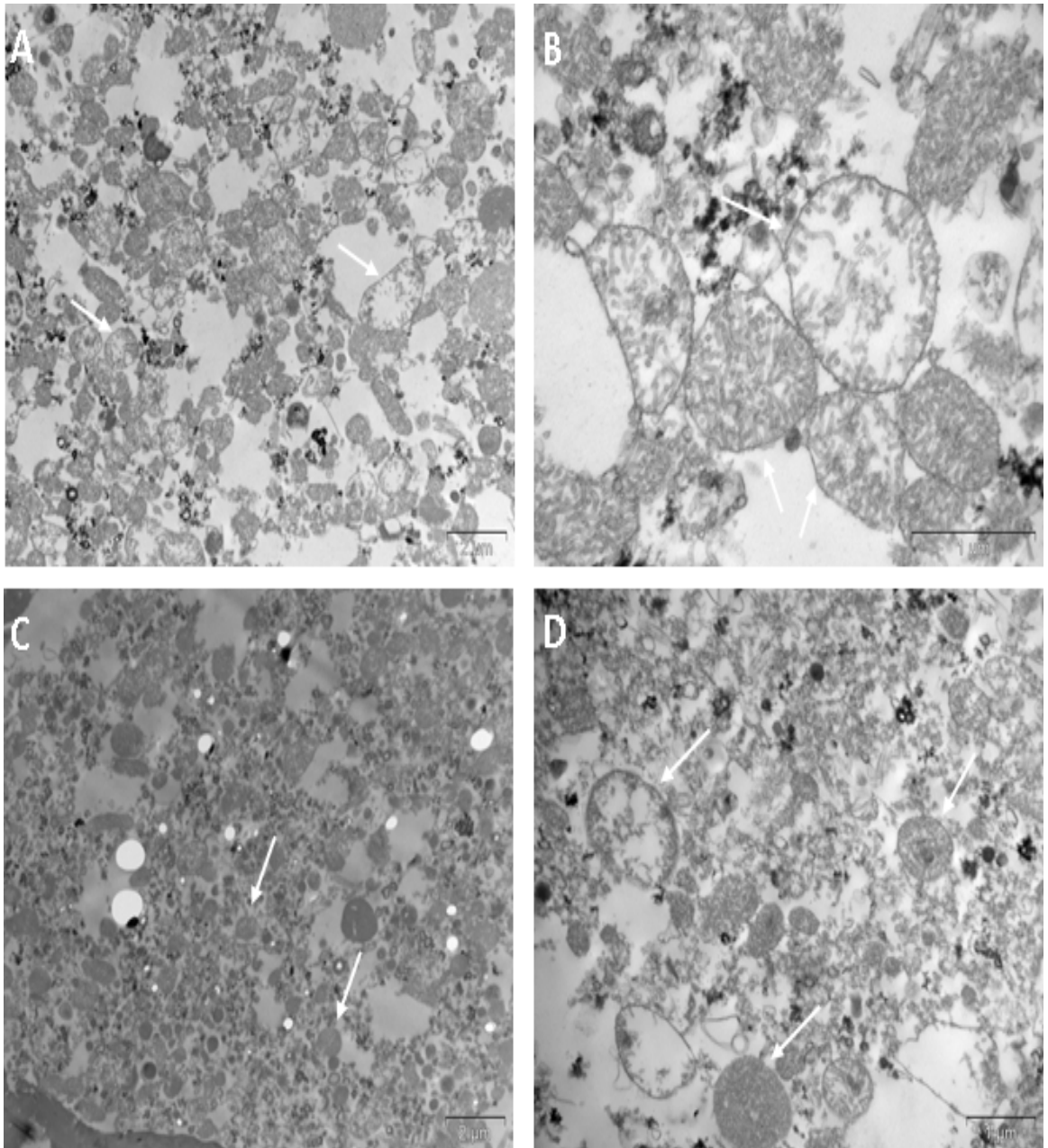


**Figure 3.5 Transmission Electron Microscope images of crude *T. thermophila* mitochondria.** a) Crude mitochondria obtained from cell disruption at 2000 psi, viewed at 4600x magnification, b) Crude mitochondria obtained at 2000 psi, viewed at 19000x magnification c) Crude mitochondria obtained at 5000 psi, viewed at 4600x magnification d) Crude mitochondria obtained at 5000 psi, viewed at 10500x magnification. Arrows indicate mitochondria. b) Percoll Discontinuous gradient-purified Mitochondria.

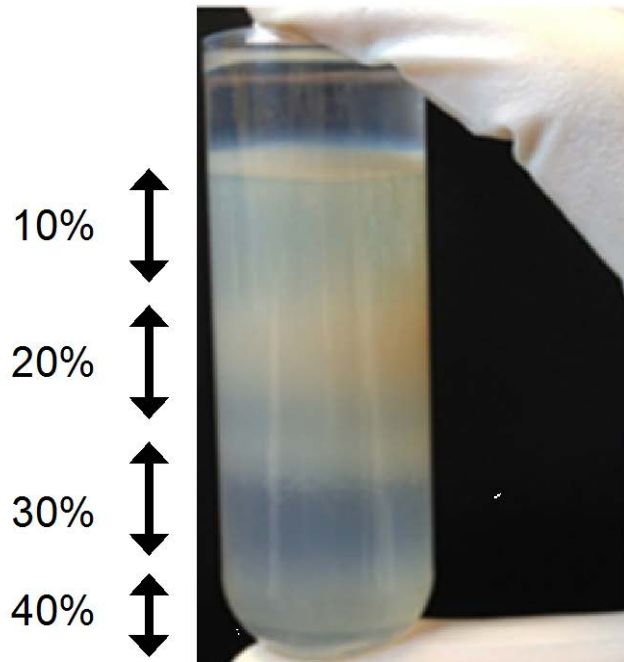


**Figure 3.6 Percoll density gradient purification of *T. thermophila* crude mitochondria.** Crude mitochondria were purified on discontinuous Percoll gradients composed of steps of 40%, 30%, 20% and 10%. The resulting fractions at the interfaces of the steps are indicated by red arrows.

These fractions were isolated and washed for analysis via transmission electron microscopy (TEM). The TEM images showed that mitochondria were distributed across all four isolated purified fractions of the crude sample. The 10% Percoll fraction gave rise to few intact mitochondria as shown by the presence of relatively few organelles containing cristae. The number of intact mitochondria in this fraction was lower when compared to other Percoll fractions (Figure 3.7a and 3.8a). This fraction also contained some other unidentified round structures which could be food vacuoles or vesicles of endoplasmic reticulum. Also present was debris from broken cells and organelles. In contrast, the 20% Percoll fraction contained many intact mitochondria. This fraction also showed mitochondria which were hollow (Figure 3.7b). The magnification at

13500 x clearly revealed the presence of cristae at the edges of the mitochondrial membrane (Figure 3.8b). This fraction was also contained some food vacuoles and broken mitochondrial debris. Intact mitochondria were also seen in the 30% fraction with different sizes varying from large to small. These mitochondria were also different with regards to their electron density. Some mitochondria were 'Orthodox', some were 'Intermediate' while some were 'Condensed' mitochondria (Figure 3.7c). This is consistent with the description of mitochondria following electron microscopy in *Tetrahymena pyriformis* (Schwab-Stey *et al*, 1971). The 13500x magnification of this fraction showed a closer view of these mitochondria. This fraction contained fewer vacuoles and other debris (Figure 3.8c). The 40% Percoll fraction revealed the maximum number of mitochondria, which had densely packed cristae (Figure 3.7d). However, the majority of these mitochondria were found to be broken. The 13500x magnification view of this fraction showed that these mitochondria were full of cristae (Figure 3.8d).

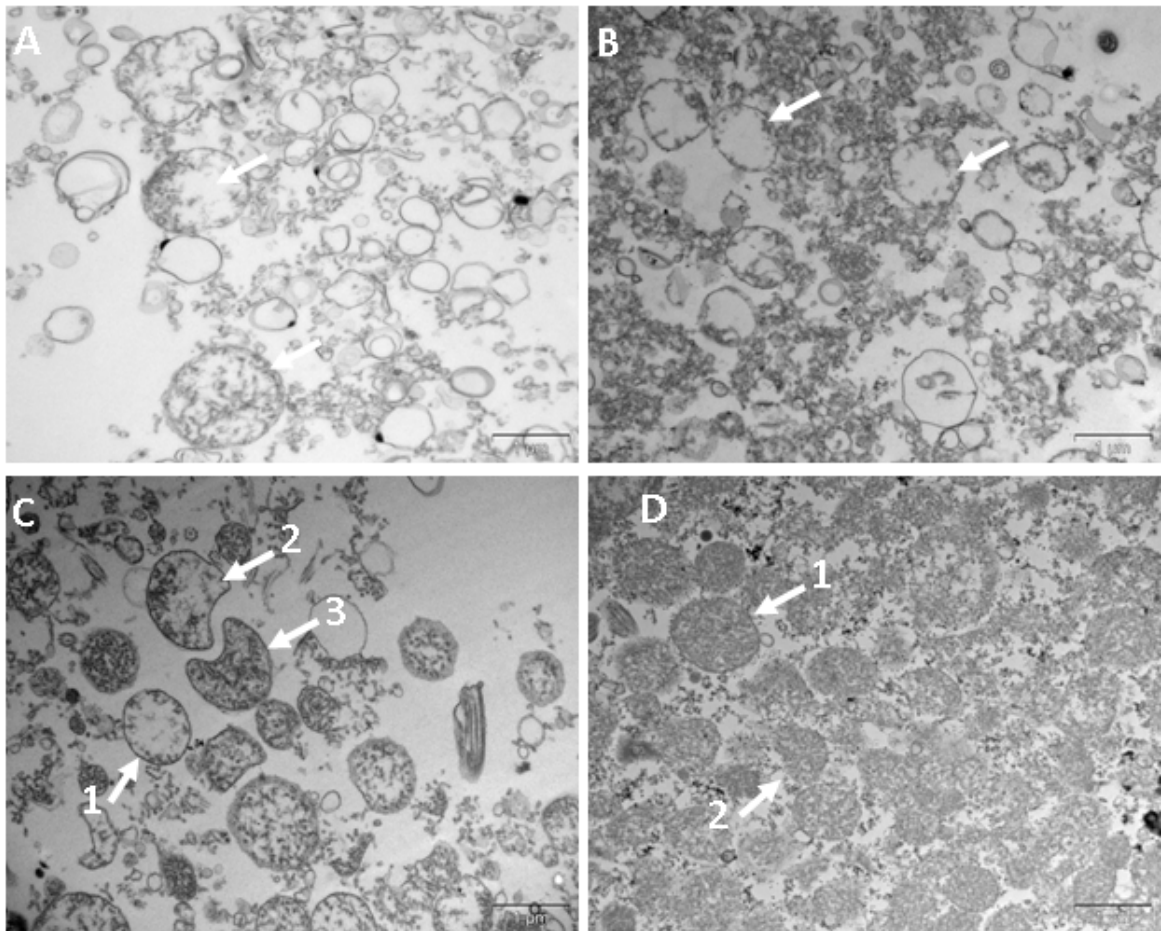


**Figure 3.7 Transmission Electron Microscopy images of Percoll purified fractions of *T. thermophila* mitochondria.** Images were taken at 10500x magnification using a Philips CM-100 EM as detailed in section 2.5.2. a) 10 % Percoll fraction b) 20 % Percoll fraction c) 30 % Percoll fraction representing 1) Orthodox mitochondria (Optically void matrix) 2) Intermediate mitochondria (medium optical density) 3) Condensed mitochondria (Electron dense matrix) d) 40 % Percoll fraction representing 1) Intact mitochondria 2) Broken mitochondria.

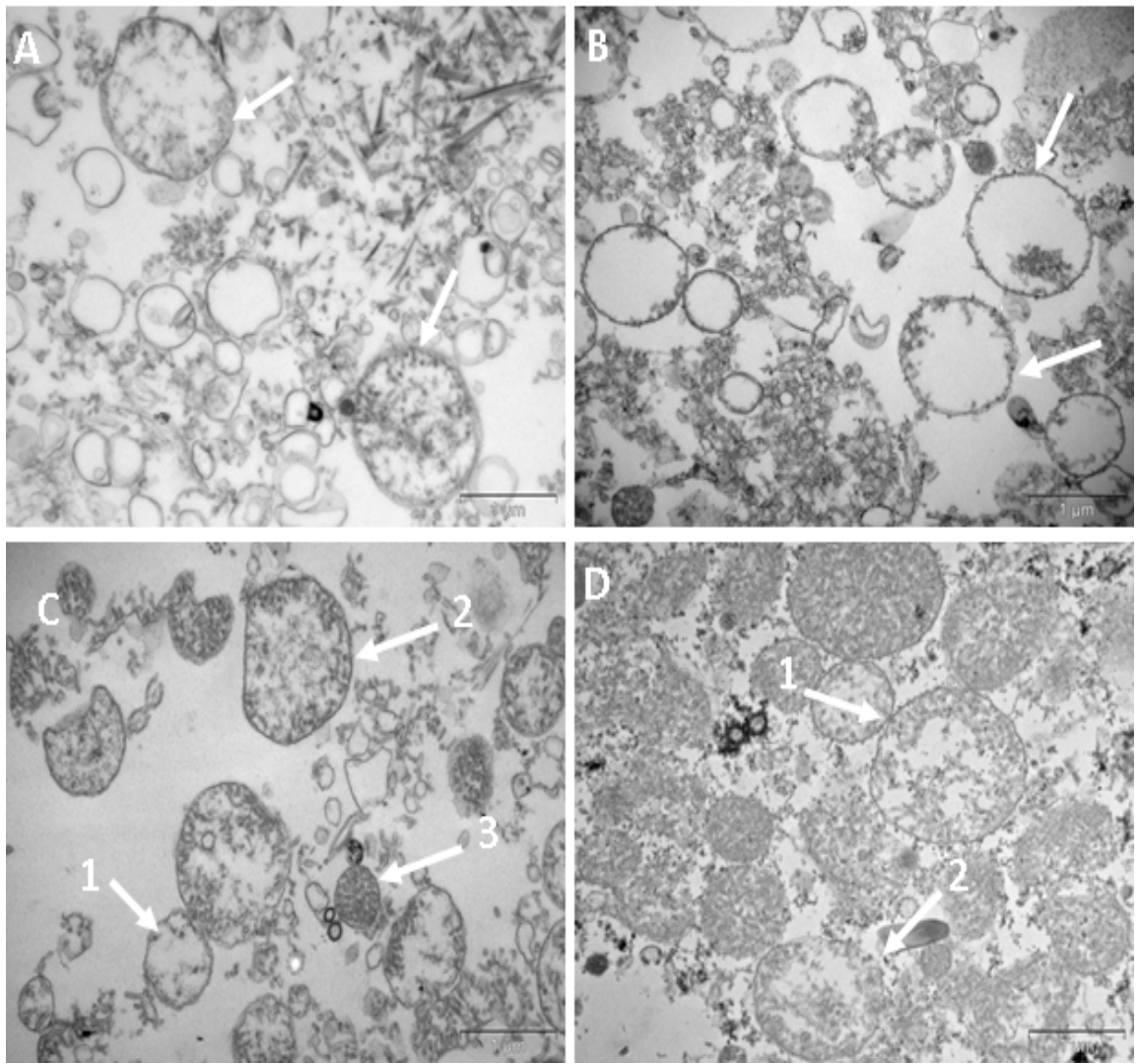


**Figure 3.8 Transmission Electron Microscopy of Percoll purified fractions of *T. thermophila* mitochondria.** Images were taken using a Phillips CM-1000 EM at 13500x magnification. a) 10 % Percoll fraction b) 20 % Percoll fraction c) 30 % Percoll fraction representing 1) Orthodox mitochondria 2) Intermediate mitochondria 3) Condensed mitochondria d) 40 % Percoll fraction representing 1) Intact mitochondria 2) Broken mitochondria.

## **3.2.2) Enzyme assays**

### **3.2.2.1) Cytochrome Oxidase (Complex IV)**

Respiratory measurements were carried out in order to identify which Percoll purified fractions contained cytochrome c oxidase activity, a marker enzyme for mitochondrial inner membranes. Oxygen consumption was enhanced in the mitochondria by the addition of an artificial electron donor ascorbate-TMPD. Two experiments were carried out in duplicate using Percoll purified total cell extract. In order to improve the purity of the mitochondrial preparation, the first experiment utilized cell fractions separated on gradients composed of 5%, 10%, 20%, and 30% Percoll. This was followed by a second experiment contained cell extract separated on gradients composed of 10%, 20%, 30% and 40% Percoll. Each experiment was carried out in duplicate, and graphs were plotted using the data obtained (Figure 3.9).

The first set of data (5-30 % Percoll, Figure 3.9 a and 3.9 b) obtained showed that the maximum activity of cytochrome c oxidase was found in the fraction corresponding to 30% Percoll, with well over 50% of activity being found in this fraction. This indicates that the majority of mitochondrial inner membranes were present in this fraction. However, as this was the top percoll fraction a second experiment was carried out, using a 10-40% Percoll column. The second set of data (10-40%, Figures 3.9c and 3.9d) showed the maximum activity of cytochrome c enzyme activity was present in the 20% and 30% Percoll fractions. Surprisingly, activity was found in the 40% fraction in one replicate (Figure 3.9c), but not the other (Figure 3.9d). This is likely due to be due to slight changes in the setup of the gradient. However, despite this, across all four replicas in both experiments the trend is clear, in that the majority of enzyme activity is in or around the 30% fraction, as shown in Figure 3.10.

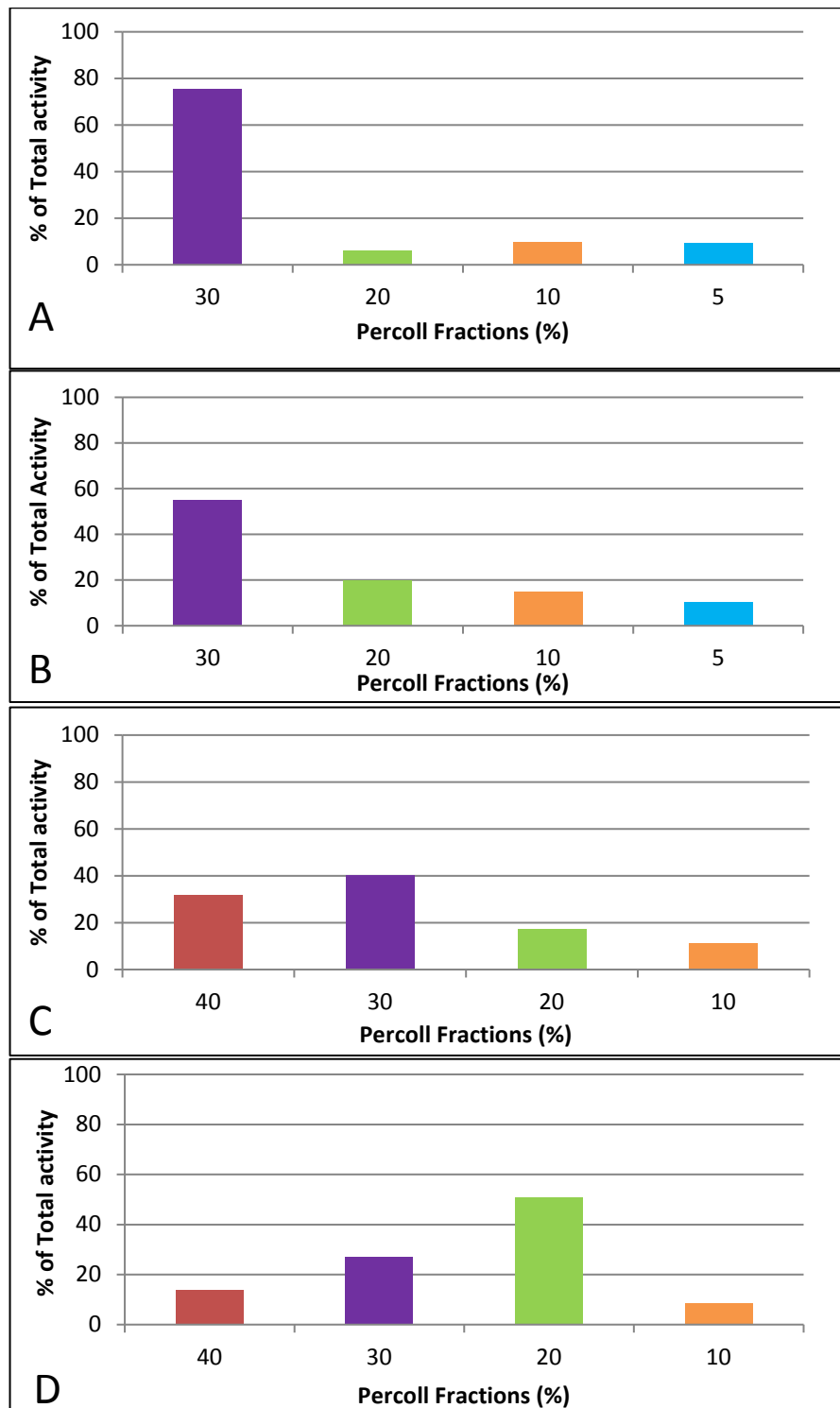


**Figure 3.9 (overleaf) Cytochrome c oxidase activity in different Percoll purified mitochondrial fractions.** A and B are from gradients containing 5%, 10%, 20% and 30% Percoll. Graph C and D are from gradients containing 10%, 20%, 30% and 40% Percoll. Each graph represents an independent experiment on a different *T. thermophila* culture and mitochondrial preparation.

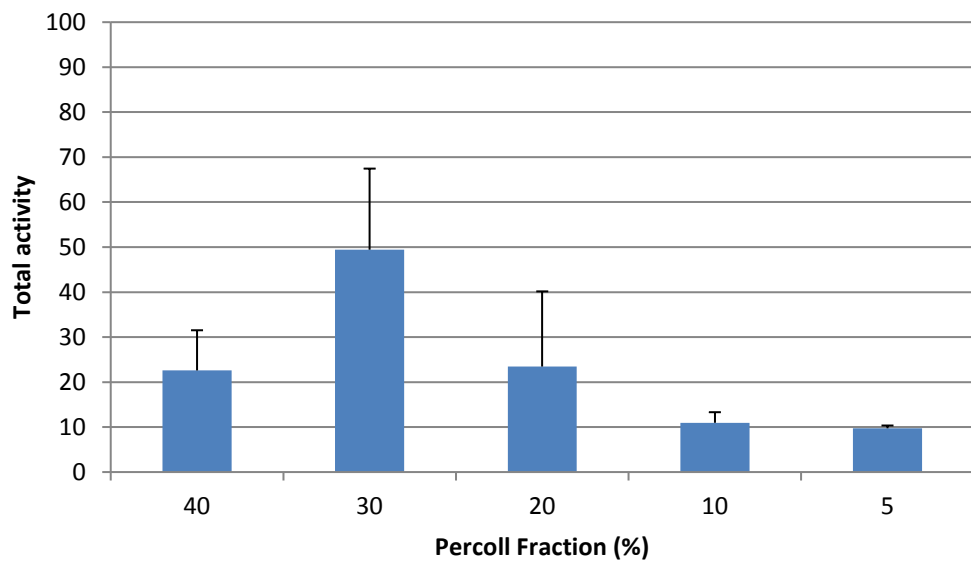


**Figure 3.10 Cytochrome c oxidase activity in different Percoll purified mitochondrial fractions.** The data comes from all four experiments in Figure 3.9, rather than one specific experiment. Error bars represent standard deviation.

### 3.2.2.2) Malate Dehydrogenase

The activity of malate dehydrogenase was measured in the presence and absence of a detergent, Triton X-100. Samples of the same four cell extracts as were used in the cytochrome c assay were used to determine their malate dehydrogenase activity in the presence and absence of detergent in the form of fold-change, as shown in Figure 3.11.

In each case, the maximum change in the enzyme activity was found in the fraction corresponding to 20% Percoll (Figure 3.11 a-d). In one case, (Figure 3.11a), the 5% fraction also showed a similar increase in activity to the 20% fraction, an observation which was not seen in the duplicate. However, the total increase in activity for the 5% fraction was around 2 fold, which is the same as for the replica experiment. In contrast, in experiment a, the 20% activity was just 2 fold instead of 4 fold, as seen in the other three experiments, suggesting that perhaps this observation was an outlier.

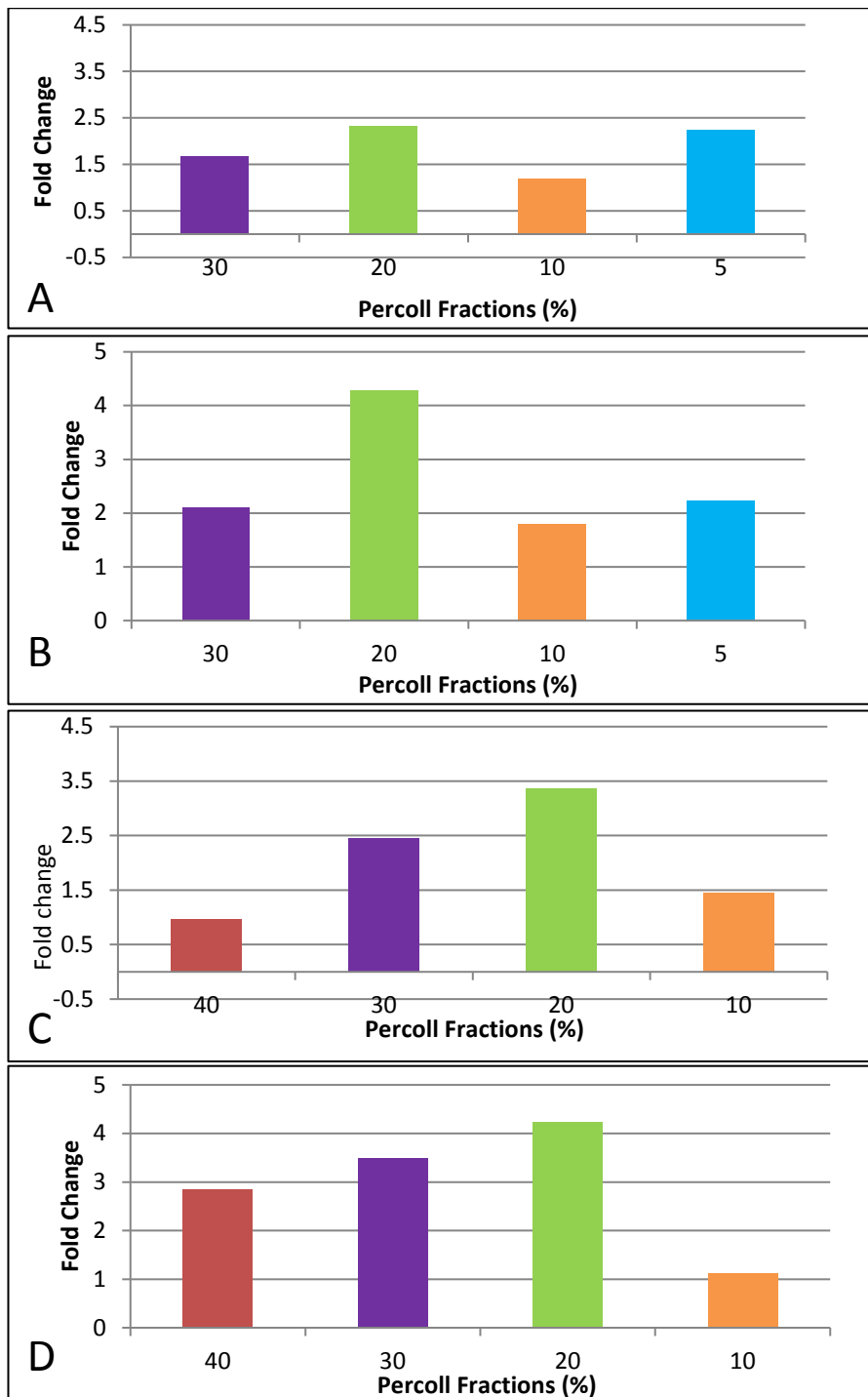


**Figure 3.11 (overleaf) Change in malate dehydrogenase activity in response to the addition of detergent for different Percoll purified mitochondrial fractions.** A and B are from gradients containing 5%, 10%, 20% and 30% Percoll. Graph C and D are from gradients containing 10%, 20%, 30% and 40% Percoll. Fold change was calculated from the increase in activity upon the addition 100  $\mu$ L of 0.4% (v/v) Triton X-100. Each graph represents an independent experiment on a different *T. thermophila* culture and mitochondrial preparation and are the same preparations used in Figure 3.9.

Overall, the results support theory that in the 20% fraction the majority of the malate dehydrogenase was contained inside the mitochondria and was released upon addition of the detergent Triton X-100. As a result, the fold change in the total activity of the enzyme in the 20% Percoll fraction was greatly increased. In contrast, the fractions corresponding to 5%, 10%, 30% and 40% Percoll showed lower changes in total activity after the addition of the detergent (Figure 3.12). This indicated that these fractions contained a much lower number of intact mitochondria.

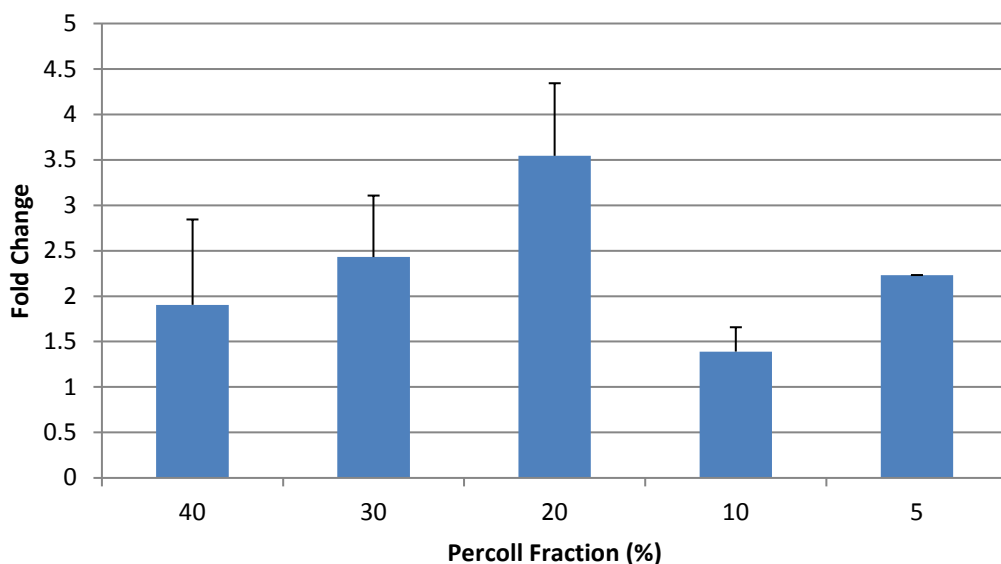


**Figure 3.12 Mean change in malate dehydrogenase activity in response to the addition of detergent for different Percoll purified mitochondrial fractions** The data comes from all four experiments in Figure 3.11, rather than one specific experiments. Error bars represent standard deviation.

### 3.2.2.3 Comparative Distribution of Malate Dehydrogenase Cytochrome oxidase Activity.

The relative distribution of both malate dehydrogenase activity and cytochrome oxidase activity was assessed in three independent experiment using the 10-40% discontinuous Percoll gradients (Figure 3.13). The malate dehydrogenase activity was predominantly located in the 30% and 40% Percoll fractions, whilst cytochrome oxidase was found throughout all fractions. This distribution is consistent with the 10% and 20% Percoll fractions containing a small percentage of intact mitochondria, with a much higher proportion of mitochondria resolving to the 30% and 40% layer. The change in relative proportions of cytochrome oxidase and malate dehydrogenase is most likely due to the 40% layer also containing peroxisomes which also contain malate dehydrogenase (Musrati *et al*, 1998) and which are usually partition to a higher density layer in Percoll gradients (Schwitzgubel and Siegenthaler, 1984).

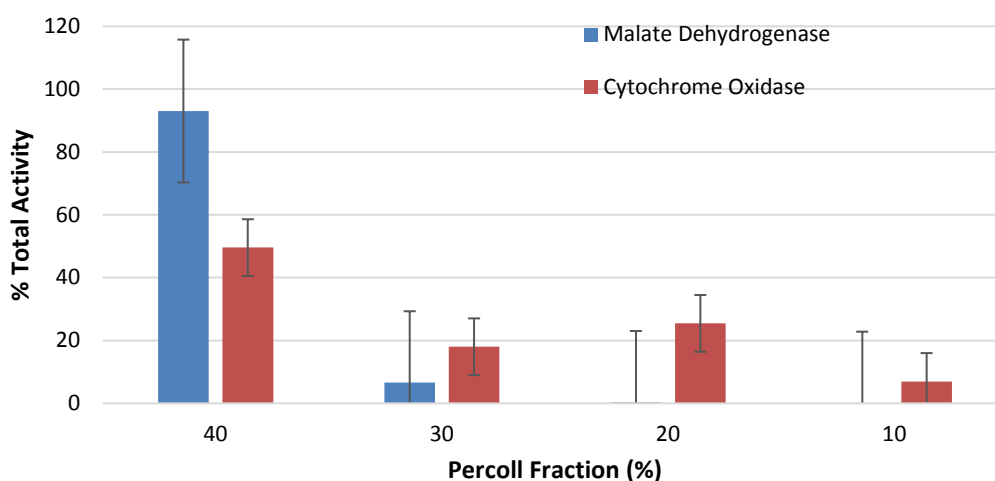


**Figure 3.13 Comparative distribution of malate dehydrogenase and cytochrome oxidase across different Percoll purified mitochondrial fractions.** Data are means of the percentage of total activity for three independent preparations purified using discontinuous 10-40% Percoll gradients. Error bars represent standard error of the mean.

### 3.3) Discussion

This research was carried out in order to determine the best method to isolate pure, intact *T. thermophila* mitochondria. In order to study the presence of mitochondria in the cell, the mitochondrial marker protein ATP synthase beta subunit was highlighted by using an immunogold-labelling technique. In the thin cross-sections of *T. thermophila* viewed by TEM, mitochondria were easily recognized. This data was further confirmed by using TEM for crude and purified mitochondrial samples. The four TEM images (Figure 3.5) of *T. thermophila* crude mitochondria revealed the presence of mitochondria in the ciliate. These mitochondria vary in shape and size. These mitochondria showed varying number of distinct cristae. Based on electron density, three different types of the mitochondria were found in *Tetrahymena pyriformis* (Schwab-Stey *et al*, (1971), Poole, 1983). These mitochondria were termed as Condensed, Orthodox and Intermediate. The research presented here also confirms the presence of three different types of mitochondria in *T. thermophila*.

As this project is based on determining the activity of the mitochondrial respiratory chain enzymes, this chapter describes the development of methods to break open the cells in a manner that did not damage the mitochondria. Of the two pressures used to break open the whole cells of *T. thermophila*, it was concluded that 2000 psi was the most suitable pressure for the cells, as it caused allowed the minimum breakage of mitochondria. In comparison, 5000 psi damaged more mitochondria leaving few intact, and therefore was not suitable as the starting material for future experiments.

Crude mitochondria obtained from cells broken open at 2000 psi were then purified using Percoll discontinuous gradients. The TEM images provided the opportunity to determine which fraction contained the most intact mitochondria. Although all four fractions showed the presence of mitochondria, it was observed that the fraction from

the lowest percentage of Percoll used in the experiment gave the most intact mitochondria. Most of the hollow mitochondria with round shape were found in the 20% Percoll fraction. Based on the cristae, the 30% Percoll fraction had all three different types of mitochondria as mentioned earlier. The 40% Percoll fraction contained mitochondria that appeared to be densely packed full of cristae, however, these also appeared to have ruptured or broken mitochondrial membranes. The shape and sizes of the mitochondria seemed to be similar in both the crude and purified mitochondrial preparations.

In comparison, Smith *et al* (2007) isolated the mitochondria from *T. thermophila* and observed them via a scanning-electron microscope (SEM) (Figure 3.14). As obvious from the SEM image, the mitochondria were shrunken in comparison to the results presented here. This is due to purification of mitochondria on sucrose rather than a gradient (Smith *et al*, 2007). Due to the process of osmosis and the high sugar concentration in the medium, water moves out of the mitochondria causing them to shrink. In addition, the Smith *et al* (2007) cells broke open the cells by using a hand-held homogenizer which broke the cells on with varying pressure or force. In contrast, the research presented here used a constant pressure to break open the cells with a cell crusher and therefore constant shear force as the sample is passed through a fixed aperture, followed by Percoll gradient centrifugation to purify the crude mitochondria. Percoll gives more efficient density separation of the cells and their organelles as it has a very low osmolarity which it preserve the cells/organelles in their original osmotic state. This is the first use of Percoll to isolate *T. thermophila* mitochondria prior to EM. For this reason the TEM images obtained in this research are more indicative of the *in situ* morphology of the mitochondria of *T. thermophila* than previously published images.

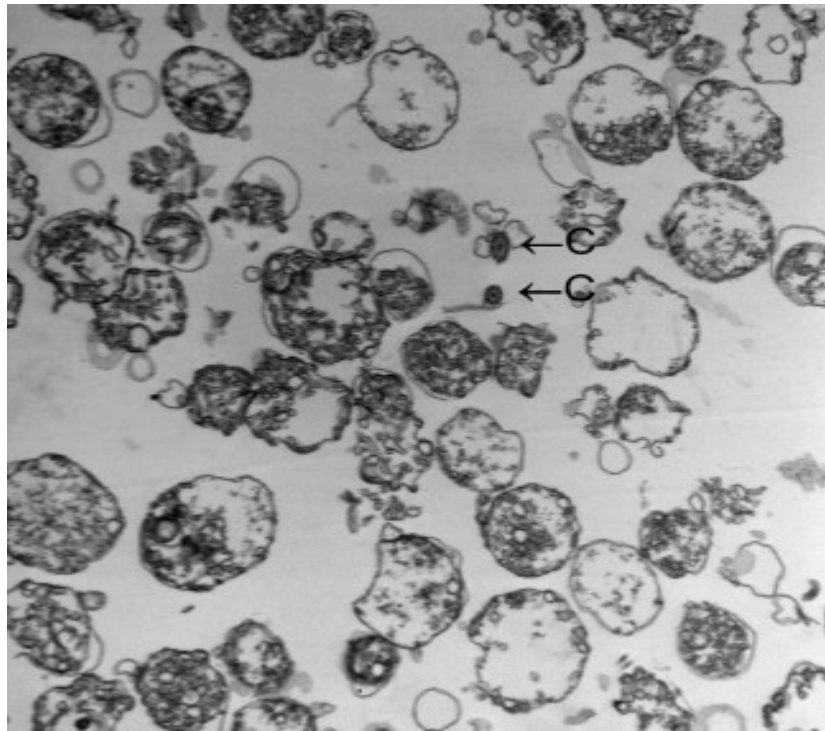


**Figure 3.14 Scanning Electron micrograph of sucrose gradient-purified mitochondria of *T. thermophila* (Smith *et al*, 2007).** Contaminating fragments of cilia are indicated by arrows.

In this chapter, the activity of two enzymes was measured to identify the presence of intact mitochondria in cell fractions of *Tetrahymena thermophila*. Cytochrome oxidase is a marker enzyme for mitochondrial membranes. Here, cytochrome c oxidase was successfully identified in the mitochondria of *T. thermophila*, with the greatest activity occurring in the fraction corresponding to 30% Percoll, thus reflecting the presence of the maximum number of mitochondrial membranes. This result is also consistent with the transmission electron microscopy findings which clearly showed that 30% and 40% Percoll fractions contained the maximum number of mitochondrial membranes. This enzyme activity was very low in the other Percoll fractions reflecting the low number of mitochondrial membranes in these layers. This result is also consistent with EM findings, and is consistent with the three different types of mitochondria (Condensed, Orthodox and Intermediate) having different functions.

The total activity of malate dehydrogenase was observed in the presence and absence of detergent in order to identify the fraction with the greatest number of intact mitochondria. The maximum change in the total activity of this enzyme was found in the 20% Percoll fraction which reflects the presence of the highest proportion of intact mitochondria. Again, these findings are consistent with the TEM images which showed the highest number of intact mitochondria in the 20% Percoll fraction. There were fewer intact mitochondria in the 30% and 40% Percoll fractions as determined by malate dehydrogenase latency, again this was consistent with TEM images which showed the presence of many broken mitochondria in these fractions. The 5% and 10% Percoll fractions also showed much less enzyme activity, reflecting that a very small number of intact mitochondria are present in these fractions.

### **3.4) Conclusion**

This research was carried out to identify methods for the isolation and purification and characterisation of mitochondria from *Tetrahymena thermophila*. Transmission Electron Microscopy and the measurement of the biochemical activity of cytochrome c oxidase and malate dehydrogenase, was used to evaluate the effect of different cell disruption pressures and different Percoll gradient compositions for the purification of mitochondria. Data from both TEM and biochemical assays indicated that the best yield and intactness of mitochondria was obtained by disrupting the cells at 2000 psi, and purification on gradients composed of 10% 20% 30% and 40% Percoll. The highest enzymatic activity was found in the 30% Percoll fraction (cytochrome c oxidase) and from the 20% Percoll fraction (malate dehydrogenase). Together with the TEM data, which showed that the greatest number of intact mitochondria around found in 20% and 30% Percoll fractions, these data suggest that these two fractions yielded the greatest

numbers of intact mitochondria. Further work, to analyse contaminating enzymes (cytosolic) could be carried out in order to clarify the purity of the fraction. These findings will be greatly beneficial to subsequent research into *T. thermophila* mitochondrial function, such as determining the precise composition of mitochondrial membranes, the function of the three types of mitochondria, and enzymatic activity under different conditions.

## Chapter 4

# Characterization of respiration and ATP synthesis in *T. thermophila* mitochondria

### 4.1) Introduction

In eukaryotic cells, oxygen is consumed by mitochondria. This process is linked with the generation of large amount of energy in the form of Adenosine Triphosphate (ATP). A series of five enzyme complexes comprise the electron transport chain (ETC), which is located in the folding of the inner mitochondrial membrane. Various substrates donate electrons to these enzymes resulting in two important simultaneous phenomenons: respiration and ATP synthesis.

Respiration in isolated mitochondria can be monitored by using a Clark-type Oxygen Electrode. The electrodes are separated from the reaction chamber, which contains the isolated mitochondria in solution, by a Teflon membrane. This membrane allows the passage of molecular oxygen from the reaction chamber to the electrodes. When oxygen interacts with the cathode, it is electrolytically reduced. This reduction results in a current flow which is proportional to the concentration of oxygen that is interacting with the electrode. Therefore, measurement of this current over time, via a chart recorder, reflects the change in dissolved oxygen concentration in the reaction chamber. Thus, the trace obtained is basically a measure of the oxygen consumption by the isolated mitochondrial sample.

Under ideal conditions, when a suitable respiratory substrate is added to the medium containing coupled mitochondria, the process of oxygen consumption is started (Figure 1). The oxygen consumption increases when Adenosine Diphosphate (ADP) is added to the system in the presence of inorganic phosphate (Pi). ATP synthase, also known as Complex V, converts ADP and Pi to ATP. The energy for this reaction is provided from the flow of protons from the intermembrane space via ATP synthase to the matrix of the mitochondria. In the presence of ADP the action of ATP synthase dissipates the proton gradient allowing, the rate of electron transport from the respiratory substrate to oxygen to increase. This state when the mitochondria are actively respiring in the presence of ADP is referred to as 'state 3' respiration (Figure 4.1). Once all the ADP is phosphorylated to form ATP, the translocation of protons by the ATP synthase ceases and as a result the rate of electron transport and respiration is lowered, known as 'state 4' respiration. Measurements from the oxygen electrode, allows the P/O ratio to be measured. This gives an indication as to the amount of ATP that is produced per molecule of oxygen used.

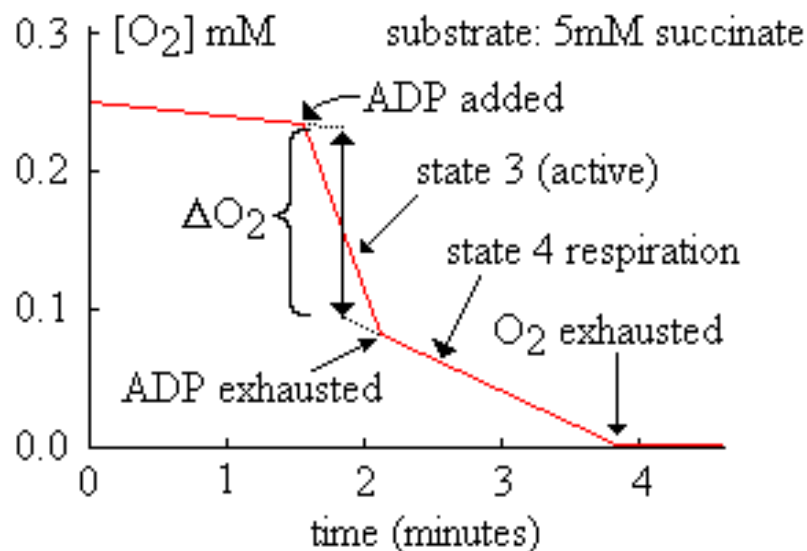


**Figure 4.1** A graph representing a typical trace from an oxygen electrode containing intact mitochondria. The addition of ADP in the presence of substrate and inorganic phosphate enhance respiration (state 3). When all the ADP is converted to ATP, the rate of respiration decreases (state 4).

The levels of oxygen consumption and ATP synthesis by the isolated mitochondria can be reduced by using specific inhibitors. These inhibitors bind to specific sites on the protein complexes of the electron transport chain. For example, oligomycin binds to the OSCP subunit (Oligomycin-sensitive conferring protein) of ATP synthase (Symersky, 2012). This stops the rotational motion of the ATP synthase which in turn stops oxidative phosphorylation. Uncouplers, such as FCCP can be added. These abolish the link between the electron transport chain and oxidative phosphorylation, and thus alter the proton permeability of intact mitochondria resulting in proton flux from the intermembrane space to the matrix. This affects the overall electrochemical gradient across the inner membrane resulting in an increase in oxygen consumption, but decreasing the rate of ATP synthesis.

It has long been known that ciliate mitochondrial ATP synthases behave differently to yeast and mitochondrial ATP synthases. In particular, many F-type ATP synthase inhibitors are ineffective in ciliates, or only work at much higher concentrations (Unitt and Lloyd, 1981). This is presumably due to missing subunits in the ATP synthase complex, as identified by genome sequencing (Eisen 2006) (Nina, 2010).

The behaviour of complexes I-IV was first characterized in the 1970s. These studies showed that electron transport was inhibited by cyanide, rotenone and antimycin A (Turner, 1971) (Conklin, 1972). Levels of antimycin A required for inhibition was found to be much levels that are higher than required for mammalian mitochondria, suggesting that *Tetrahymena* lacks complex III (Conklin, 1972). However, all these experiments were carried out before a ciliate genome sequence was available.

The aim of this chapter is to examine the functional roles of the electron transport chain in *T. thermophila* mitochondria. In particular, the effect of the uncoupler FCCP and hydrogen cyanide (KCN), which inhibits complex IV were examined.

## **4.2) Results**

In this chapter various experiments were performed to investigate the functional behaviour of the electron transport chain in the mitochondria of *T. thermophila*. Experiments were carried out to measure the oxygen consumption rates with different substrates, as well as an uncoupler and inhibitors which act upon different enzymes of the ETC. Experiments were carried out with crude mitochondrial preparations, following Turner 1971 and Conklin 1972.

### **4.2.1) Effect of various substrates on oxygen consumption**

Succinate proved to be an excellent substrate and gave the highest rate of oxygen consumption amongst the four natural respiratory substrates tested (succinate, NADH, isocitrate and malate, Figure 4.2). The second highest rate was observed with the substrate malate, while comparatively, isocitrate and NADH showed very low rates of oxygen consumption (Figure 4.2). The artificial substrate TMPD-ascorbate, which reduces endogenous cytochrome c (the substrate for complex IV) also showed a high rate of oxygen consumption (Figure 4.2). Based on these results, succinate was selected as a substrate for further experiments investigating oxidative phosphorylation in the mitochondria of *T. thermophila*.

### **4.2.2) Effect of ADP on oxygen consumption in the presence of different substrates**

Oxygen consumption rates were measured in the presence of ADP with various natural respiratory substrates. It was found that the addition of ADP together with succinate slightly increased the rate of oxygen consumption compared to the succinate only rate (Figure 4.2). An increase in the rate of respiration was also observed with the substrates TMPD-ascorbate, and isocitrate, when ADP was included, relative to the rate with the

substrate alone. The increase of TMPD was particularly large. These experiments were repeated three times, and results presented are representative. In contrast no increase in the rate of oxygen consumption was seen when ADP was included with the substrates malate and NADH. However, the overall rate of oxygen consumption in these cases both with and without ADP was much lower than that with succinate (Figure 4.2).

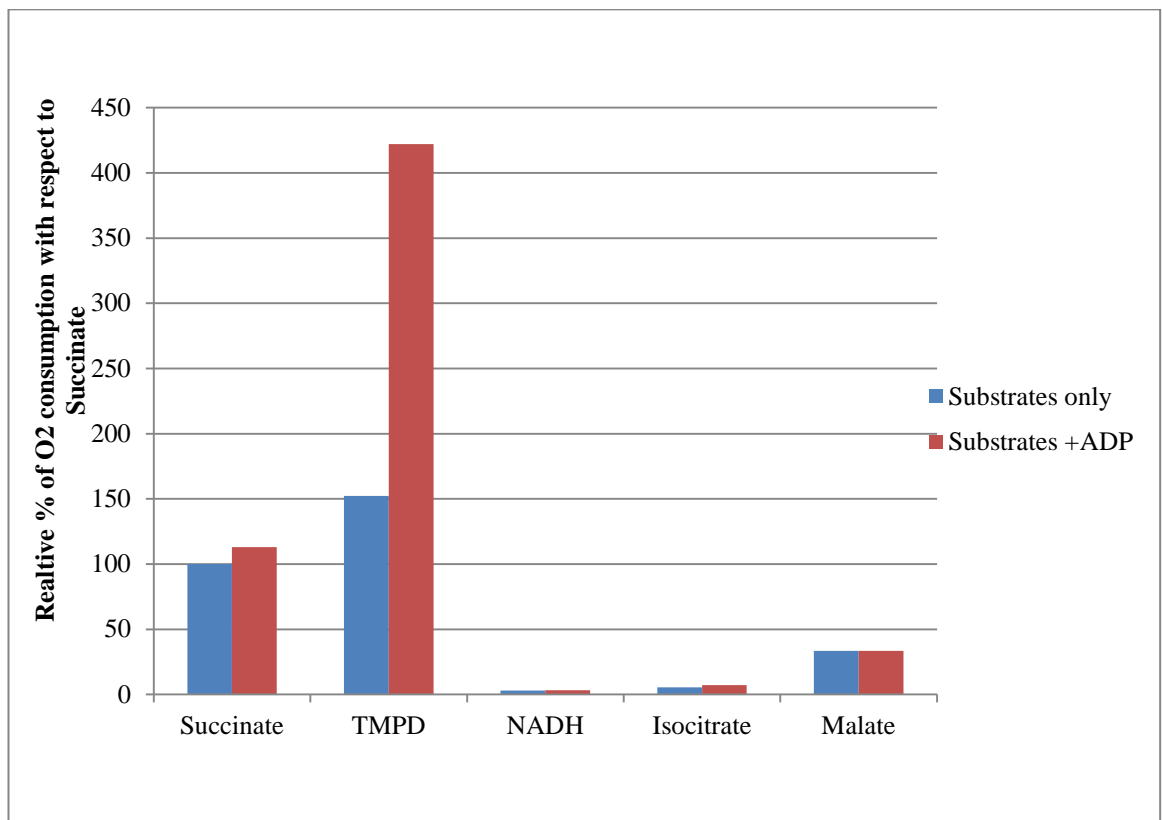


**Figure 4.2 Effect of TMPD, NADH, Isocitrate and Malate on relative respiratory rates with respect to succinate (blue bars) in the presence and absence of ADP.** Relative oxygen consumption rates with respect to the rate in the presence of 5 mM succinate. Blue bars represent the rate with the substrate alone, red bars represent the initial rates with the substrates plus 0.06 mM ADP. Results are representative, and repeated experiments showed the same effects.

### **4.2.3) Observation of typical respiratory state 3 and state 4 transitions in the presence of succinate and ADP**

The addition of succinate to the mitochondria resulted in an initial high rate of oxygen consumption, however, over time this rate decreased (Figure 4.3). This decrease in rate was not found to be due to the decrease in concentration of substrate, as further additions of succinate did not restore the original rate (data not shown). In contrast, the addition of the uncoupler FCCP resulted in slightly higher initial rates of oxygen consumption that did not decrease over time (Figure 4.4). The addition of ADP showed a greater initial rate of oxygen consumption relative to succinate alone that rapidly decreased over time (Figures 4.3 and 4.4). However, addition of further ADP did not increase the rate of oxygen consumption, as would be expected if the reduction in the rate of oxygen consumption was due to reduction in the ADP concentration (State 3/State 4 transition, Figure 4.4). The initial rate of oxygen consumption with succinate as the substrate was higher when both the uncoupler FCCP and ADP were present compared with FCCP alone (Figure 4.4).

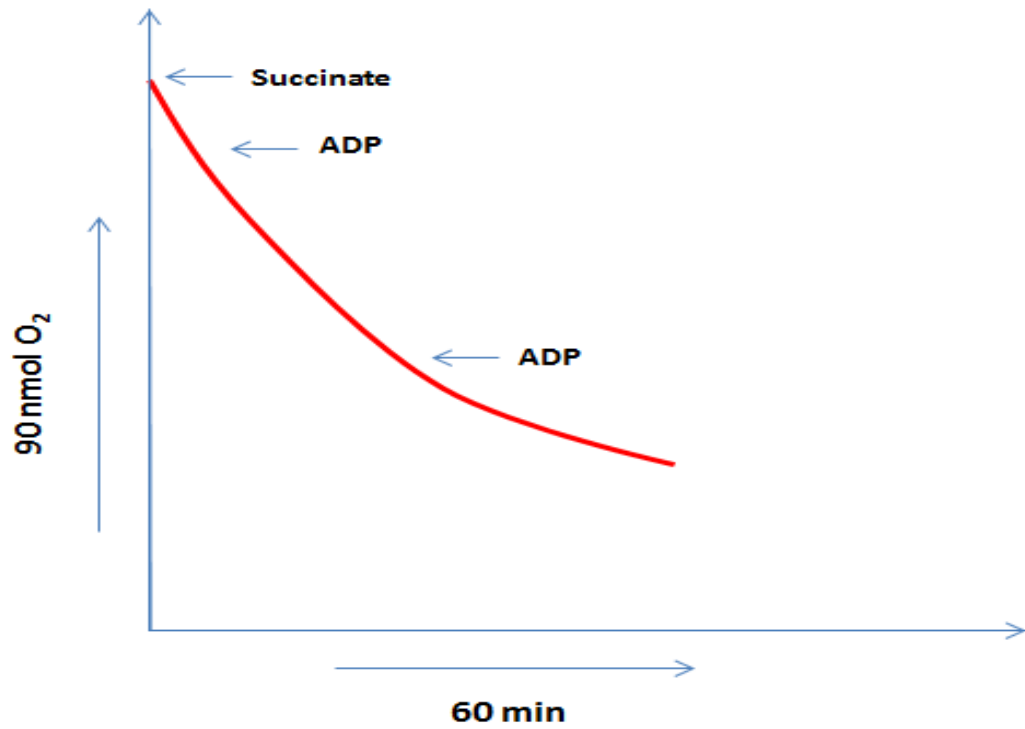


**Figure 4.3** The effect of ADP on oxygen consumption by *T. thermophila* mitochondria in the presence of succinate. Oxygen electrode traces showing the rate of oxygen consumption in the mitochondria of *T. thermophila* in the presence of 5 mM succinate with two additions of 0.06 mM ADP at different points. Typical State 3 and State 4 were not observed following the addition of ADP.

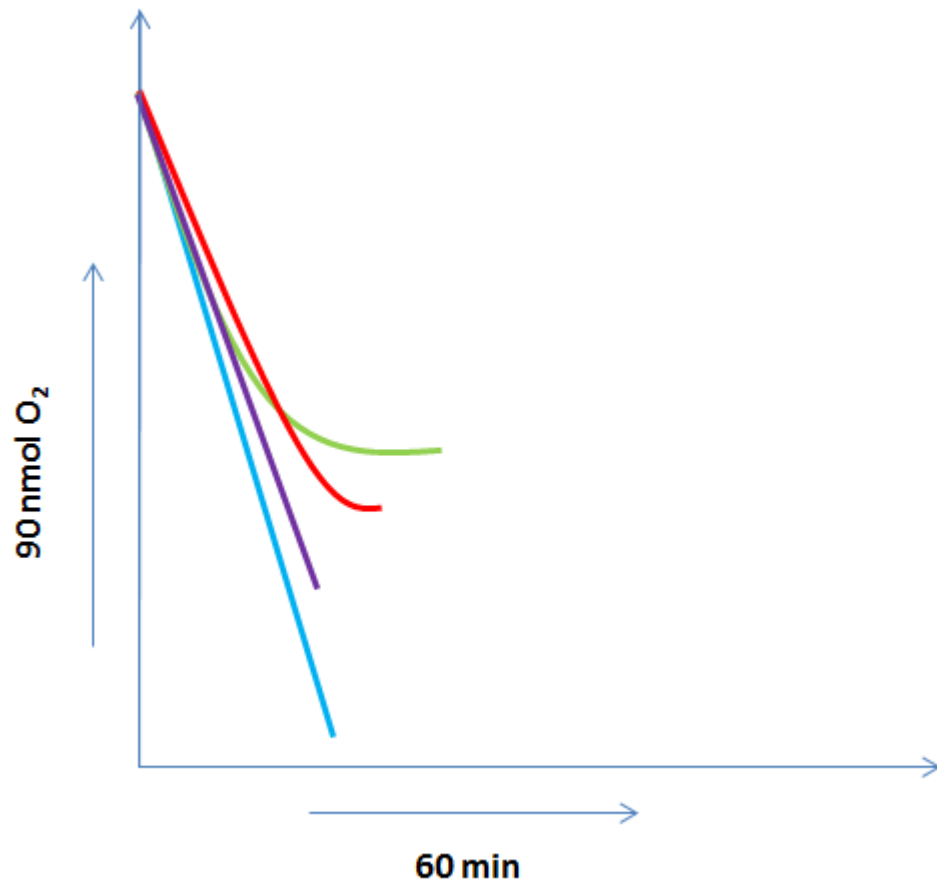


**Figure 4.4** The effect of ADP and FCCP on oxygen consumption by *T. thermophila* mitochondria. A typical oxygen electrode trace showing the rates of oxygen consumption in the mitochondria of *T. thermophila* in the presence of succinate (red line) only, 5 mM succinate + 0.06 mM ADP (green line), succinate and 1.25 nM FCCP (purple line) and succinate + ADP + FCCP (blue line) when added together in the reaction.

#### 4.2.4) Experiments in the presence and absence of phosphate using crude mitochondria

##### a) Respiratory measurements

As typical State 3 and State 4 were not observed in the mitochondria of *T. thermophila* (Figure 4.3), further experiments were designed in order to examine if the reduction in the rate of oxygen consumption in the absence of uncoupler was linked to low phosphate concentration in the reaction medium. The results showed that when  $\text{KH}_2\text{PO}_4$

was not included in the reaction medium, the rate of oxygen consumption with succinate was highest in the presence of both ADP and FCCP (Figure 4.5), while high rates were also observed when ADP and FCCP were added alone with succinate. The addition of the ATP synthase inhibitor oligomycin showed inhibition of oxygen consumption by *T. thermophila* mitochondria. This inhibition was similar in both the presence and absence of added ADP to the reaction (Figure 4.5). In contrast, the addition of  $\text{KH}_2\text{PO}_4$  to the reaction medium decreased the rates of oxygen consumption regardless of whether ADP, FCCP and oligomycin were added together or in combination (Figure 4.5).

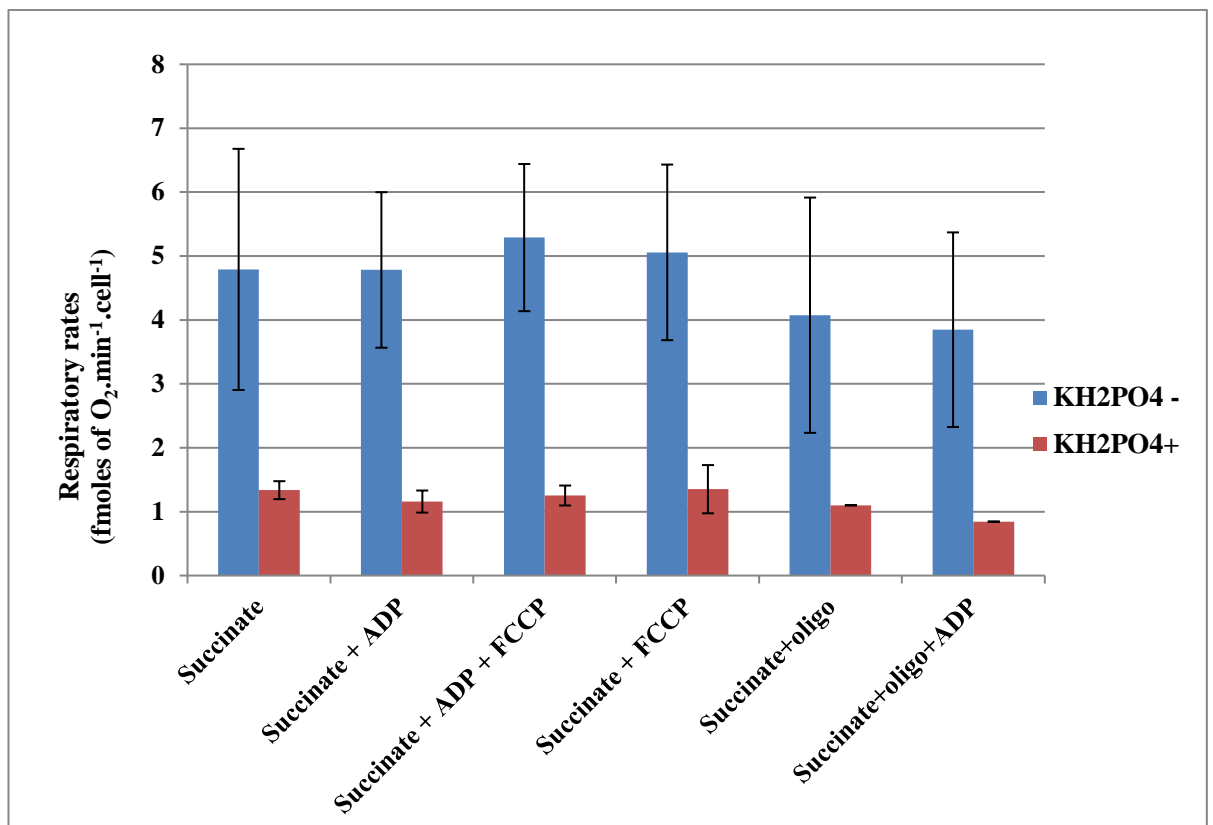


**Figure 4.5 Respiratory rates of *T. thermophila* mitochondria in the presence and absence of  $\text{KH}_2\text{PO}_4$ .** Average Oxygen consumption rates were measured in isolated *T. thermophila* mitochondria reaction media containing (red) or not containing (blue) 10 mM  $\text{KH}_2\text{PO}_4$  in the presence of 1.67 mM succinate, 0.06 mM ADP, 1.25 nM FCCP and oligomycin (0.0167 mg/mL) when added separately or in combination. Error bars represent  $\pm$  SEM (n=4).

The relative percentages of the oxygen consumption in the presence of these chemicals were also determined with respect to succinate (Figure 4.6). This data showed that when phosphate was absent in the reaction medium the rate of oxygen consumption when succinate was used as a substrate was highest in the presence of ADP and FCCP together. This rate was 30% higher than that of succinate only. There was a 5% and 20% increase in the oxygen consumption rate with ADP and FCCP respectively when added in two separate reactions in the presence of succinate as a substrate. The presence of  $\text{KH}_2\text{PO}_4$  decreased the overall rate of oxygen consumption (Figure 4.5). The oxygen consumption rate was reduced to 40% and 70% of the rate with succinate following the addition oligomycin in the absence and presence of  $\text{KH}_2\text{PO}_4$  respectively (Figure 4.6). A similar reduction was also observed when oligomycin was added in the presence of ADP (Figure 4.6).

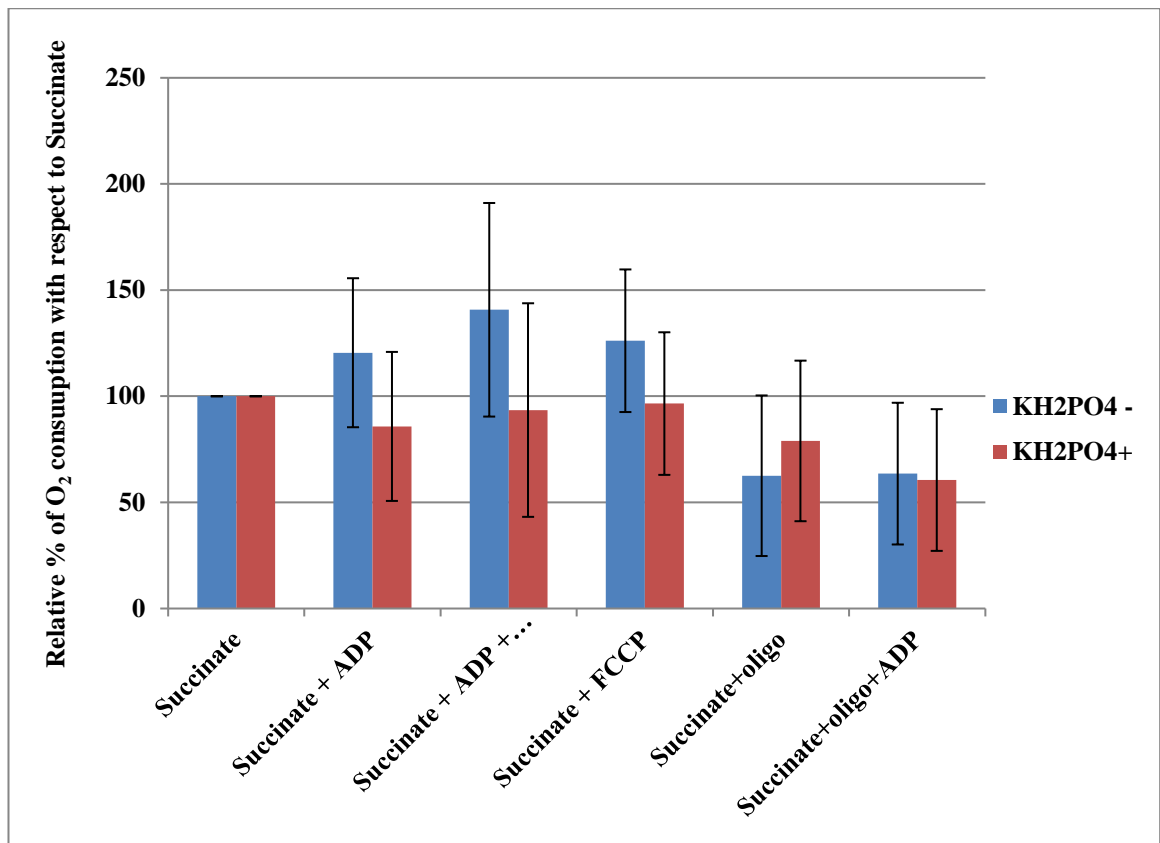


**Figure 4.6** The effect of ADP, FCCP and oligomycin on relative respiratory rates in the presence and absence of KH<sub>2</sub>PO<sub>4</sub>. Relative oxygen consumption rates in the presence (red) or absence (blue) of 10 mM KH<sub>2</sub>PO<sub>4</sub> with 1.67 mM succinate, 0.06 mM ADP, 1.25 nM FCCP and oligomycin (0.0167 mg/mL) added separately or in combination. All rates are normalised to corresponding rate with succinate. Error bars represent  $\pm$  standard deviation of the mean (n=4).

## b) Bioluminescent ATP assay/ Luciferase assay

To further investigate the function of the *T. thermophila* ATP synthase, experiments were carried out by directly measuring the ATP concentration at time points during oxygen consumption assays. Result showed that the presence of phosphate in the reaction medium in the absence of ADP not only decreased the overall rate of oxygen consumption (Figure 4.7) but also resulted in a net decrease in the ATP concentration (Figure 4.8), indicating that the rate of ATP hydrolysis in the presence of KH<sub>2</sub>PO<sub>4</sub> was greater than the rate of ATP synthesis. In contrast, in the absence of added KH<sub>2</sub>PO<sub>4</sub> there was a net increase in ATP concentration (Figure 4.7). When the mitochondria

were incubated with both succinate and ADP, although the respiratory rates were similar to succinate only, there was a net decrease in ATP concentration regardless of whether  $\text{KH}_2\text{PO}_4$  was present (Figure 4.8). This data indicated that the mitochondria of *T. thermophila* contained an ATP hydrolysing activity that was much greater than the ATP synthesising activity. This activity also affected the apparent P/O ratio which was near zero in case of succinate only and lower than zero when succinate and ADP were added together in the reaction medium (Figure 4.9).

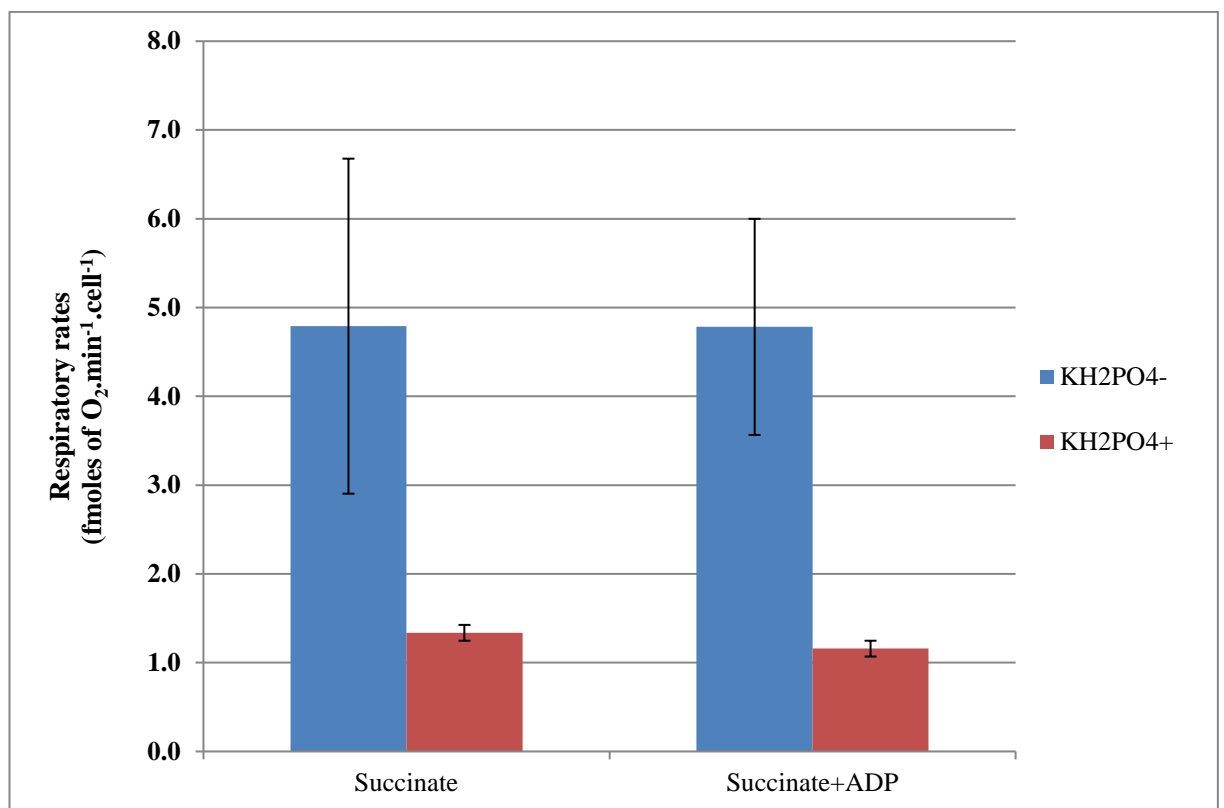


**Figure 4.7 Respiratory rates in *T. thermophila* mitochondria in the presence and absence of phosphate in the reaction medium.** Average Oxygen consumption rates were measured in isolated *T. thermophila* mitochondria reaction media containing (red) or not containing (blue) 10 mM  $\text{KH}_2\text{PO}_4$  in the presence of 1.67 mM succinate only and in combination with 0.06 mM ADP. Error bars represent  $\pm$  SEM (n=4).

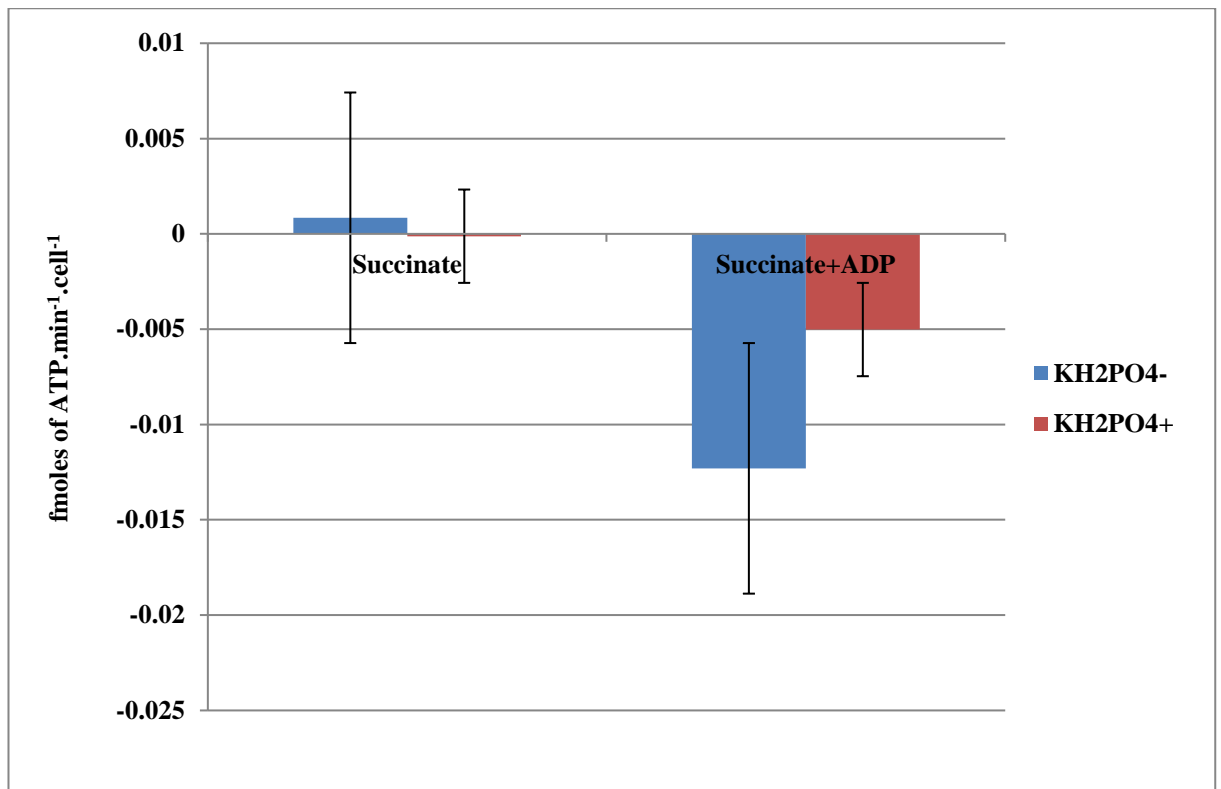


**Figure 4.8 Rate of ATP concentration change in *T. thermophila* mitochondria in the presence and absence of phosphate.** Average change in the rates of ATP concentration was measured in isolated *T. thermophila* mitochondria in reaction media containing (red) or not containing (blue) 10 mM KH<sub>2</sub>PO<sub>4</sub> in the presence of 1.67 mM succinate or 1.67 mM succinate and 0.06 mM ADP. Error bars represent ± SEM (n=4).

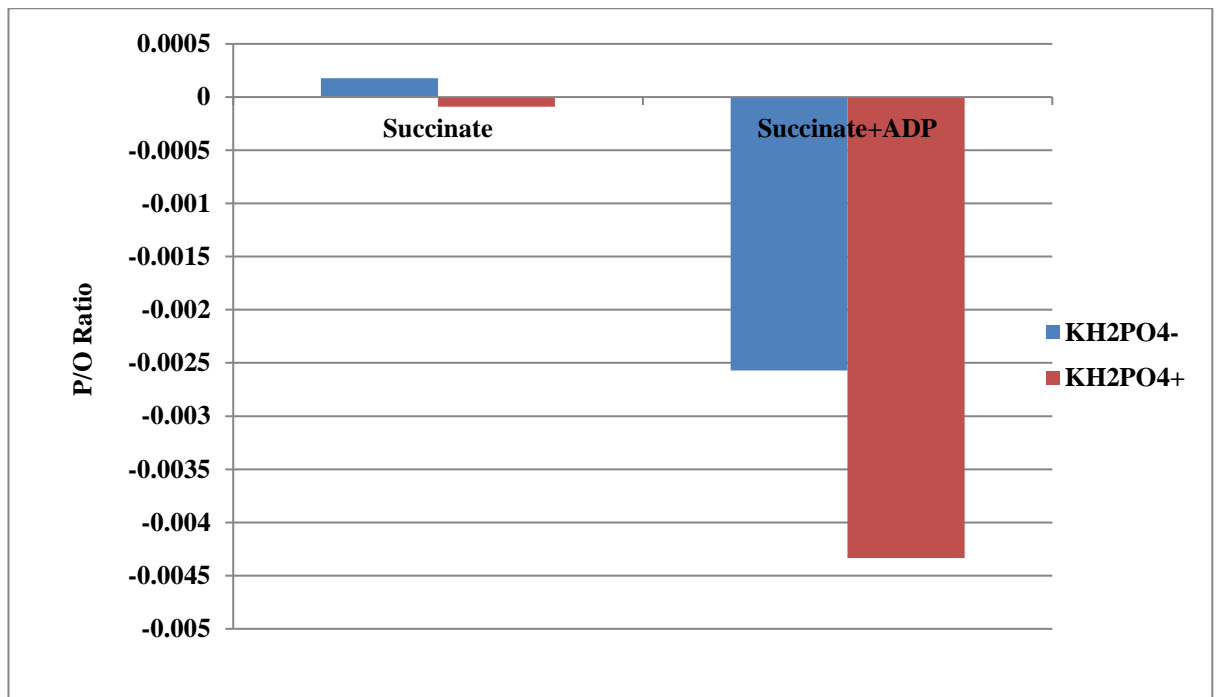


**Figure 4.9 P/O ratio for oxidative phosphorylation in *T. thermophila* mitochondria in the presence and absence of phosphate.** P/O ratio was measured in isolated *T. thermophila* mitochondria in reaction media containing (red) or not containing (blue) 10 mM KH<sub>2</sub>PO<sub>4</sub> in the presence of 1.67 mM succinate or 1.67 mM succinate and 0.06 mM ADP. Ratios were calculated from data presented in Figures 4.7 and 4.8.

#### **4.2.5) Effect of inhibitors and uncoupler on oxygen consumption**

The effect of the uncoupler FCCP and inhibitors KCN and oligomycin on respiration in the presence of succinate was measured. It was observed that the respiratory rate was enhanced by 33% when FCCP was added (Figure 4.10). In contrast, the addition of KCN decreased the respiratory rate by 68% (Figure 4.10). Oxygen consumption decreased 90% when oligomycin was added (Figure 4.10).

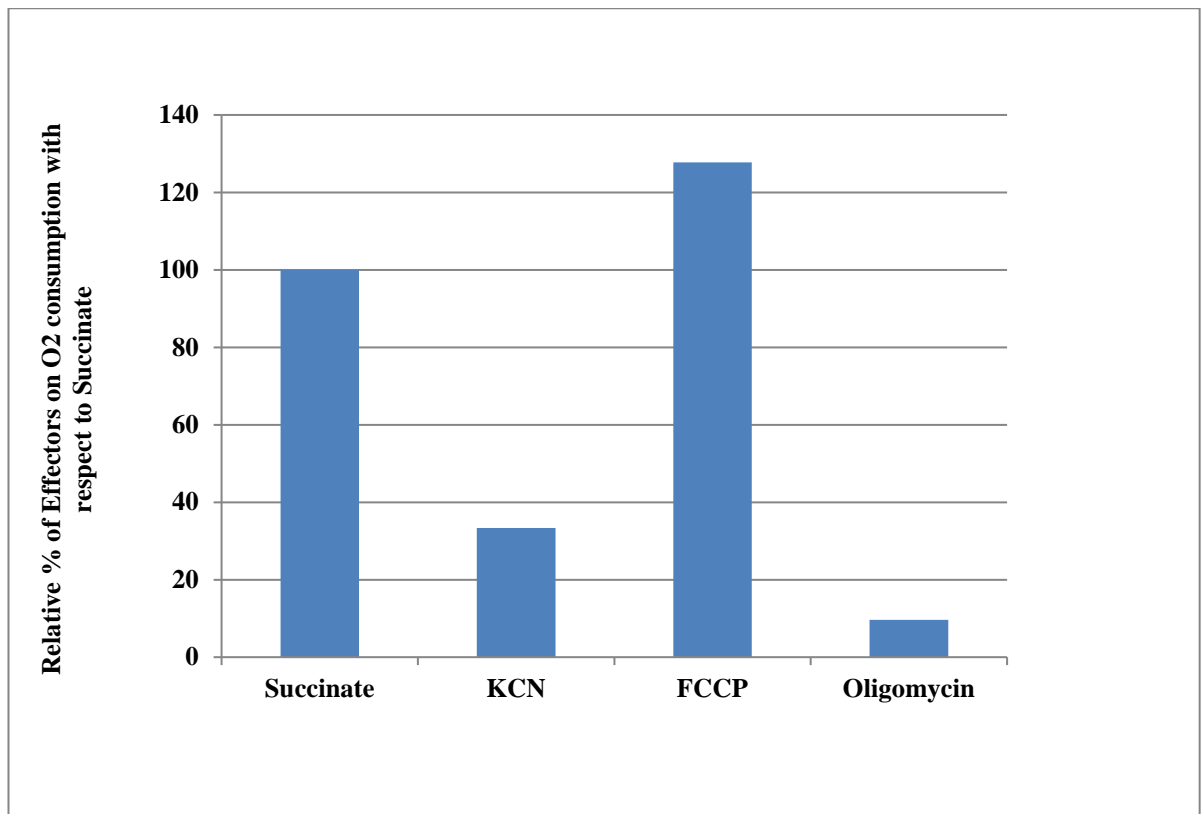


**Figure 4.10 The effect of KCN, FCCP and oligomycin on relative respiratory rates with succinate as substrate.** Relative oxygen consumption rates in the presence of 5 mM succinate with 0.83 mM KCN, 1.25 nM FCCP and oligomycin (0.0167 mg/mL) when added separately. All rates are normalised to the corresponding rate with succinate only. Results are representative, and repeated experiments showed the same effects.

## 4.2.6) Experiments using purified mitochondria from *T. thermophila*

### a) Respiratory measurements

In order to determine if mitochondrial activity was affected by an external ATP hydrolysing (ATPase) activity *T. thermophila*, a series of experiments were performed using Percoll purified mitochondria, from fractions two and three (which were shown in Chapter 3 to contain intact mitochondria). It was observed that out of four fractions obtained by Percoll gradient purification, oxygen consumption activity was highest in fraction two, while fraction three had a lower level of oxygen consumption (Figure

4.11). These experiments also showed that the timing of the addition of ADP could significantly affect the rate of oxygen consumption. The respiratory rate was higher when ADP was added at the same time as succinate compared to succinate alone. However, if the mitochondria were incubated with succinate for 5-10 minutes prior to the addition of ADP, the rate of respiration was about 60% lower than when succinate and ADP were added together (Figure 4.11).

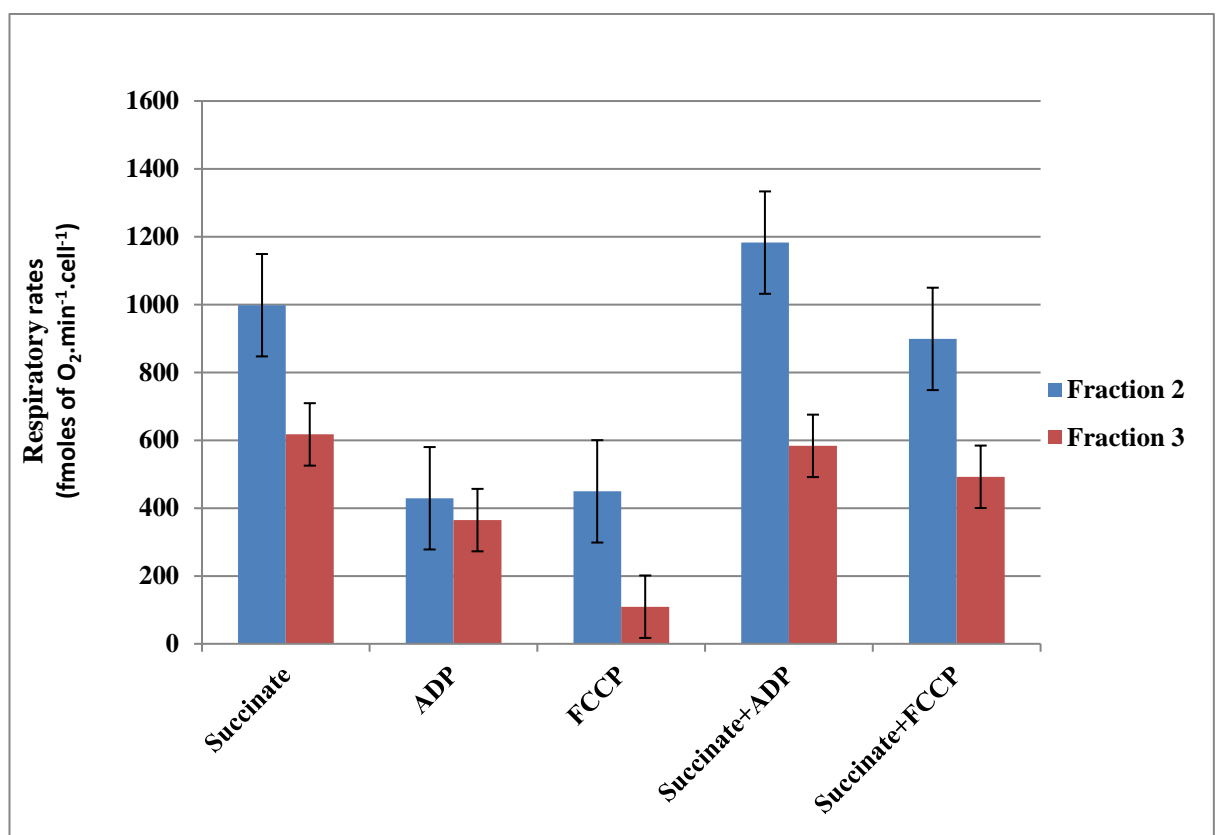


**Figure 4.11 Respiratory rates of Percoll gradient-purified *T. thermophila* mitochondria.** Average Oxygen consumption rates were measured in two fractions, fraction 2 (blue) and fraction 3 (red), from the Percoll gradient purified *T. thermophila* mitochondria using standard reaction media in the presence of 10 mM succinate, 0.06 mM ADP and 1.25 nM FCCP when added separately or in combination. Error bars represent  $\pm$  SEM (n=3).

## b) Bioluminescent ATP assay/luciferase assay

Respiratory measurements with Percoll purified mitochondria of *T. thermophila* showed that the fraction two had the highest rate of oxygen consumption (Figure 4.12). However, similar to crude mitochondria, a net increase in ATP concentration was only observed in the absence of ADP (Figure 4.13). Mitochondria from fraction three had the greatest level of ATP synthesis activity relative to the ATP hydrolysing activity. However the purification of mitochondria was not helpful in eliminating the ATPase activity. The apparent P/O ratio was also observed to be very small in the absence of ADP with purified mitochondria (Figure 4.14).

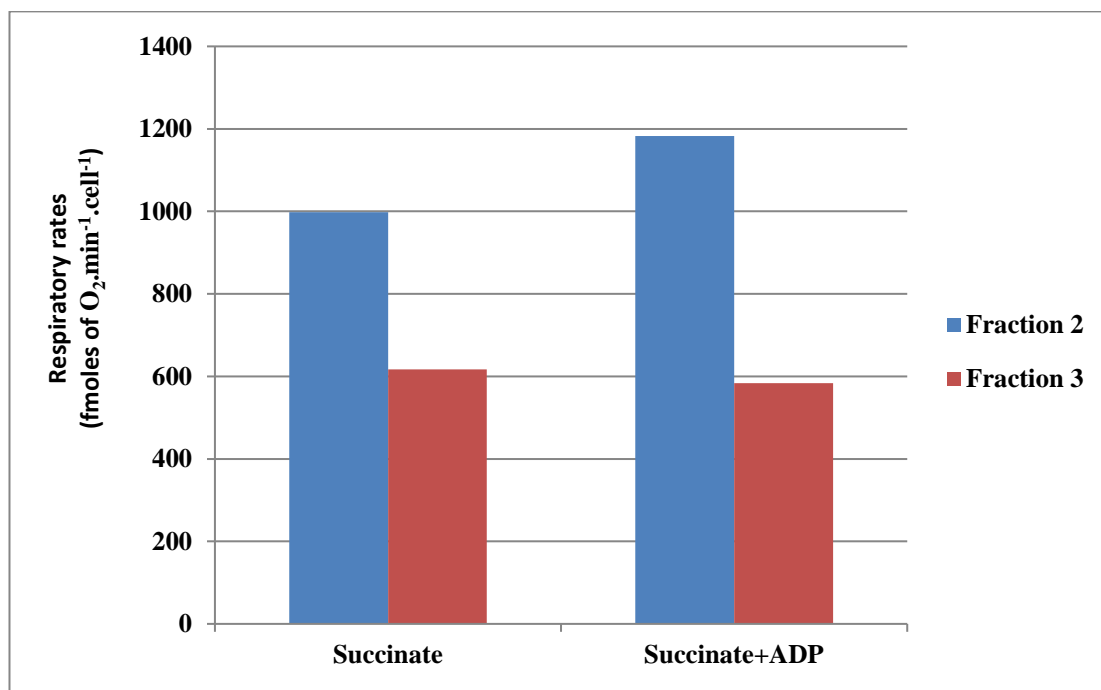


**Figure 4.12** Rate of oxygen consumption in the isolated fractions of percoll gradient-purified mitochondria of *T. thermophila*. Oxygen consumption rates were measured in two fractions of isolated purified *T. thermophila* mitochondria using standard reaction media in the presence of 10 mM succinate only or 10 mM succinate and 0.06 mM ADP. Results are representative, and repeated experiments showed the same effects.

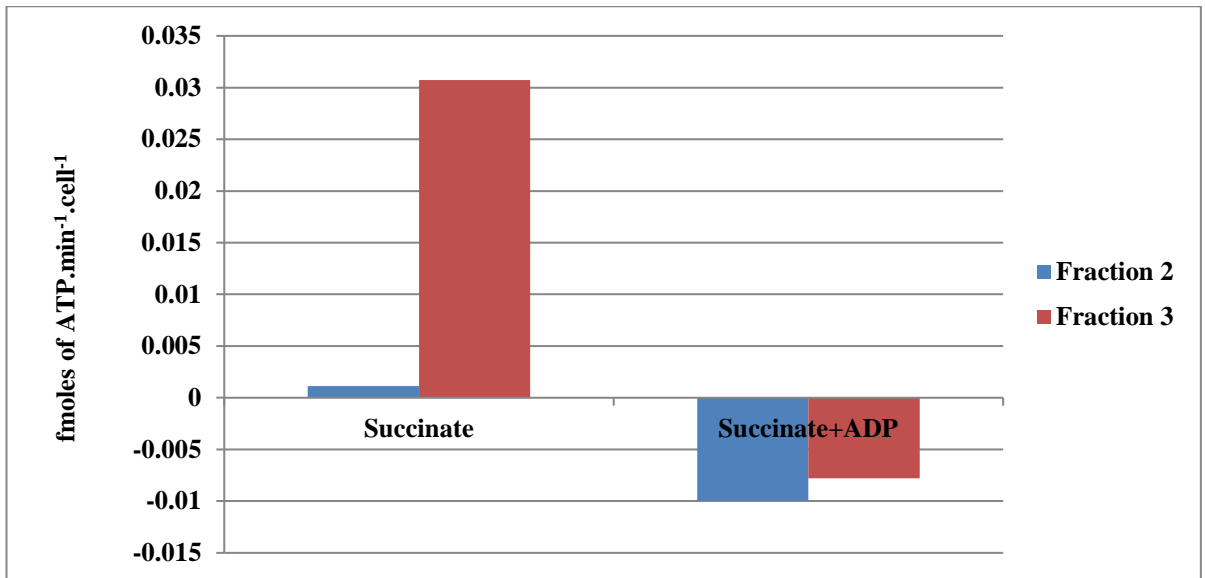


**Figure 4.13 ATP measurements in the percoll gradient-purified mitochondria of *T. thermophila*.** Rates of ATP synthesis were measured in two fractions of isolated purified *T. thermophila* mitochondria using standard reaction media in the presence of 10 mM succinate or 10 mM succinate and 0.06 mM ADP. Results are representative, and repeated experiments showed the same effects.

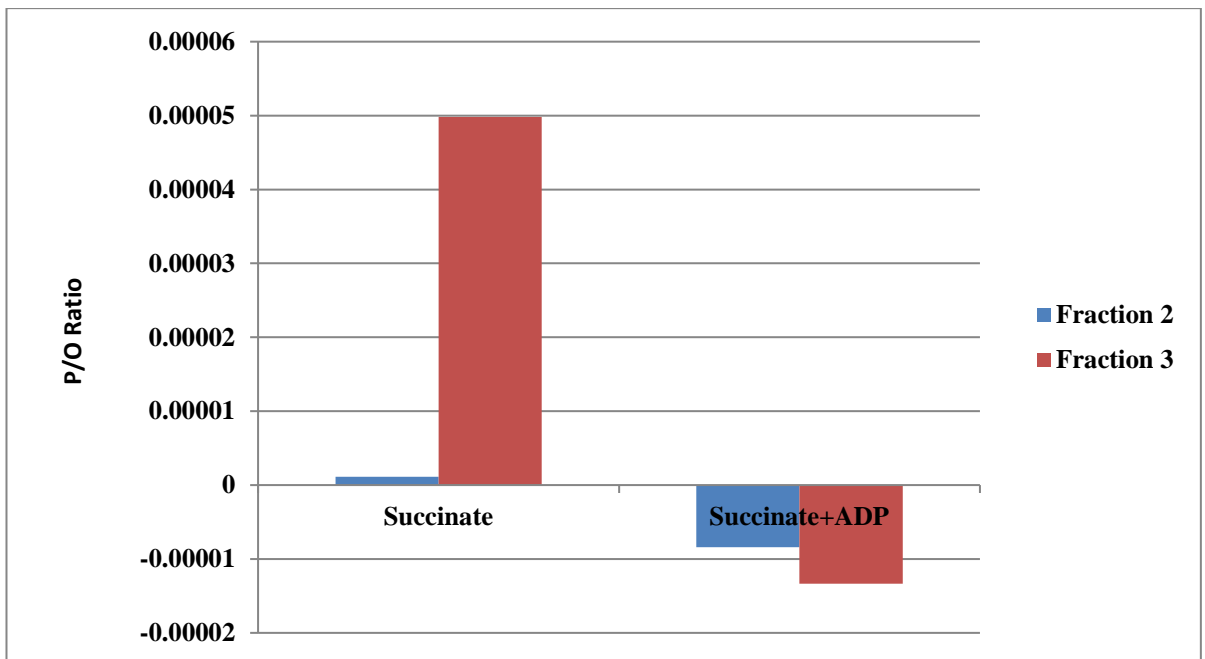


**Figure 4.14 Apparent P/O ratios in the Percoll gradient-purified mitochondria of *T. thermophila*.** P/O ratio was measured in two fractions of isolated purified *T. thermophila* mitochondria using standard reaction media in the presence of 10 mM succinate or 10 mM succinate and 0.06 mM ADP. Ratios were calculated from data presented in Figures 4.12 and 4.13.

#### **4.2.7) Measurement of ATP in crude mitochondria of *T. thermophila* in the presence and absence of phosphatase inhibitor cocktail (sodium fluoride, sodium orthovanadate, tetrasodium pyrophosphate)**

In order to eliminate the ATP hydrolysis activity from the mitochondria, an experiment was designed based on the use of a combination of phosphatase inhibitors in the reaction medium. Experiments were carried out by measuring the respiratory rates and changes in ATP concentration in the presence and absence of a phosphatase inhibitor cocktail. It was observed that the addition of a phosphatase inhibitor slightly reduced the rate of oxygen consumption (Figure 4.15). The oxygen consumption rates both with and without the phosphatase inhibitor cocktail, was higher in the presence of ADP than with succinate alone (Figure 4.15). This result agreed with previous findings when the standard reaction medium was used (Figure 4.5).

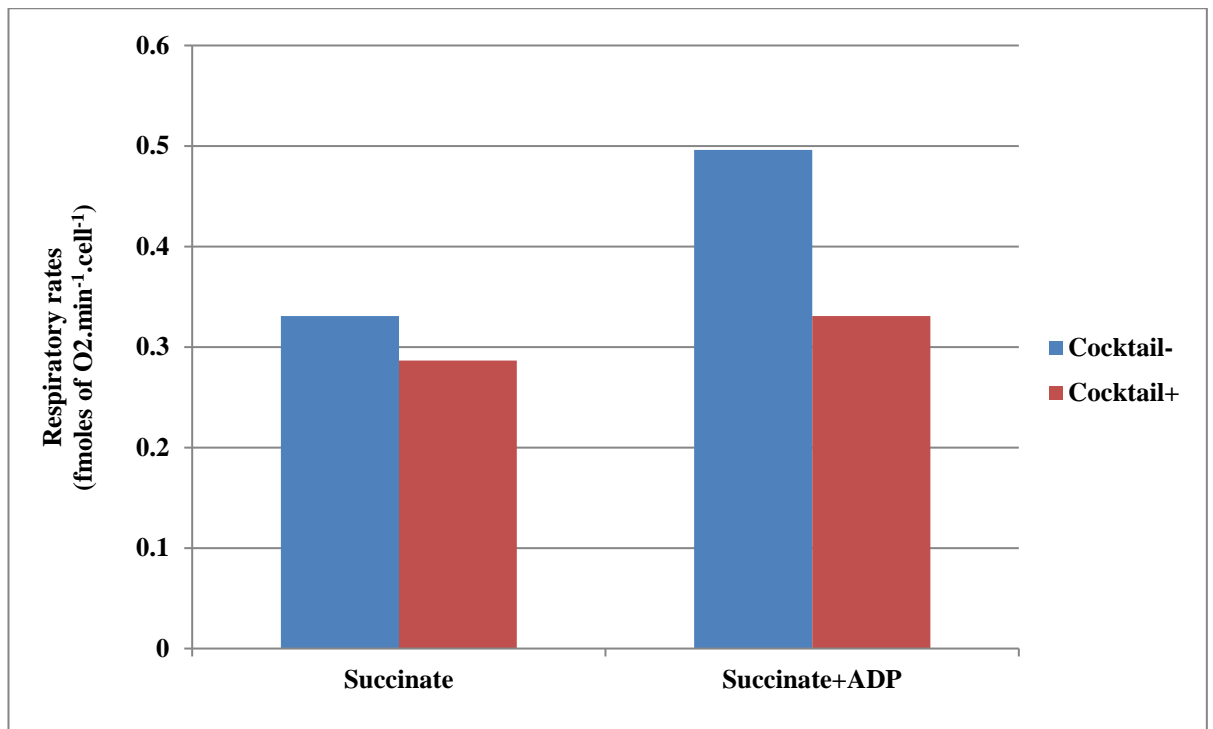


**Figure 4.15** Rate of oxygen consumption in the isolated crude mitochondria of *T. thermophila* in the presence and absence of phosphatase inhibitor cocktail. Reaction medium containing phosphatase inhibitor cocktail (red) or not (blue). Oxygen consumption rates were measured in isolated *T. thermophila* mitochondria in the presence of 10 mM succinate or 10 mM succinate and 0.06 mM ADP. Results are representative, and repeated experiments showed the same effects.

The increase in oxygen consumption rate in the presence of the phosphatase inhibitor (47%) was more marked than in its absence (17%). In line with this, the presence of the phosphatase inhibitor cocktail prevented a net decrease of ATP, and may have resulted in a net increase in the ATP concentration even in the presence of ADP (Figure 4.16). This indicates that phosphatase inhibitor cocktail inhibited the ATP hydrolysing activity to some extent. The P/O ratios under these conditions were lower than those normally expected from intact mitochondria with succinate as substrate (Figure 4.17), but were greatly improved in comparison with the previous findings in the absence of the cocktail (Figure 4.14).

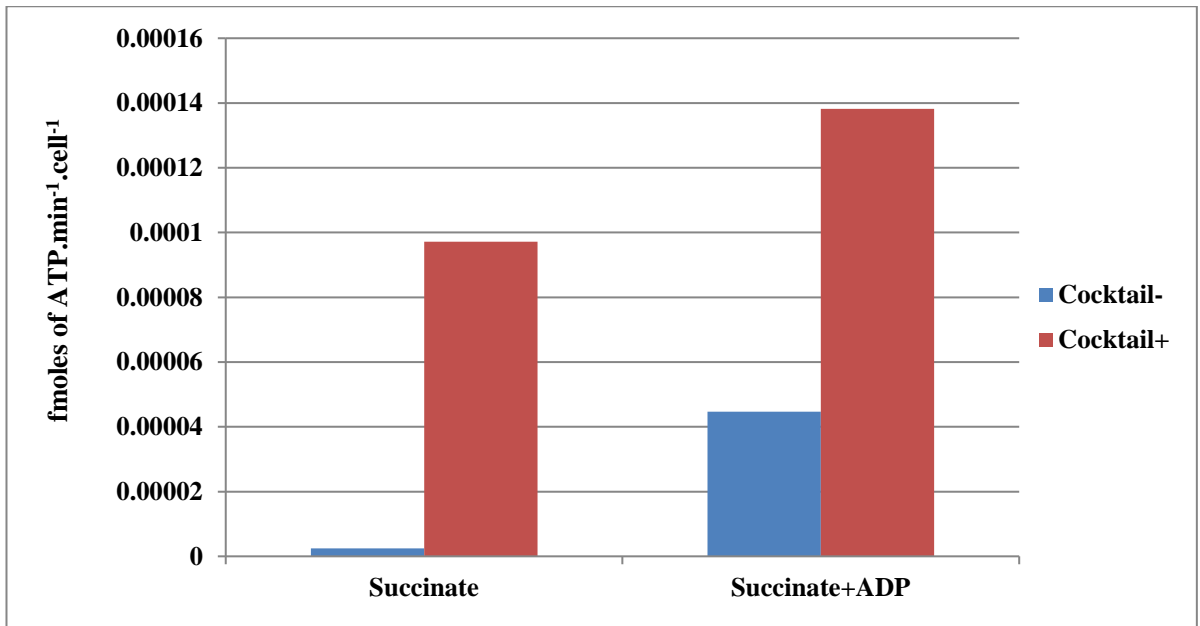


**Figure 4.16 Rate of ATP synthesis in crude *T. thermophila*. Mitochondria.** Reaction medium containing phosphatase inhibitor cocktail (red) or not (blue). Rates of ATP synthesis were measured in isolated *T. thermophila* mitochondria in the presence of 10 mM succinate or 10 mM succinate and 0.06 mM ADP. Results are representative, and repeated experiments showed the same effects.

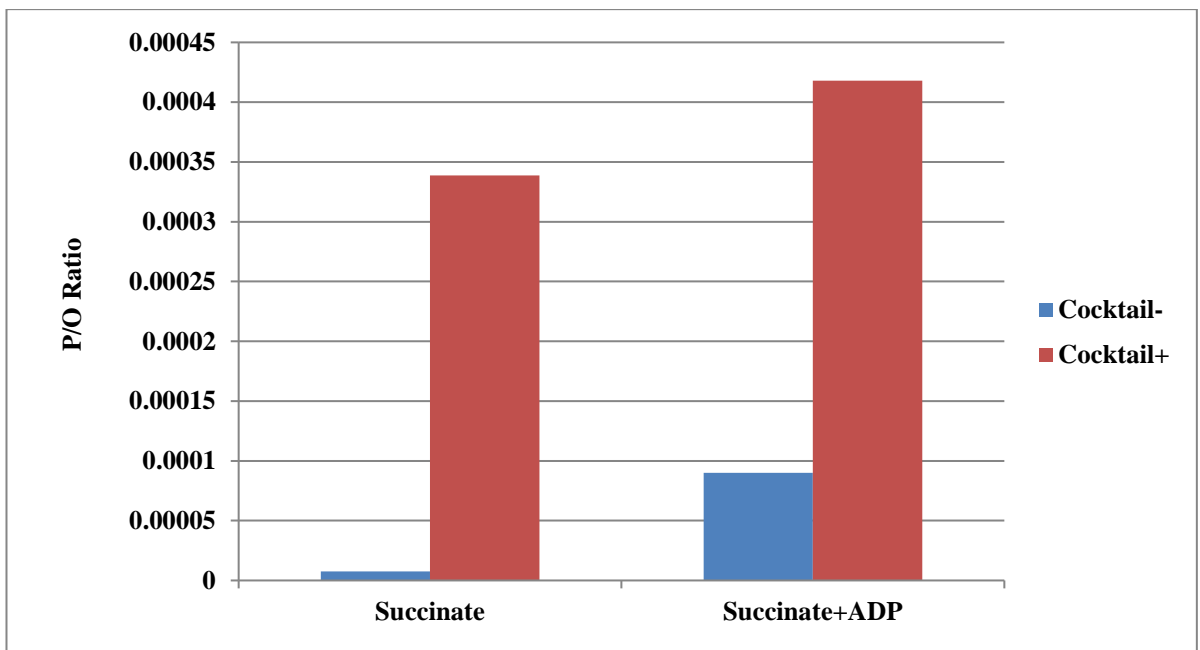


**Figure 4.17 P/O ratio in the isolated crude mitochondria of *T. thermophila*.** Reaction medium containing phosphatase inhibitor cocktail (red) or not (blue). P/O ratio was calculated in isolated *T. thermophila* mitochondria in the presence of 10 mM succinate or 10 mM succinate and 0.06 mM ADP. Ratios were calculated from data presented in Figures 4.15 and 4.16.

### 4.3) Discussion

Respiratory measurements were carried out in order to investigate the functionality of the electron transport chain (ETC) in the mitochondria of *Tetrahymena thermophila*. The data presented here shows that the mitochondria are capable of synthesising ATP, however to measure this ATP synthesis a contaminating phosphatase activity must be removed or inhibited. This indicates that a functional ATP synthase is present, as is a functional electron transport chain, despite missing genes (Eisen 2006). It is also in agreement with data from other alveolate species, including dinoflagellates and apicomplexa (Mogi and Kita, 2009). Like apicomplexan, dinoflagellates have also missing pyruvate dehydrogenase but still possess the functional TCA in their mitochondria (Danne, 2013). Similarly Butterfield *et al* (2013) analysed dinoflagellates EST (Expressed sequence tag) data where they reported the presence of a bacterial origin subunit in place of a key subunit ( $E_1$ ) of pyruvate dehydrogenase. These findings are also in broad agreement with early biochemical analyses of ciliate mitochondria (Turner, 1971) (Conklin 1972).

Amongst the different natural respiratory substrates tested in this experiment, succinate proved to be the best substrate with the highest rate of oxygen consumption. In comparison, malate showed the second highest respiratory rate. NADH and isocitrate had almost no or very little effect on the oxygen consumption, and may indicate that the enzymes responsible for oxidation of these substrates are absent or in extremely low abundance in *T. thermophila* mitochondria. Hence these are not suitable substrates for respiratory measurements. The high respiratory rate with TMPD-ascorbate showed that it can be used as a good substrate where respiratory measurements are based on the activity of complex IV in the electron transport chain.

The addition of ADP with succinate, isocitrate and TMPD-ascorbate enhanced the rate of oxygen consumption but had no effect when NADH and malate were used as substrate. In the research presented here, following the addition of small amounts of ADP, typical transitions from respiratory state 3 to state 4 were not observed. Although initially rapid, the rate of oxygen consumption with succinate as a substrate decreased over time. This effect was independent of the presence or absence of ADP, but could be eliminated by the addition of the uncoupler FCCP. It was therefore hypothesised that this reduction in oxygen consumption was mediated by a change in the ability of the ATP synthase to dissipate the transmembrane proton gradient. This was further supported by the finding that oligomycin inhibited the rate of respiration by up to 90% (Figure 4.10). Oligomycin specifically binds to the OSCP subunit of ATP synthase (complex V) inhibiting rotational catalysis and therefore proton translocation in the presence of ADP and Pi by ATP synthase (Ko *et al.*, 2003). This could suggest that the proton pore through the ATP synthase is the major route of proton flow into the mitochondrial matrix. Variation (15-90%) in inhibition of respiration by oligomycin observed with different preparations most likely varies due to the degree of coupling the mitochondria exhibit with highly coupled mitochondria being particularly sensitive to oligomycin.

In order to answer whether the decrease in respiratory rate over time in the absence of FCCP was due to a reduction in the inorganic phosphate concentration, experiments were performed in the presence and absence of phosphate in the reaction medium. The rate of oxygen consumption was greatly reduced if phosphate was present. This is most likely due to the phosphate affecting the dicarboxylate carrier (DIC) which is an antiporter which transports succinate (dicarboxylic acid) across the mitochondrial membrane in exchange for phosphate (Kolarov *et al.*, 1972) (Lancar-Benba *et al.*, 1996). Therefore, increasing the phosphate concentration outside the mitochondria

results in a reduction of the succinate concentration in the matrix which in turn decreases the rate of oxygen consumption. This phosphate inhibition of succinate oxidation has been previously observed in mammalian mitochondria (Johnson and Chappell, 1974) Together, these observations strongly suggest that the inner mitochondrial membrane of the purified mitochondria was intact, preventing the free exchange of both succinate and protons between the matrix and the intermembrane space. The initial aim of adding  $\text{KH}_2\text{PO}_4$  was to determine if phosphorylation was being inhibited by a lack of phosphate. However, although it is evident that phosphorylation was occurring without the addition of phosphate, from the experiments conducted it is unclear whether at lower concentrations ( $<1$  mM) of phosphate may have enhanced the respiratory rates.

In order to understand the function of ATP synthase in *T. thermophila* mitochondria, ATP measurements were carried out. Results showed that in a reaction where succinate was used as a substrate with isolated crude mitochondria, there was a net increase in ATP synthesis while the P/O ratio was nearly zero. While the addition of ADP resulted in the faster rate of ATP hydrolysis with P/O ratio lower than zero. To answer whether this decrease in the rate was due to a limited phosphate supply, the experiments were repeated with the further addition of phosphate in the reaction medium. As a result, a faster rate of ATP hydrolysis was observed. Therefore experiments were conducted to remove the phosphatase activity in the mitochondria of *T. thermophila*. For this purpose, gradient purified mitochondria were used. After observing the obtained fractions by electron microscopy, fraction two and fraction three were used in an ATP synthesis activity assay. The findings showed that the rate of ATP synthesis was higher in fraction three when succinate was used as substrate while P/O ratio was very small. When ADP was added to the reaction medium, the rate of ATP synthesis was much

reduced, with a P/O ratio lower than zero suggesting that the rate of ATP hydrolysing activity was higher than the rate of ATP synthesis.

Further experiments were therefore designed to eliminate the ATPase activity from the mitochondria of *T. thermophila*. A set of a combination of phosphatase inhibitors was used for this purpose. The data obtained showed that the presence of a phosphatase inhibitor cocktail enhanced the rate of ATP synthesis when only succinate was added. This rate was elevated when succinate and ADP were used together in another experiment. Small increases in both P/O ratios were observed in comparison to when no inhibitor cocktail was added. This suggests that the phosphatase inhibitor cocktail was able to greatly reduce the phosphatase activity, though it was not able to stop it completely. These results strongly suggest that the mitochondria of *T. thermophila* have an external ATPase activity which is greater than the rate of ATP synthesis.

#### **4.4) Conclusion**

In conclusion, this study showed that the mitochondria isolated from the ciliate *Tertahymena thermophila* had an intact inner mitochondrial membrane which facilitates the coupling of mitochondrial electron transport to ATP synthesis. A functional ATP synthase which synthesizes ATP was identified, as should be expected for typical eukaryotic mitochondria. In addition, it was found that *T. thermophila* mitochondria have an ATP hydrolysing activity, which was unexpected.

# Chapter 5

## Identification of mitochondrial ATP synthase subunits of *T. thermophila*

### 5.1) Introduction

ATP synthase is the final complex of the mitochondrial oxidative phosphorylation chain. It is one of five enzymes complexes associated with the electron transport chain (ETC) and is located in the inner membrane of mitochondria. There are numerous copies of each electron transport chain component within a single mitochondrion. A serial transfer of electrons through the four enzymes complexes (complexes I-IV) occurs, accompanied by the build-up of a proton gradient in the inter-membrane space. The ATP synthase complex carries out the translocation of protons from the inter-membrane space to the mitochondrial matrix, with the consequence that ATP is synthesised from ADP and inorganic phosphate. These ATP molecules act as a fuel for the biosynthetic functions of the cell (Figure 1.2, section 1.3).

ATP synthase (which is more formally known as F-type ATP synthase (Futai *et al*, 1989)) consists of two domains, F<sub>o</sub> and F<sub>1</sub>. The F<sub>o</sub> domain is membrane bound and contains several subunits including a, b, c and OSCP (oligomycin sensitivity conferring protein) (Figure 5.1).

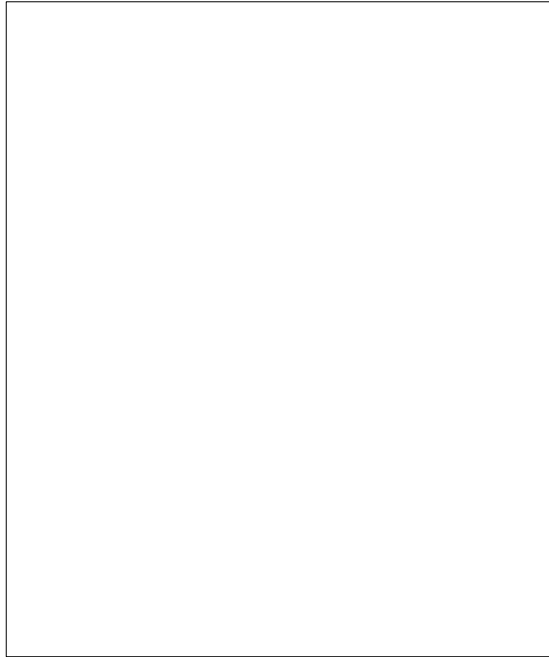


**Figure 5.1 Eukaryotic mitochondrial ATP synthase (Gledhill and Walker, 2006)**

In contrast, the  $F_1$  subunits protrude into the matrix and consist of nine subunits of five different types which include  $\alpha_3$ ,  $\beta_3$ ,  $\gamma$ ,  $\delta$ ,  $\epsilon$  in bovine ATP synthase (Stock, 1999). Note that bacterial ATP synthase subunits have similar, but different names, with some proteins having two distinct names, and some names being used for different proteins. Eukaryotic nomenclature will be used in this chapter. Table 1 shows the expected size of each subunit, based on the mammalian ATP synthase.

**Table 1** Expected size of each subunit, based on the mammalian ATP synthase.

<b>Subunits</b>	<b>Size kDa</b>	<b>Subunits</b>	<b>Size kDa</b>
<b><math>\alpha</math></b>	60	<b>c</b>	14
<b><math>\beta</math></b>	57	<b>d</b>	18
<b><math>\gamma</math></b>	33	<b>e</b>	8
<b><math>\delta</math></b>	17	<b>f6</b>	13
<b><math>\epsilon</math></b>	6	<b>g</b>	13
<b>a</b>	25	<b>a6L</b>	8
<b>b</b>	29		

ATP synthase is found across all alveolate species and has been shown to be active (Nina, 2011; Uyemura, 2004; Strum, 2015). For example, Nina *et al* (2011) reported the presence of ATP synthase in the mitochondrion of *P. falciparum* in a dimeric form. In apicomplexa, Uyemura (2004) have shown that the electron transport chain is essential in *Plasmodium* species. The ciliate *T. thermophila* also contains a functional ATP synthase as the addition of oligomycin prevented the synthesis of ATP.

Several of the genes for the main subunits of ATP synthase are not identifiable by sequence homology in any of the alveolate species for which genome or EST sequence is available. These subunits play a pivotal role in the function of ATP synthase. For example, the *Plasmodium* parasite does not appear to contain the genes necessary for functional ATP synthase on either the nuclear or the mitochondrial genomes (Gardner *et al*, 2002; Carlton *et al*, 2002; Vaidya and Mather, 2005). It was initially thought that the parasite could fulfil its ATP requirement mainly with glycolysis (Carlton *et al*, 2002). Although there are genes which code for a well conserved F<sub>1</sub> domain, the parasite appears to lack many F<sub>0</sub> subunits including *b*, *d* and F<sub>6</sub>. The key subunit *a* of the F<sub>0</sub> region, which is essential for proton translocation in ATP synthase, also appears to be missing (Gardner *et al*, 2002). However, as *Plasmodium* mitochondria contain a functional electron transport chain which is linked to oxidative phosphorylation and a mitochondrial proton gradient, the ATP synthase complex must be functional (Uyemura, 2004; Painter, 2007). Mogi *et al* (2009) identified potential candidates for various F<sub>1</sub> subunits ( $\alpha$ ,  $\beta$ ,  $\gamma$ ,  $\delta$ ,  $\epsilon$ ) and F<sub>0</sub> subunits (*a*, *b*, *c*, and *d*) in *Plasmodium* spp. using a bioinformatics approach. This suggests that *Plasmodium* mitochondria may contains some alternative, highly divergent proteins to fulfil the roles of the apparently missing proteins, in order to create a functional ATP synthase.

As *Plasmodium* has only one mitochondrion per cell, this limits the amount of material that can be obtained without undertaking large-scale cell culture. As a result, very little biochemical information is known about the ATP synthase of this parasite. Therefore in this study the ciliate *T. thermophila* is used as a model organism to study mitochondrial ATP synthase in species belonging to the super phylum Alveolata, which includes *T. thermophila* and *Plasmodium*. *T. thermophila* has 800 mitochondria per cell (Hill, 1972) and like other members of the same group; *T. thermophila* is also apparently missing genes for the same subunits as *Plasmodium*.

Nina *et al* (2010) purified ATP synthase from the alveolate *T. thermophila* in order to identify the apparently missing subunits of ATP synthase. They purified *T. thermophila* mitochondria by using sucrose gradient centrifugation and also permeabilized mitochondria using Digitonin. Following blue native gel electrophoresis, Nina *et al.* (2010) electro-eluted the ATP synthase complex from the gel. The results showed that ATP synthase in *T. thermophila* is a large complex. Nina *et al* (2010) identified three bands corresponding to ATPase activity which were excised from the blue native gel and subjected these to trypsin/chymotrypsin digestion followed by Liquid chromatography-tandem mass spectrometry (LC/MS/MS). In the analysis of this data, Nina *et al* (2010) identified six orthologues of ATP synthase subunits and 13 novel proteins were identified which are ciliate specific and not found in other alveolates species.

One of the missing proteins is subunit a, which contains five transmembrane helices, and is responsible for formation of a proton channel and passing H<sup>+</sup> to the c subunit. A putative protein Ymf66 was identified as a potential candidate for the missing a subunit in *T. thermophila*. Nina *et al* (2010) reported that this protein contains multiple

transmembrane domains, and an important arginine residue consistent with the features expected of the a subunit Figure 5.2a.

However, the situation may not be as clear-cut. Firstly, the identified protein is significantly larger than conventional a subunits at 446 aa vs 226aa (*Homo sapiens*). Secondly, an alignment with human, maize and *E. coli* a subunit residues shows that the conserved arginine residue (R210, *E. coli* numbering) is not conserved. In addition, an alignment of the full protein shows that it shares little sequence homology to other a subunits (Figure 5.2b). Finally, all a subunits contain 5 trans-membrane helices. A TMMpred analysis of the Nina *et al* (2010) subunit Ymf66 reveals this protein to contain 8 transmembrane helices.

**a)**



b)

```

Human_a : -----*-----20-----*-----40-----*----- : -
Maize_a : -MMMTRWSSTDMKRRNRILANMVPPIRNLSLPDYEEYEEEEYHPVSREATR : 49
E_coli_a : ----- : -
YMF66 : MGRENVLPVHNDVYEDFVFTTPYFQPESTFKSVPKLFSDDLGGVVEWVYT : 50

Human_a : -----60-----*-----80-----*-----100----- : 5
Maize_a : GVCILLRIDRYLSSIGRSIQDREVLRDFCQRLLFPQREAGHSFSEIYDDI : 99
E_coli_a : -----MASENMTPQDYIGHHLNQLDL : 23
YMF66 : TSESVLAYDYKLWYLWVSGVSNLDESDFMFFNQYWALSLSLSTSVFQLFYAVI : 100

Human_a : -----*-----120-----*-----140-----*----- : 16
Maize_a : FASFIAPTILG-----RAHGVEASRLGQPLRDLYDEMERNGEIVNNGSIIIPEGGGPVPT--ESPLD : 147
E_coli_a : RTFSLVDP-----QNPFA : 36
YMF66 : LDRYLSVLFQNTFYTNDWFRMMLHSEKETALIWLHYFELSWHINGLNQFFT : 150

Human_a : -----160-----*-----180-----*-----200----- : 34
Maize_a : QFGIHPILDNLIGKYYVSFTNLSLSMLLTIGLVLIVFVVTKKGGGKSV : 196
E_coli_a : TF-----WTINIDSMFFS-----VVLGLLFLVLF-----RSVAKKA : 67
YMF66 : FYGGILEFVYFDKSNPDMCIHVHTLWIHLILFLIFTGFVTILFSFYGN : 200
f 1 L L

Human_a : -----*-----220-----*-----240-----*----- : 84
Maize_a : KYLINNRLITTQQWLIKLTSKQMMTMHNTKGRTWLSMLVSLIIFIATNLI : 246
Maize_a : PNAFQSLVELIYDFVPNLVNEQIGGLSGNVKHKFFPCISVTFPSLFRNP : 246
E_coli_a : TSGVPGKFQTAIELVIGFVNGSVKDMYHGKSKLIAPLALTFVWVFLMLI : 117
YMF66 : PNTEENTIDSDYLAASGTVEAEKEITSIDDYLGVLVFAIAYVGVFFVYHG : 250
v f n

Human_a : -----260-----*-----280-----*-----300----- : 118
Maize_a : -----LGLLPHSFTPTTQLSMNLAAMAIPLWACTVIMGFR : 280
E_coli_a : MDLLPIDLLPYIAEHVLCIPALRVVPSADVNVTLISMAIGVFIILFYSIK : 167
YMF66 : -----WTSMLSHAVILLSCYSIIIMFLFILGMPITLLLYDFGFFFLAYL : 293
lgl s l gi

Human_a : -----*-----320-----*-----340-----*----- : 156
Maize_a : SKIKNALAHFIPQG--TPTPLIP-----MLVLIETISLIQEMAL : 318
Maize_a : RHGLHFFSFLIPAG--VPLPIAP-----FLVILPLISHCFRALSS : 318
E_coli_a : MKGIGGFTKEITLQPFNHWAFIP-----VNLILEGVSLSKPVSIL : 207
YMF66 : KGAGKYISSVAEMMFDTACTVIFYIRILAQWIRVVLVVVFISLSHYVSD : 343
l l p e s l s

Human_a : -----360-----*-----380-----*-----400----- : 197
Maize_a : AVR---LTANITAGHLLMHLIGSATLAMSTINIP-----STLIIFTILI : 363
Maize_a : GIR---LFANMMAGHSSVKILSGFA--WTMLFINNIFYFLGDLGPLFIVL : 363
E_coli_a : GLR---LFGNMYAGELIFILIAGLLPWWSQWILN-----VPWAIFHIL : 247
YMF66 : FDITNSALIGSENQSDSMNELNTNFSMTYYILTVPVPGKFIYWIYEILHTF : 393
r l n ag l

Human_a : -----*-----420-----*-----440-----*----- : 226
Maize_a : LLTILEIAVALIQAYVFTLLVSLYIHDNT----- : 410
Maize_a : ALTGLELGVAISCAHVSTISICIIYINDATNLHQNESFHNCKTRRSQS--- : 410
E_coli_a : IIT-----LQAFIEMVLTIVYISMASEEH----- : 271
YMF66 : FVVCNQFVAFFAIVFWLFLFLYTFYIIEKHEDFFSKKREERKKKLKLWN : 443
t qa yl

Human_a : --- : -
Maize_a : --- : -
E_coli_a : --- : -
YMF66 : LKN : 446

```

**Figure 5.2 (overleaf) Alignment of a conserved region of ATP synthase a subunits and the *T. thermophila* Ymf66 a-like protein.** In *E. coli*, the conserved arginine R210 is a key residue, and is embedded in the C-terminal transmembrane helix of the a subunit. Alignment (a) as published by Nina *et al* (2010), conserved residues in green and b) a full alignment using T-Coffee. Yellow residues are conserved in two species, green residues in three and blue residues across all four species.

It also is interesting to note that Ymf66 was not identified in non-ciliate alveolate species, despite the protein apparently playing a key role in ATP synthesis. While it is possible that each alveolate lineage evolved a different replacement protein for subunit a (and other missing proteins), the simplest explanation is that all alveolates share the same replacement proteins. The discovery that different sub-groups of the Alveolata have evolved independent  $F_0$  architecture is surprising. Given that it does not meet Occam's razor, and that the proposed protein is too large, seemingly missing the conserved R210 residue and has too many transmembrane helices. Therefore independent confirmation of the role of Ymf66 is necessary.

The aim of the research presented here is to purify the ATP synthase from the mitochondria of *T. thermophila* and to investigate its subunit composition in order to confirm the presence of Ymf66 or identify other proteins that are substituting for the apparently missing subunits. In contrast to the Nina *et al* (2010) protocol, the complex will be isolated using a variety of pull-down methods in order to ensure that identified proteins are specific to ATP synthase. Three different biochemical pull-down techniques will be used: with a specific antibody, using an inhibitor protein and following chemical crosslinking. Mammalian ATP synthases are inhibited by the inhibitor protein, which binds to the F1 domain (Cabezón, 2003), preventing hydrolysis and synthesis of ATP. A pull-down assay using recombinant inhibitor protein (IF1) fused to GFP was successful in isolating bovine ATP synthase (Bason 2011). Although there is no ciliate inhibitor protein, the significant conservation of ATP synthase structure across all eukaryotes means that it is likely that a mammalian inhibitor protein would inhibit ciliate ATP synthase.

Here, I present data showing that the proteins identified by Nina *et al* (2010) were not identified, and instead present evidence for a novel a subunit, conserved across all alveolates. I also present evidence for the identification of a putative b subunit, which has not previously been identified in ciliates. The ciliate ATP synthase complex was successfully isolated using the mammalian inhibitor protein. This is the first use of the inhibitor protein to pull down the ATP synthase complex in a lineage that does not have an inhibitor protein, so the work presented here presents a new molecular tool.

## **5.2) Results**

### **5.2.1) Production and purification of the inhibitor protein IF<sub>1-60</sub>-His**

The plasmid pRun-IF1-60-His (containing the bovine inhibitor protein fused to a his-tag, Bason, 2011) was used to transform *E. coli* BL21 (DE3). The plasmid was extracted and the DNA concentration was measured as 162 ng/μl. After analysis of the plasmid using agarose gel electrophoresis it was observed that the larger band in the digested sample was consistent with the pRun vector at approximately 2500 bp while the smaller band (800 bp) was consistent with the IF<sub>1-60</sub>-His insert (198bp) plus 600bp of the vector. This plasmid was used for all later protein expression. The inhibitor protein was purified through a nickel affinity column using fast protein liquid chromatography (FPLC) (Section 2, Figure 2.2). The final protein concentration was found to be 11.87 mg/mL. This purified inhibitor protein was stored at -20 °C until required. SDS-PAGE was used to confirm the presence of purified IF<sub>1-60</sub>-His, as shown in section 2, Figure 2.3. Several bands were observed including some contaminating proteins. However, the dominant band observed at 26KDa, was as expected for the successful purification of IF<sub>1-60</sub>-His (section 2, Figure 2.3).

## **5.2.2) *T. thermophila* ATP synthase pull down techniques**

Three different techniques were used to pull down the ATP synthase complex from *T. thermophila*. The first two techniques were based on the idea of pulling down the ATP synthase with the purified IF<sub>1-60</sub>-His protein alone or with purified IF<sub>1-60</sub>-His in combination with pre-treatment of the mitochondria with a chemical cross-linker DTBP (Dimethyl 3,3'-dithiobispropionimidate.HCL).

### **5.2.2.1) ATP synthase pull down using the inhibitor protein**

#### **IF1-60-His**

In this technique, the purified IF<sub>1-60</sub>-His was incubated with detergent solubilised crude mitochondria from *T. thermophila* (section-5.2.1). The IF-ATP synthase complex sample was isolated using a Nickel HiTrap™ HP IMAC column. This resulted in the elution of a broad protein peak, as shown in Figure 5.3. Those fractions which were included in this protein peak (10 mL to 25 mL) were collected. The presence of protein was further confirmed by measuring the protein concentration of each fraction. Several runs of FPLC were performed in order to obtain the appropriate amount of proteins required for Mass spectrometry.

The final, pooled protein concentration ranged between 9 mg/mL and 15 mg/mL. This isolated purified protein was then analysed using a glycine gel, as shown in Figure 5.4a. Bands of various sizes were present. There was a prominent band corresponding to IF<sub>1-60</sub>-His at 26KDa (Figure 5.4a). Further bands represent proteins co-purifying with the inhibitor protein, presumably proteins of the ATP synthase complex. These bands were excised for tryptic digest and Mass spectrometry analysis to confirm identity (Figure 5.4b).

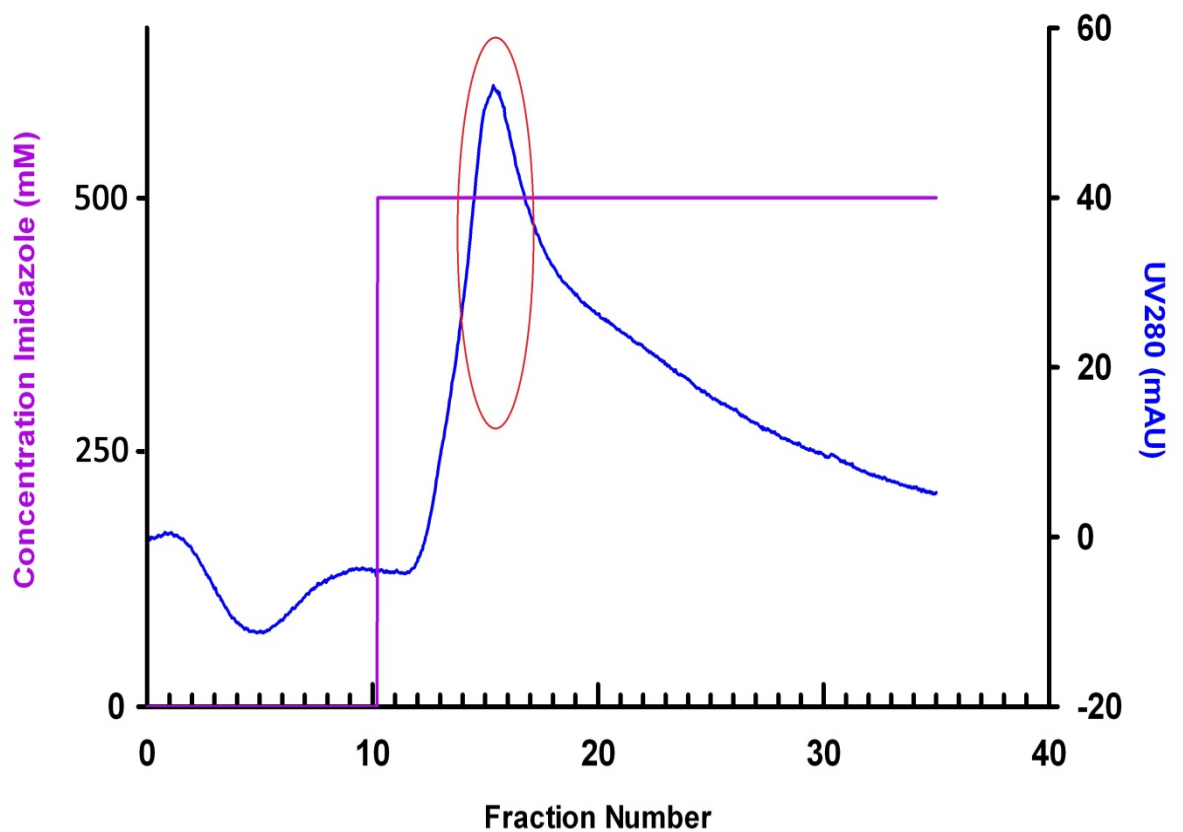


**Figure 5.3** A chromatogram showing the elution profile of IF<sub>1-60</sub>-His purified ATP synthase. The complex was pulled-down with IF<sub>1-60</sub>-His followed by a step gradient purification on a nickel affinity HiTrap™ HP IMAC column. Imidazole concentration is represented by the purple line and the linear gradient varied from 25 mM to 500 mM. The ATP synthase peak is represented by a red circle. The blue line represents the absorbance at 280 nm and is indicative of the protein concentration. The fraction number is represented on the x-axis scale.

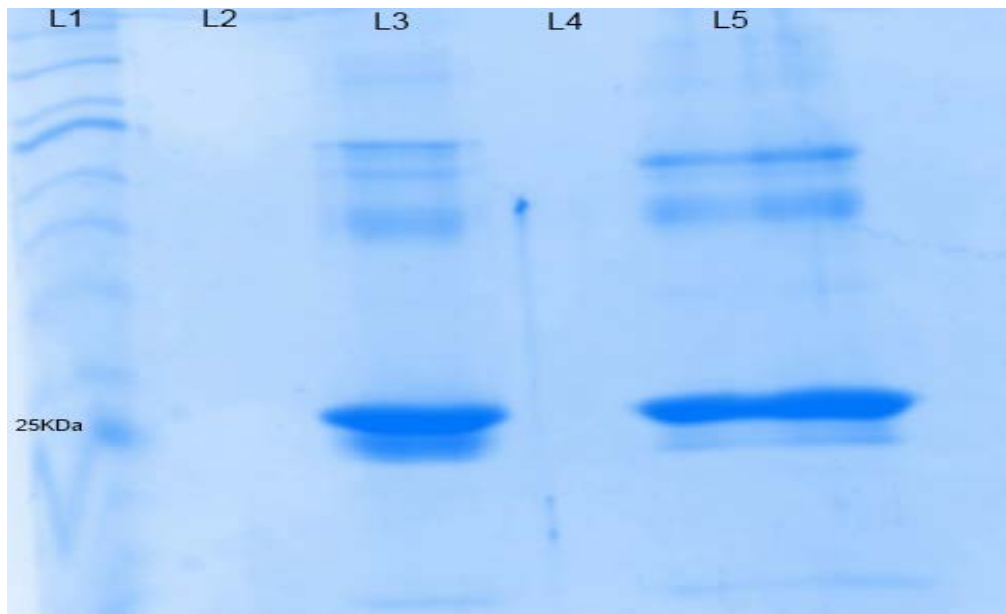


**Figure 5.4a** Coomassie stained Glycine gel of ATP synthase complex pulled down by inhibitor protein IF<sub>1-60</sub>-His and purified using Nickel affinity chromatography. IF<sub>1-60</sub>-His band can be seen at 26KDa in L3 and L5. Protein marker was in L1. Lanes 2 and 4 are empty.

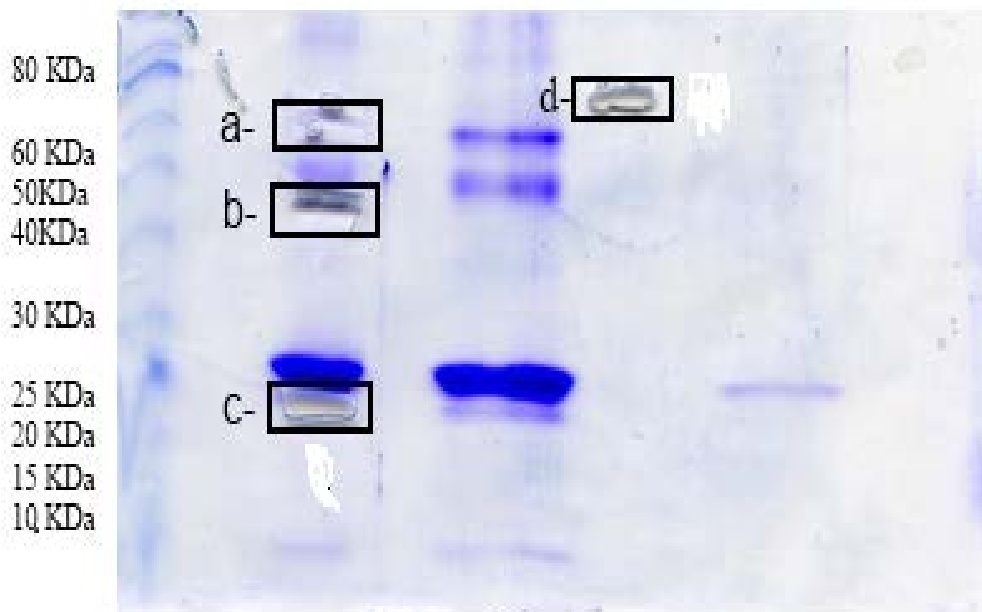


**Figure 5.4b** Coomassie gel showing the bands that were excised and analysed by Mass Spectrometry. Key; a= G65-1, b=G49-3, c=G23-2, d=G70-4 (where G refers to glycine, 65, 49, 23 refers to predicted size of the protein and -1,-2,-3,-4 refers to individual bands cut out from a single gel).

### **5.2.2.2) ATP synthase pull down using a cross linker and an inhibitor protein**

This second technique included the addition of a chemical crosslinker DTBP (Dimethyl 3,3'-dithiobispropionimidate.HCL) as there were concerns the ATP synthase complex may disassociate during purification. Initially, an ATPase activity assay was carried out to identify the maximum concentration of DTBP that could be added without loss of ATP synthase activity. A final concentration of 20 mM DTBP was found to be optimum. Therefore, 0.5 mL of 60 mM DTBP was incubated with 1 mL of crude mitochondrial sample for an hour at room temperature (data not shown). The sample was then processed as before (i.e. without the addition of cross-linker), using the same FPLC protocol to pull down and purify the ATP synthase complex by the addition of the inhibitor protein IF<sub>1-60</sub>-His. The resulting elution profile showed an A280 absorbance peak when eluted with 300 mM imidazole corresponding to the elution of the cross-linked ATP synthase and IF<sub>1-60</sub>-His (Figure 5.5). Those fractions which showed the specific peak of protein in the chromatograph were selected including fractions 9 to 12. The protein concentration was determined using a NanoDrop-1000. The fractions were then pooled and precipitated using methanol precipitation. After resuspending the protein in 10 µl of resuspension buffer, the sample was stored at -80 until required. The final protein concentration was measured and found to be 13.05 mg/mL. This protein was stored at -80 °C until required. Several runs of FPLC were performed in order to obtain the appropriate amount of purified ATP synthase complex required for Mass spectrometry. The final protein concentration ranged between 9 mg/mL and 15 mg/mL. All the protein samples were stored at -80 °C until used. Before performing SDS-PAGE, all the stored proteins were pooled together. This isolated

purified protein sample was then loaded on a glycine gel which was used to excise bands for MS analysis.

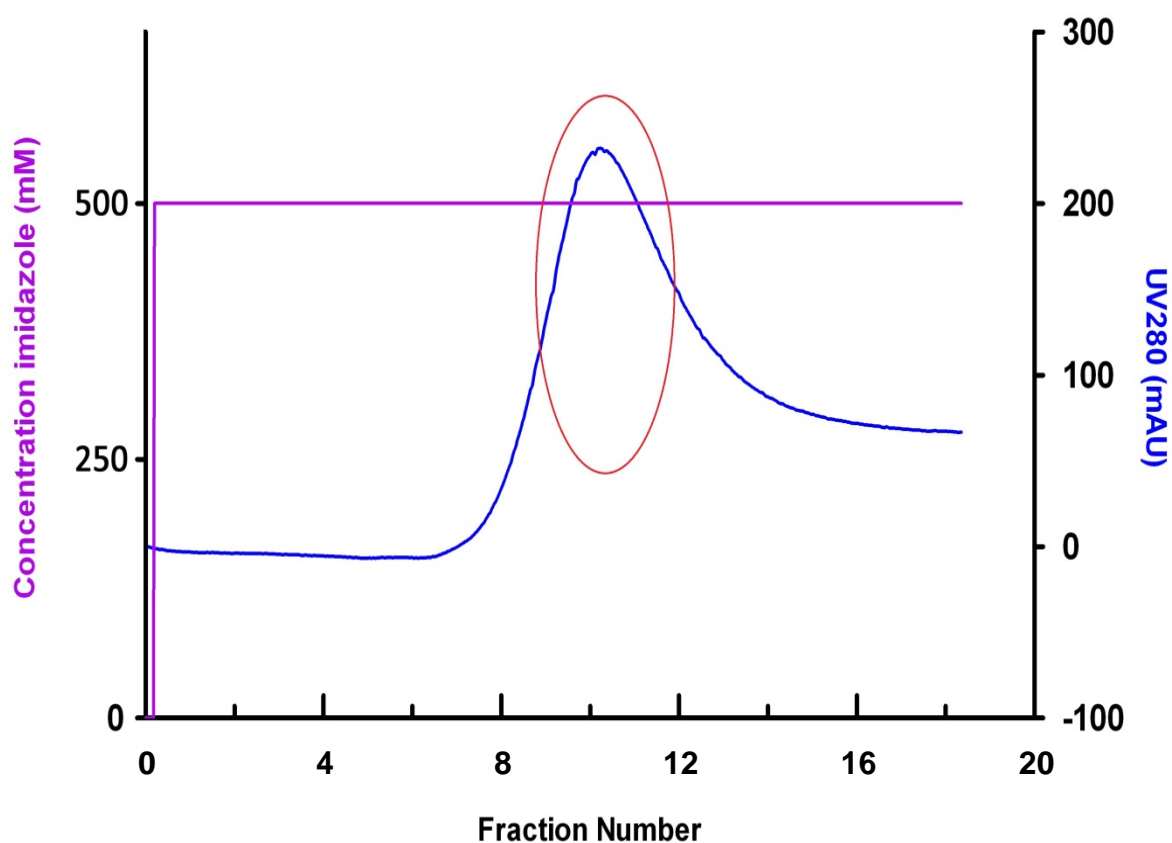


**Figure 5.5** A chromatogram showing the elution profile of IF<sub>1-60</sub>-His purified DTBP cross linked ATP synthase. The complex was pulled-down by IF<sub>1-60</sub>-His following crosslinking DTBP. A step gradient purification using a nickel affinity HiTrap<sup>TM</sup> HP IMAC column. The imidazole concentration is represented by the purple line and the gradient varied from 25 mM and 500 mM. The ATP synthase peak is represented by a red circle. The blue line on y-axis represents the absorbance at 280 nm, representing the protein concentration. The 0.5 mL fractions were collected and the fraction number is represented on x-axis.

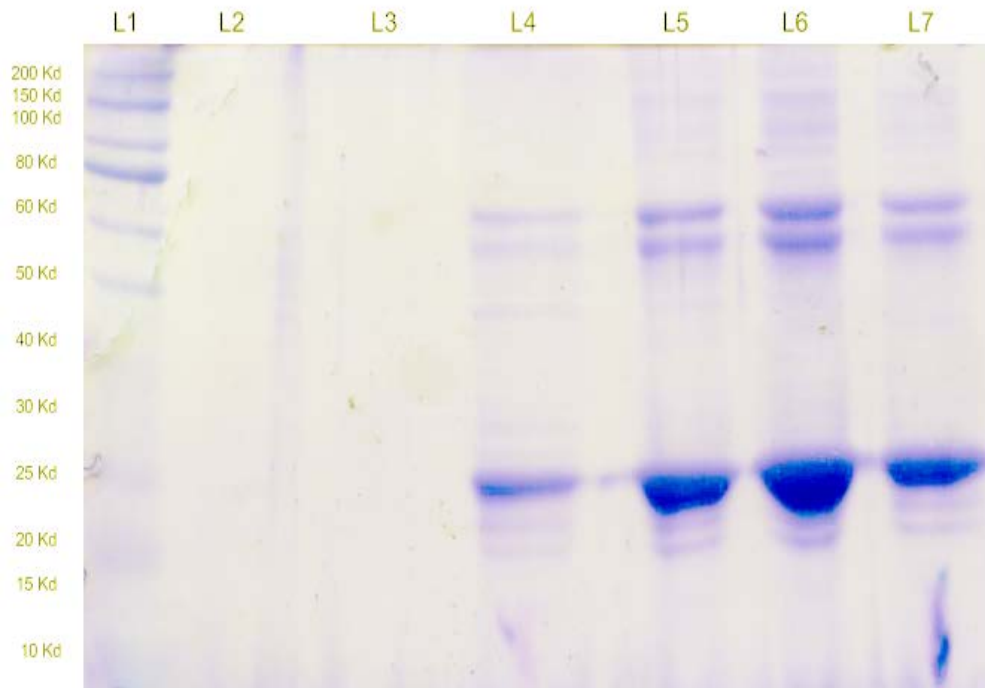


**Figure 5.6** Coomassie stained SDS-PAGE of Nickel affinity column purified fractions of ATP synthase treated with DTBP crosslinker and pulled down using IF<sub>1-60</sub>-His . Lane 1 is protein ladder (size to the left), lanes 2 and 3 are empty, and Lane 4-7 corresponds to fractions 9-12 as depicted in Figure 5.7.

After performing SDS-PAGE of the eluted protein via FPLC (Figure 5.6) it was evident that several proteins were present including the 26KDa - IF<sub>1-60</sub>-His protein and two prominent bands between 55KDa and 60KDa which were likely to represent the  $\alpha$  and  $\beta$  subunits. A western blot was performed, using an anti- $\beta$  subunit antibody (Figure 5.7). A clear band at 54 kDa was obtained as expected, in the lanes corresponding to fractions 11 and 12, as shown in Figure 5.7. This confirmed the successful pulldown of a  $\beta$ -subunit of ATP synthase of *T. thermophila*. The western blot was then repeated, using an anti-c subunit antibody. A clear band of 9 kDa was obtained as expected for subunit c in the lane corresponding to fraction 12 (Figure 5.8).

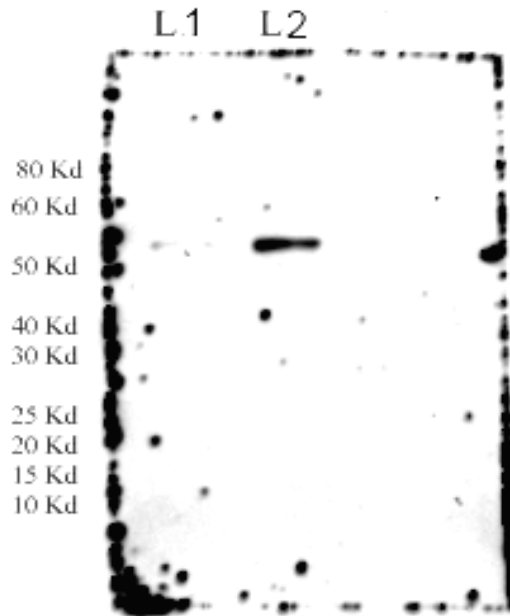


**Figure 5.7** A ChemiDoc image of a Western blot using anti- $\beta$  subunit antibody on ATP synthase pulldown fraction treated with a crosslinker DTBP. Lane 1 and lane 2 both contain a purified ATP synthase showing a specific band of  $\beta$ -subunit of ATP synthase of *T. thermophila* at 54 KDa.

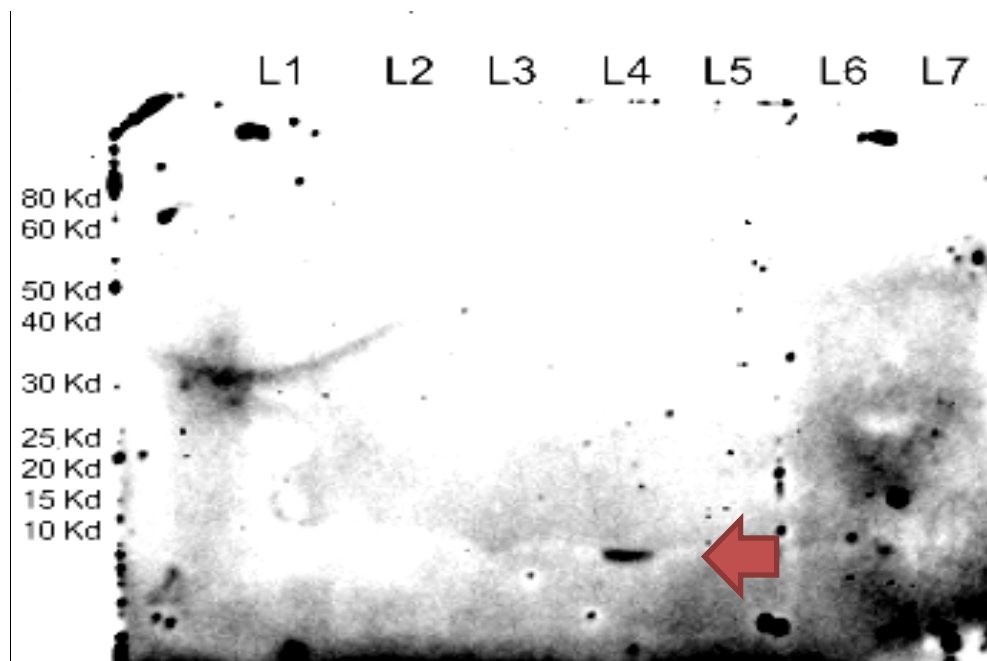


**Figure 5.8** A ChemiDoc image of a Western blot using anti-C subunit antibody on ATP synthase pull down fractions treated with a crosslinker DTBP. Lane 1 contains protein markers. Lanes 2-7 contain purified ATP synthase showing a specific band of C-subunit of ATP synthase of *T. thermophila* at 9 KDa (red arrow) in lane 4.

### 5.2.2.3) ATP synthase pull down using the anti- $\beta$ subunit antibody

A western blot was performed to identify the  $\beta$ -subunit of the ATP synthase of *T. thermophila* mitochondria. A commercially available anti- $\beta$  subunit antibody raised against the *Arabidopsis thaliana* ATP synthase  $\beta$  subunit was used. *T. thermophila* crude mitochondria (15mg/mL) were loaded on a glycine gel alongside isolated mitochondria from *A. thaliana* as a positive control. The proteins were transferred on to PVDF membrane in order to perform western blotting (Section 2.11.6). Results, as shown in Figure 5.9 show a clear band at 59 kDa in the *A. thaliana* mitochondria which corresponds to the expected size of the  $\beta$ -subunit of the *A. thaliana* ATP synthase. A band of 54KDa was obtained in the lane containing the *T. thermophila* crude mitochondrial sample, indicating that the  $\beta$ -subunit of ATP synthase of *T. thermophila* mitochondria was successfully identified using the *A. thaliana* ATP synthase, anti-  $\beta$  subunit antibody.

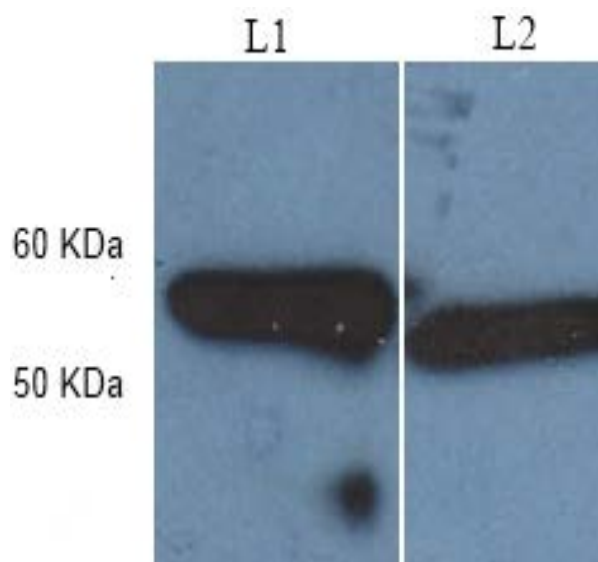


**Figure 5.9 Western blot using anti-  $\beta$ -subunit of ATP synthase.** Lane 1, *Arabidopsis thaliana* mitochondrial sample used as a positive control. Lane 2, *T. thermophila* mitochondrial sample. Lane 1 showed a band at 59KDa and Lane 2 showed a clear band at 54 KDa, corresponding to the expected size of the  $\beta$ -subunit of ATP synthase.

The *A. thaliana* anti- $\beta$  antibody was therefore able to bind to the *T. thermophila* ATP synthase  $\beta$  subunit and could be used to pull down the ATP synthase complex and an anti- $\beta$  subunit antibody method was developed to purify detergent solubilised ATP synthase as detailed in section 2.11.3 the detergent solubilised ATP synthase was bound to the affinity column, and then washed to remove unbound proteins. The bound ATP synthase protein was eluted with high salt concentration (1.5 M NaCl) which gave a distinct absorption peak at 280 nm in the chromatogram, as shown in Figure 5.10.

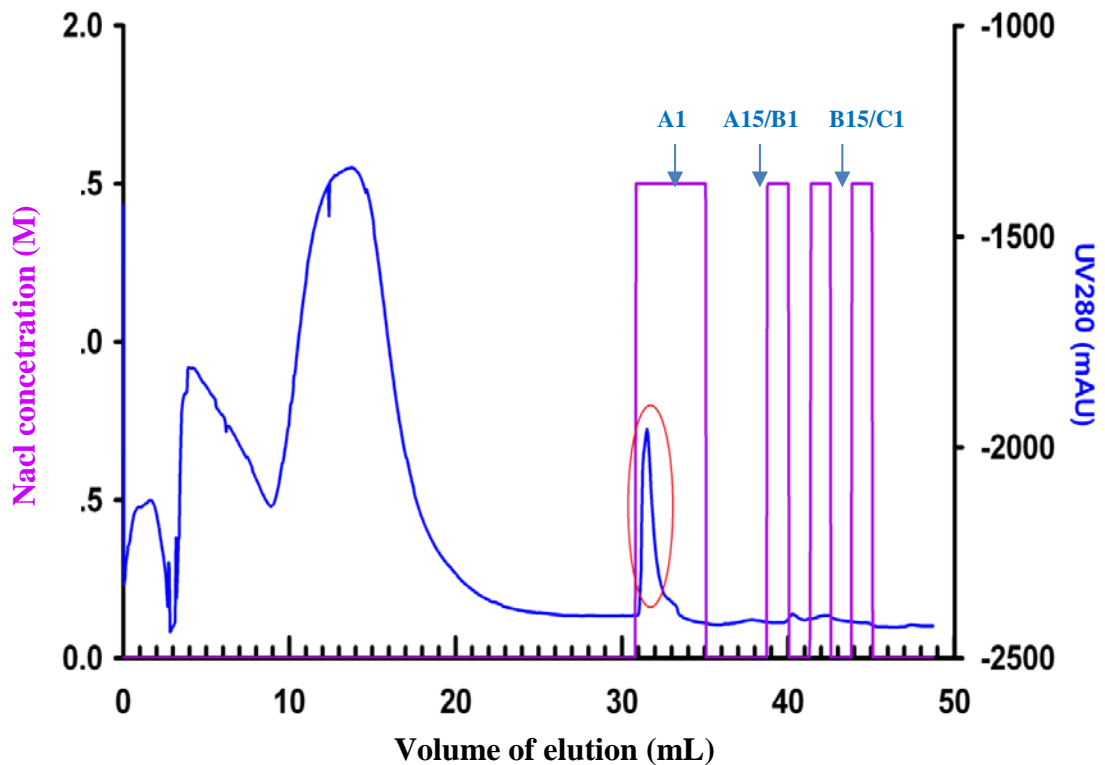


**Figure 5.10** A chromatogram showing the elution profile of ATP synthase purified using an anti- $\beta$  subunit antibody. The complex was pulled-down by an anti- $\beta$  subunit antibody coupled to a CN-Br sepharose 4B column. Salt concentration is represented by the purple line and the linear gradient varied from 50 mM to 1.5 M NaCl concentrations. Fractions of 0.3 mL were collected when the high salt elution commenced. The ATP synthase peak is represented by a red circle. The blue line on y-axis represents the absorption at 280 nm, representing the protein concentration. The position of fractions is indicated by the arrows.

Fractions corresponding to the A280 absorption peak were collected (A1, A4, A7, A11, A15 and B12 in the graph) and were measured for the presence of protein with the NanoDrop-1000. The protein concentration was found to be in the range of 0.5 mg/mL to 1 mg/mL. These fractions were then analysed using a western blot with the anti- $\beta$  subunit antibody. The appearance of a clear band at 54 KDa showed the successful pull down of the  $\beta$  subunit (Figure 5.11).

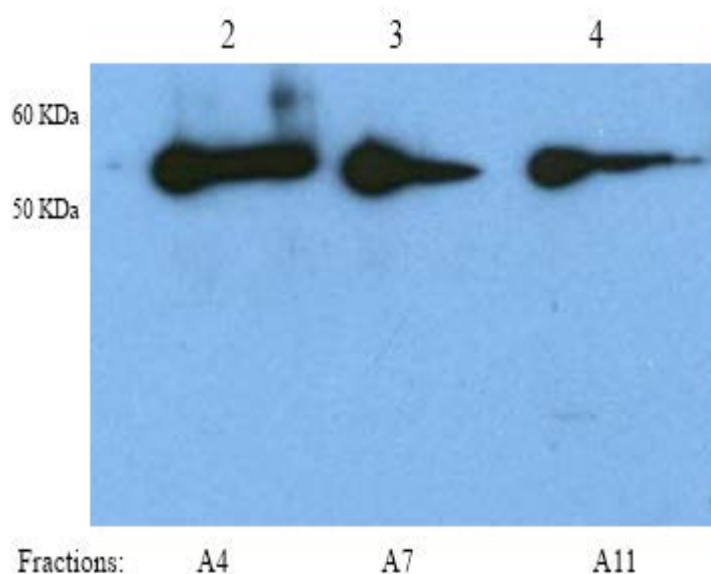


**Figure 5.11** Western blot of eluted fractions of ATP synthase purified by pull down with an anti- $\beta$  subunit antibody coupled to a CNBr (Cynobromide) column. Lanes 2, 3 and 4 correspond to fractions A4, A7 and A11 respectively. Bands obtained at 54 KDa representing the successful identification of the  $\beta$ -subunit of *T. thermophila* ATP synthase.

The fractions were pooled and precipitated via methanol precipitation. The dried protein was then resuspended in 150  $\mu$ L buffer A (0.05% DDM, 0.02 M imidazole, 0.05 M NaCl, pH adjusted at 6). The protein concentration was measured by a Bradford assay and the final concentration was found to be 7 mg/mL. The protein was then stored at -80  $^{\circ}$ C until used for Mass Spectrometry analysis.

### 5.2.3) Mass Spectrometry protein analysis via MALDI-TOF

As discussed above, three different approaches were used to isolate and purify ATP synthase from the mitochondria of *T. thermophila*. In each case the purified samples were subject to SDS-PAGE which resulted in multiple protein bands of different sizes being resolved. To identify the proteins present in these samples, bands were excised from the gels under aseptic conditions and subject to proteomic analysis by mass spectrometry. Figure 5.6b shows an example of an SDS-PAGE following excision of some protein bands and the labelling convention used for these samples.

The bands were digested with trypsin in preparation for fragment analysis via Mass Spectrometry using a MALDI/TOF/MS-MS instrument (section 2.12.6). The overall workflow for identification of *Tetrahymena* proteins is depicted in Figure 5.12. Firstly, mass peaks corresponding to known common contaminants of proteomics analysis were filtered using MASCOT (Perkins *et al*, 1999) and the C-Rap database (<http://www.thegpm.org/crap/>). During this process peaks predominantly corresponding to human keratin and porcine trypsin were filtered from the raw data. The remaining data was then subject to smooth calibration using Mmass ([www.mmas.org](http://www.mmas.org)) before identification of proteins by fragment mass using Protein Prospector MS-Fit (<http://prospector.ucsf.edu/prospector/cgi-bin/msform.cgi?form=msfitstandard>). The protein sequences were then identified using Blast 95% identity of >95% against the translated genomic database of *Tetrahymena thermophila*. The full data can be seen in Table 5.2.

Trypsin-digested protein samples



MALDI-TOF/MS-MS

(Fragment analysis)



MASCOT + C-Rap database

(To remove contaminant peaks)



Mmass

(Smooth calibration of data)



Protein Prospector MS-Fit

(Searches for sequences and best matches are selected)

**Figure 5.12 Work Flow for the identification of proteins by Mass Spectrometry**

**Table 5.2 Proteins identified using all pull-down techniques.** Red indicates contaminants, green indicates ATP synthase proteins, and blue indicates proteins with no known function. Pull-down: Beta indicates anti-beta antibody, IF indicates inhibitor protein pull-down, cross-linker indicates inhibitor protein plus cross-linker. Proteins identified with \* were identified in an inhibitor-pull down experiment conducted by Imogen White, an honours student under the direction of Anjum Naqvi.

Accession #	GI code	Sample ID	Description	MW (kDa)	Technique
NP_149381	15027647	F-T7	ATP synthase F0 subunit 9 (subunit c)	7.9	IF
XP_001007296.2	146161492	J-blank	hypothetical	124.2	antibody
XP_001009289.1	118352031	T100-5	hypothetical	8	crosslinker
XP_001010233.1	118353936	G90-2	C2 domain containing protein	96.3	crosslinker
XP_001010233.1	118353936	G160-2	C2 domain containing protein	96.3	crosslinker
XP_001010459	118354393	F-G23	hypothetical	231.9	IF
XP_001010660.1	118354798	A2-32	hypothetical	37	antibody
XP_001010761.1	118355000	F-T28	ATP synthase F1, gamma subunit family protein	32.7	IF
XP_001010761.1	118355000	S30*	ATP synthase F1, gamma subunit family protein	32.7	IF
XP_001010839.1	118355156		cation channel family protein	226.6	IF
XP_001010914.1	118355308	J4-15	hypothetical	92.8	antibody
XP_001011569.1		T7	hypothetical	91.4	IF
XP_001011629.1	118356751	T50-3	hypothetical	112.9	crosslinker
XP_001011633.1	118356759	G95-1	hypothetical	116.7	crosslinker
XP_001011633.1	118356759	G49	hypothetical	116.7	IF
XP_001011786.1	118357072	G65	hypothetical	123.2	IF
XP_001011815.1	118357131	G95-3	hypothetical	104.9	crosslinker
XP_001011830.1	118357161	T100-3	hypothetical	10	crosslinker
XP_001011904.1	118357309	G90-4	hypothetical	103.4	crosslinker
XP_001012056.1	118357615	A7-18	hypothetical	101.7	antibody
XP_001013690.1	118360918	G90-3	EF hand family protein	111.9	crosslinker
XP_001014631.1	118363488	IF-2	hypothetical	123.2	crosslinker
XP_001015264.1	118364083	L-120*	ATPase, putative	122.2	IF
XP_001015305.1	118364166	A9-21	hypothetical	79.3	antibody
XP_001015517.2	146165634	G25-1	hypothetical	39	crosslinker
XP_001015731.1	118365020	G95-5	hypothetical	112.2	crosslinker
XP_001016593.1	118366755	A4-14	Histone H4, putative	11	antibody
XP_001016788.2	146168336	G70-3	hypothetical	119.6	crosslinker
XP_001017043	118367661		ABC transporter family protein	160.5	IF
XP_001017179.2	229595475	G60-1	NADH-ubiquinone oxidoreductase 75 kDa subunit,	80.3	crosslinker

			mitochondrial		
XP_001017197.1	118367975	T28	Cyclin, N-terminal domain containing protein	115.7	IF
XP_001017238.3	229595483	T140-2	hypothetical	115.3	crosslinker
XP_001017678.1	118368944	G70-4	hypothetical	107.3	crosslinker
XP_001019412.1	118372431	S-78*	hypothetical	83.7	IF
XP_001019725.1	118373062	T35-1	hypothetical	78.3	crosslinker
XP_001019781.2	146175330	G48-2	hypothetical	55.5	crosslinker
XP_001021209.1	118376052	G160-1	hypothetical	106.1	crosslinker
XP_001021372.3	229594884	G95-2	hypothetical	116.1	crosslinker
XP_001022746.1	118379158	A9-19	hypothetical	46	antibody
XP_001022967.1	118379603	T35-3	hypothetical	101	crosslinker
XP_001022972.1	118379613	G70-2	DNA ligase I	93.3	crosslinker
XP_001022980.1	118379629	G70	hypothetical	98.7	IF
XP_001023092.1	118379853	G70-1	hypothetical	86.4	crosslinker
XP_001023430.1	118380533	J6-16	hypothetical	12	antibody
XP_001023497.1	118380667	T35-4	hypothetical	71.5	crosslinker
XP_001023731.1	118381140	J-A2-32	cation channel family protein	148.3	IF
XP_001024017.1	118381713	G25-2	hypothetical	78.3	crosslinker
XP_001024314.1	118373815	T100-1	hypothetical	6.7	crosslinker
XP_001024314.1	118382313	T100-4	hypothetical	116.9	crosslinker
XP_001024492.1	118382672	G60-2	Pyridine nucleotide-disulphide oxidoreductase family protein	69.8	crosslinker
XP_001024757.1	118383205	T100-2	hypothetical	108.6	crosslinker
XP_001025180.2	146182760		ATP synthase F1, delta subunit family protein	24.6	IF
XP_001025757.3	229594051	A5-24	hypothetical	49	antibody
XP_001025928.2	229593955	IF-1	Protein kinase domain containing protein		crosslinker
XP_001026289.1	118386340		hypothetical	118.3	IF
XP_001027129.1	118388057	T35-2	hypothetical	124.1	crosslinker
XP_001027692.2	146184059	F-G49	ATP synthase F1, alpha subunit family protein	59.5	IF
XP_001029662.1	118394593	J4-13	hypothetical	7.5	antibody
XP_001030602.2	146184973	J2-18	hypothetical	104	antibody
XP_001030723.1	118396772	S-60-68*	phytanoyl-CoA dioxygenase (PhyH)	40.9	IF
XP_001030819.1	118396966	L-49*	hypothetical	41.2	IF
XP_001032513.1	118400381	G90-1	hypothetical	114.5	crosslinker
XP_001032631.2	146185860	G48-1	ATP synthase beta chain,	53.3	crosslinker
XP_001032631.2	146185860	F-G60	ATP synthase beta chain	53.3	IF
XP_001033190.1	118401740	G48-3	Protein kinase domain containing protein	107.5	crosslinker

XP_001033221.2	146186228	T140-1	hypothetical	118.5	crosslinker
XP_001012937.1	118359395	G95-4	hypothetical	121.7	crosslinker
XP_001008507.1	118350452	T140-3	cyclic nucleotide-binding domain containing protein	99.2	crosslinker
XP_001010012.1	118353492	T-blank	Protein kinase domain containing protein	111.8	IF
XP_001014386.1	118362318	T70	D-alanyl-D-alanine carboxypeptidase family protein	113	IF

The results show that all of the ATP synthase subunits which can readily be identified in the genome by sequence homology ( $\alpha$ ,  $\beta$ ,  $\gamma$ ,  $\delta$  (OSCP) and  $c$ ) were identified. Seven proteins were identified that have well characterised functions which are unlikely to be part of the ATP synthase complex. However, three of these proteins were only identified in samples that had been subject to chemical cross-linking which would increase the likelihood of non-ATP synthase subunits being present. In addition, 57 proteins were identified whose function has yet to be elucidated (annotated as hypothetical protein or containing a specific domain). These are the proteins that are likely to include missing ATP subunits. Although many proteins were only identified using one technique, two proteins (the  $\beta$  subunit and a hypothetical protein) were identified using two techniques. This hypothetical protein is therefore more likely to form part of the ATP synthase complex.

The aim of this study was to identify proteins that were fulfilling the role that subunit **a** and subunit **b** play in ATP synthase from other organisms. Therefore, *Tetrahymena* homologs of subunit **a** and subunit **b** would:

- a) be targeted to the mitochondria if they are nuclear encoded,
  - b) have orthologues in organisms belonging to the dinoflagellates and apicomplexans,
- and

c) have similar structural characteristics to subunit a and subunit b from other organisms.

Hence, the proteins without defined function that were identified by mass spectrometry were evaluated using a variety of bioinformatics tools (Table 5.3) to identify candidates that meet these criteria.

**Table 5.3 Work flow for the identification and characterisation of proteins identified through mass spectrometry**

Step	Program	Function
1	TargetP/PlasMit/ WoLF PSORT	To identify mitochondrially-targeted proteins
2	TMHMM/ TMpred	To predict transmembrane helices
3	MPEX	To infer hydropathy plots for membrane proteins
4	BLAST	To identify further proteins in related species and to identify proteins
5	MCoffee	Multiple sequence alignments

As localization prediction software are not designed for use with ciliate sequences and so may not identify all mitochondrial-targeted proteins, sequences were analysed using all available mitochondrial-targeting identification software (TargetP, PlasMit, iLoc/mPLOC, WoLF PSORT, and MitoPred). For example, the known mitochondrial b subunits in *Arabidopsis* are not predicted to be localized to the mitochondria using PlasMit, and TargetP, or WoLF PSORT (subunit a is mitochondrially encoded). Although the b subunits of the comparative organisms, maize and human, were predicted to be targeted to the mitochondria by at least one tool. Secondly, as we hypothesise the missing ATP synthase subunits should be found in all alveolate species (ciliates, dinoflagellates and apicomplexa), searches were carried out against all alveolates (apicomplexa genomic data and dinoflagellate EST databases, as there was

no fully sequenced dinoflagellate genome at the time of this research) to see which proteins were conserved across the group.

Finally, as many of the ATP synthase proteins are membrane proteins, the data were analysed using MPEx, TMHMM and TMPred which are tools for identifying transmembrane protein segments and calculating hydropathy plots. These plots show how hydrophobic each amino acid is in a polypeptide versus where it is located on the polypeptide. The hydropathy plot is used to find clusters of hydrophobic amino acids. In general, a grouping of among 20-30 is required for a peptide to cross a membrane, which would indicate that the polypeptide in question is a transmembrane protein. A transmembrane protein has hydrophilic parts which protrude out on either side of the cellular or organelle membrane, and a hydrophobic alpha helix which lies within the membrane. Therefore, the hydropathy plot for all the identified proteins that were potentially mitochondrial targeted, were pair wise compared to the hydropathy plots of the a and b subunits from human, maize (*Zea mays*) and *E. coli* ATP synthase they were considered to match if they were of similar length (within 10%) contained the same number of hydrophobic peaks (transmembrane helices) and the number of residues between the top of the peak and the bottom of the trough matched within 20%.

Table 5.4 summarises those proteins, of unknown function which are likely to be targeted to the mitochondria, and provides details on whether these proteins have orthologues in apicomplexa and/or dinoflagellate species and whether they match the hydropathy profiles of subunit a or subunit b from human pea or *E.coli*. The BLAST search results (for orthologue identification) are shown in Appendix 1.

**Table 5.4 Mitochondria-targeted proteins, of unknown function identified in the pull-down assays.** All proteins listed were identified as being targeted to the mitochondria by at least one of the targeting programs. Alveolate BLAST comparison column indicates if the protein is found in either dinoflagellates or apicomplexa or both (yes). Hydropathy match column indicates if the protein has a structural similarity to either subunit a or subunit b in human, pea or *E. coli* ATP synthase.

Accession #	Sample ID	Description	MW (kDa)	Alveolate BLAST comparison	Hydropathy match
XP_001015517.2	G25-1	hypothetical protein	39	Yes	b subunit
XP_001019781.2	G48-2	conserved hypothetical protein	55.5	Yes	-
XP_001015305.1	A9-21	hypothetical protein	79.3	Yes	-
XP_001010660.1	A2-32	hypothetical protein	37	Yes	a subunit
XP_001023092.1	G70-1	hypothetical protein	86.4	ciliates only	-
XP_001022967.1	T35-3	hypothetical protein	101	ciliates only	-
XP_001021209.1	G160-1	hypothetical protein	106.1	ciliates only	-
XP_001013690.1	G90-3	EF hand family protein	111.9	Yes	-
XP_001010012.1	T-blank	Protein kinase domain containing protein	111.8	Yes	-
XP_001016788.2	G70-3	hypothetical protein	119.6	ciliates only	-
XP_001023497.1	T35-4	hypothetical protein	71.5	ciliates only	-
XP_001011830.1	T100-3	hypothetical	10	not dinoflagellates	-
XP_001014631.1	IF-2	hypothetical	123.2	Yes	-

## 5.2.4) Identification of subunit a

Following bioinformatics analyses, the protein A2-32 was found to be of interest. It was identified in samples purified by pull down with the anti- $\beta$  subunit antibody by using Cyanogen Bromide-activated-sepharose affinity column.

This protein (XP\_001010660.1) is predicted to be targeted to the mitochondria and BLAST results suggested that it is found across all alveolates. The molecular size of this protein is 37 KDa. Comparative analysis of potential transmembrane segments in this protein and those for other subunit a protein sequences was conducted using MPEx (Snider *et al*, 2009; Figure 5.13), TMpred (Hofmann & Stoffel, 1993; Table 5.5) and TMHMM (Erik *et al*, 1998; Table 5.5). In the majority of cases the analysis with all three software packages predicts 5 transmembrane regions, for both the putative *Tetrahymena* a subunit and the known a subunits of *Zea mays*, *E. coli* and human. The exceptions are TMHMM (Table 5.5) which predicts 4 and 6 transmembrane segments respectively for the *Zea mays* and human proteins and MPEx which predicts 4 (not including the targeting sequence) and 6 transmembrane segments for *Tetrahymena* and *E. coli* respectively (Figure 5.13). Subunit a contains a series of conserved amino acids L179, N182, H193 (E193 in *E.coli*), G186, T178 or R178. The protein sequence was therefore aligned with *Zea mays*, *E.coli* and human mitochondrial ATP synthase a-subunits. This showed that although there were significant differences in the sequence, the most important amino acids were conserved. The arginine at position 210 (*E. coli* numbering), is known to be essential for the deprotonation of an asparagine residue located in the c subunit (position 61 in *E. coli*), and hence plays a key role in H<sup>+</sup> transport through the complex (Angevine *et al*, 2007), This residue is conserved in the putative a subunit, as shown in blue, Figure 5.14. Mutagenesis studies have recently shown that many other supposedly essential residues are not essential, so the fact that

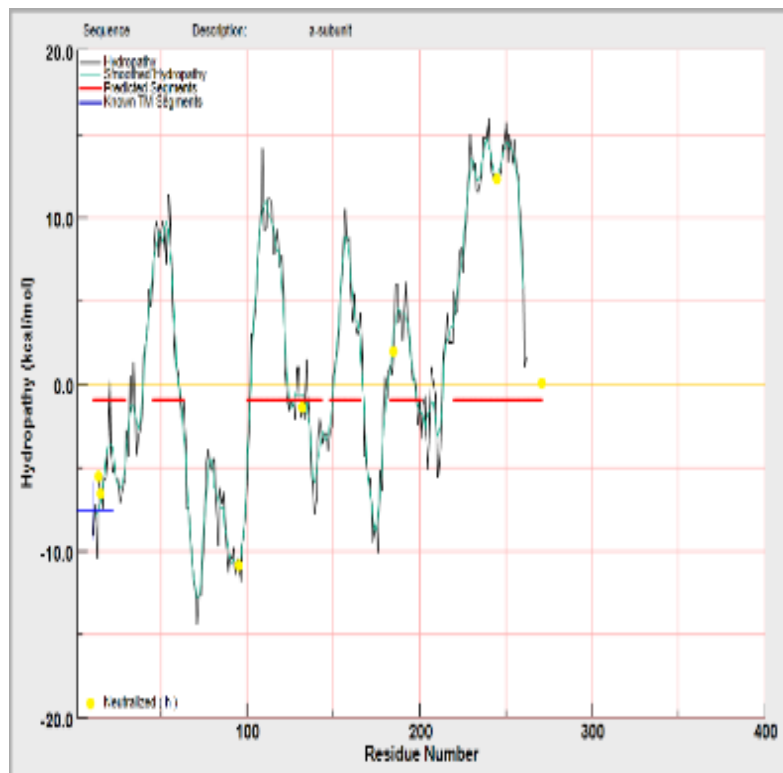
they are not present in the putative *Tetrahymena* a subunit does not discount it as a potential a subunit (Kuruma *et al*, 2012).

**Table 5.5 Prediction of Transmembrane segments of ATP synthase a subunits.**

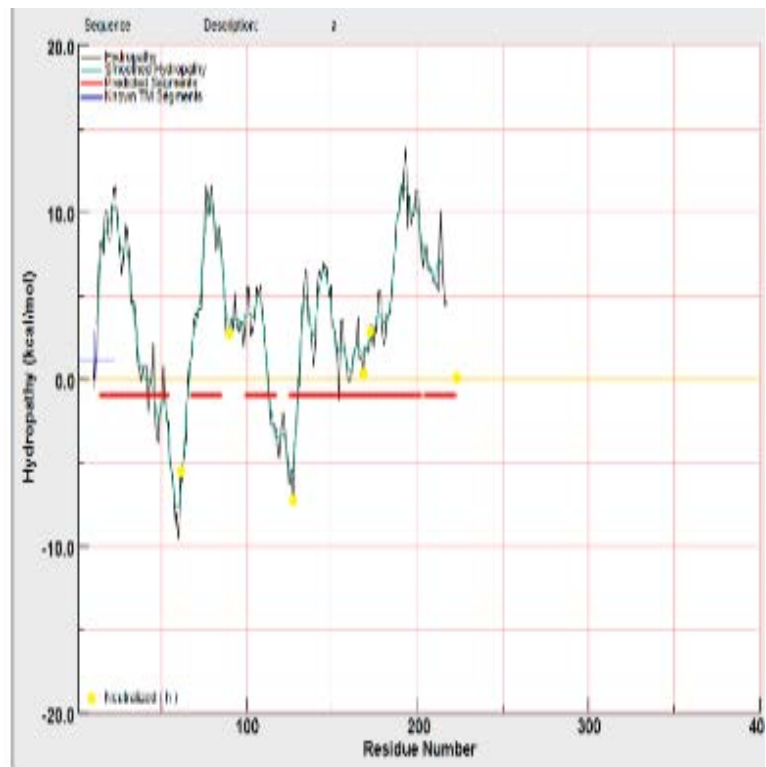
Predicted position of transmembrane segments is indicated by residue numbers.

\*Probability does not exceed auto assignment threshold.

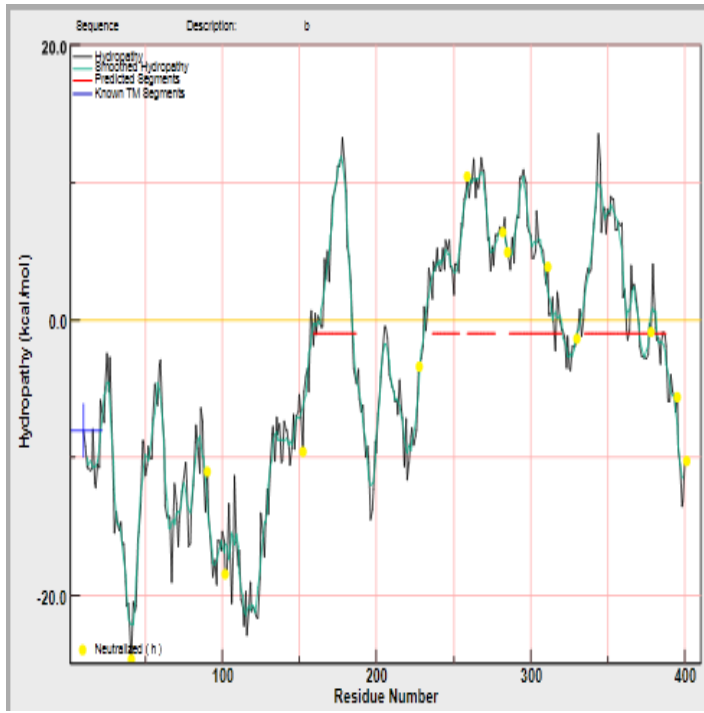
	<i>Tetrahymena</i> (A2-32)	<i>E. coli</i>	Maize ( <i>Zea mays</i> )	Human
TMpred	128 - 148 155 - 176 207 - 223 235 - 251 277 - 296	41 - 60 100 - 118 149 - 166 215 - 233 246 - 264	50 - 69 141 - 160 167 - 191 216 - 235 220 - 245	14 - 34 70 - 89 100 - 117 136 - 157 186 - 209
TMHMM	125 - 150* 153 - 180* 203 - 230* 235 - 260* 275 - 300*	38 - 60 100 - 122 147 - 166 211 - 233 243 - 265	47 - 69 136 - 158 165 - 187 230 - 252	5 - 27 67 - 89 98 - 117 132 - 151 164 - 186 191 - 222



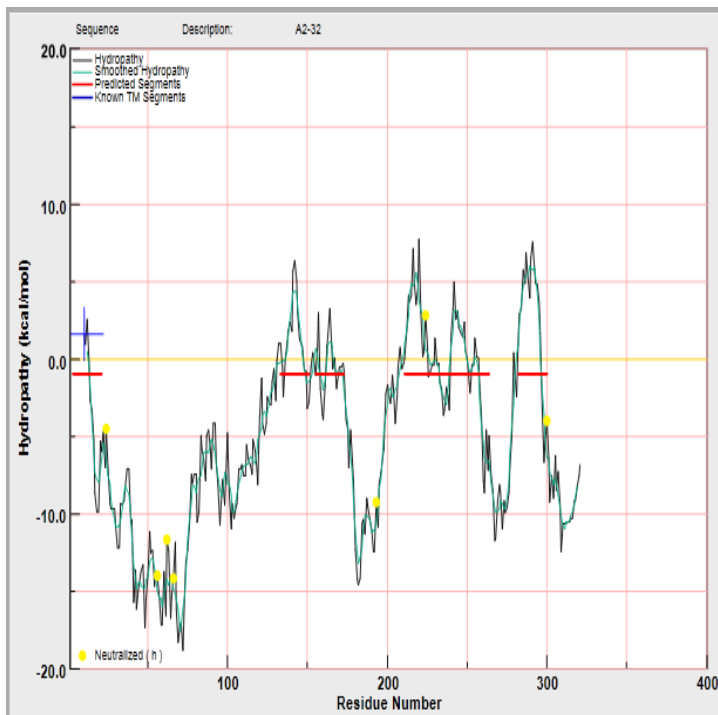
A



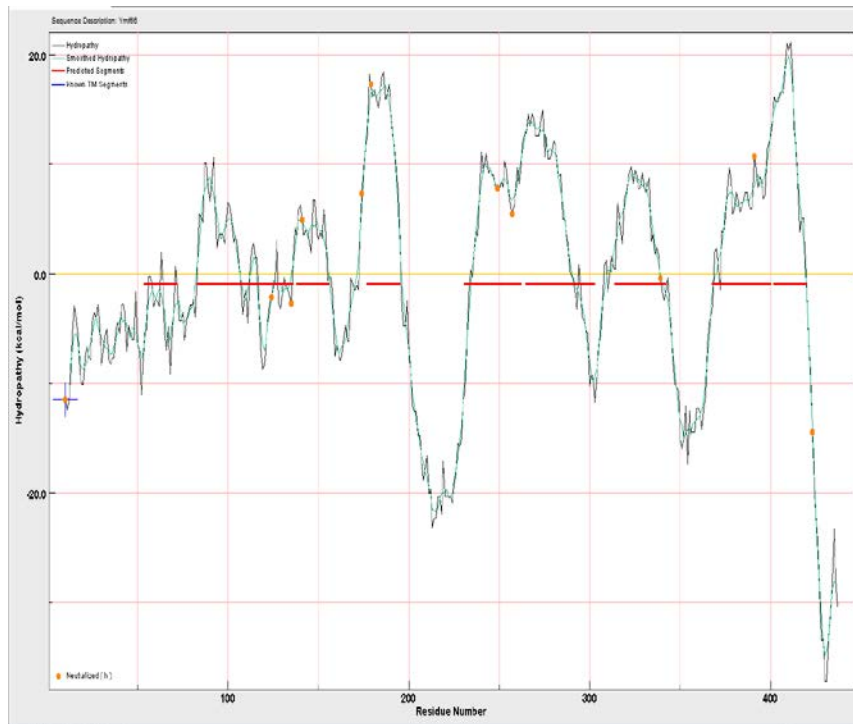
B



C



D



E

**Figure 5.13** Hydropathy plots of mitochondrial ATP synthase a subunit from a) *E. coli* (b) *Homo sapiens* (c) *Zea mays* d) *T. thermophila* sample A2-32 e) the putative *T. thermophila* a subunit (ymf66) identified by Nina *et al* (2010). Hydropathy, plots were generated with MPEX (Snider *et al.*, 2009). The red line indicates putative trans-membrane segments whilst the blue line indicates known trans-membrane segments identified from the MPtopo database (Jayasinghe *et al.*, 2001).

```

      *           20           *           40           *
Maize_a  : MMMMTRWSSTDMKRRNRILANMVPPIRNLSLPDIYEEYEEYYHPVVSREATRG : 50
Human_a  : ----- : -
E_coli_a : ----- : -
89292427 : -----MANFVIPY LKPVADFWSN : 18

      60           *           80           *           100
Maize_a  : VCILLRIDRYLSSIGRSIQDREVLRFQCRLLFPQREAGHSFSEIYDDIR : 100
Human_a  : ----- : -
E_coli_a : -----MASENMTPEQDYIGHHLNN----- : 18
89292427 : LCIDQHQP SFLQFKG---QTGSLGTLWTSKYLRSEQDVYNHKYLQYHKRV : 65

      *           120           *           140           *
Maize_a  : AHGVEASRLGQPLRDLYDEMERNGEIVNNGSIIIPGGGGPVTEP LLDQFG : 150
Human_a  : -----MNENLFASFI : 10
E_coli_a : -----LQLDLRTS : 27
89292427 : HEAP-----ELTDVISDNVY : 80
                                     f

      160           *           180           *           200
Maize_a  : IHPILD LNIGKYVSEFTNLSLSMLLTLGLVLLL VLVVTKKGGCKSVPNAF : 200
Human_a  : AP TILGLPAAVL IILFP---PLLIPTSKYL IINNRLITITQ----- : 46
E_coli_a : LVDPQNPPATFWTINIDSMFFSVV LGLLFLVLFVRSVAKKATSG-----V : 71
89292427 : RL TLFAGVERVLSVRQAQAILKTQFAGATENISGAFQITVLNCG-----IFR : 126
                                     t       g

      *           220           *           240           *
Maize_a  : QSLVELIYDFVFNLVNEQIGGLSGNVKHKFFPCISVTFTEFSLFRNPQGM : 250
Human_a  : -----QWL I KLTSKQMMTMHNTKGR TWSLMLVSLIIFIATTNLLGLL : 88
E_coli_a : PGKFQTAIELVIGFVNGSVKDMYHGKSKLIAPLALTI FVWVFLMNLMDLL : 121
89292427 : RGYFRGALLNLLQFCGAPYQSLIWSRNSGITNQVIVSSIFEAFFYPLDTV : 176
                                     f       n

      260           *           280           *           300
Maize_a  : EFSFT-----VTSHFLITIALSFSIFIGITIVGFQRHGL : 284
Human_a  : EFSFT-----PTTQLSMNLAMAIPLWAGTVIMGFRSKIK : 122
E_coli_a : PIDLLPYIAEHVGLPALRVVPSADVNVTTISMA LGVFILILFYSIKMKGI : 171
89292427 : KTLIYN-----DVQGKYKGAFHCA SQVVQNAGWSRLYAGIF : 212
                                     l       a

      *           320           *           340           *
Maize_a  : HFFSFLIPAG-----VPLPIAIFFLVLIELISHCFRALSSGIRIFANMMAG : 329
Human_a  : NALAHFIPAG-----TPTPLIIFMLVIEETISLLIQPMALAVRITANITAG : 167
E_coli_a : GGF TKEITLQ---PFNHWAFIEVNLIIEGV SLLSKPVSIGLRIFGNMYAG : 218
89292427 : QKLIENSALIFHLNQVWDGSSQQWASLALVAAAYPLLV LKTRFQVAGTPL : 262
                                     l       p       l e s       l Rl n ag

      360           *           380           *           400
Maize_a  : HSSVKILSGFAWTMLFLN NIFYFLGDLGPLFIVLALTGIELGVAISCAHV : 379
Human_a  : HILMHLLIGSATLAMSTIN---LPSTLIIFTILILLTILEIAVALICAYV : 213
E_coli_a : ELIFILIAG-----LLPWWSQWILNVPWAI FHI IITLQAFIFMV : 258
89292427 : ALATSNEVLKVN RKT---LYAGLVPYLI FNTLFA YEFAAWHSSTACERV : 308
                                     l       l       q       v

      *           420           *
Maize_a  : STISICIYINDATNLHQNESFHNCIKTRSQS : 410
Human_a  : FLLVSLYLHNT----- : 226
E_coli_a : LTIIVYLSMASEEH----- : 271
89292427 : IGGIQNAMKQFSSPAAEQVWSS----- : 330
                                     t

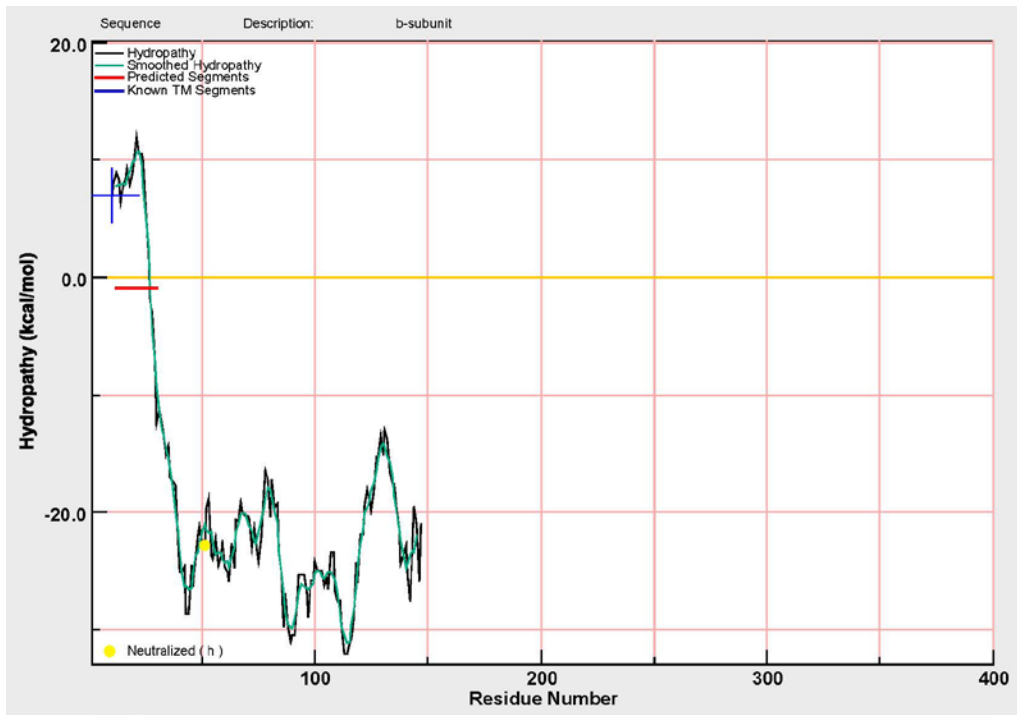
```

**Figure 5.14** Alignment of maize, *E. coli* and human a subunit with the putative *Tetrahymena* a subunit (labelled 89292427). Green residues are conserved across three species; blue residues are conserved across all four.

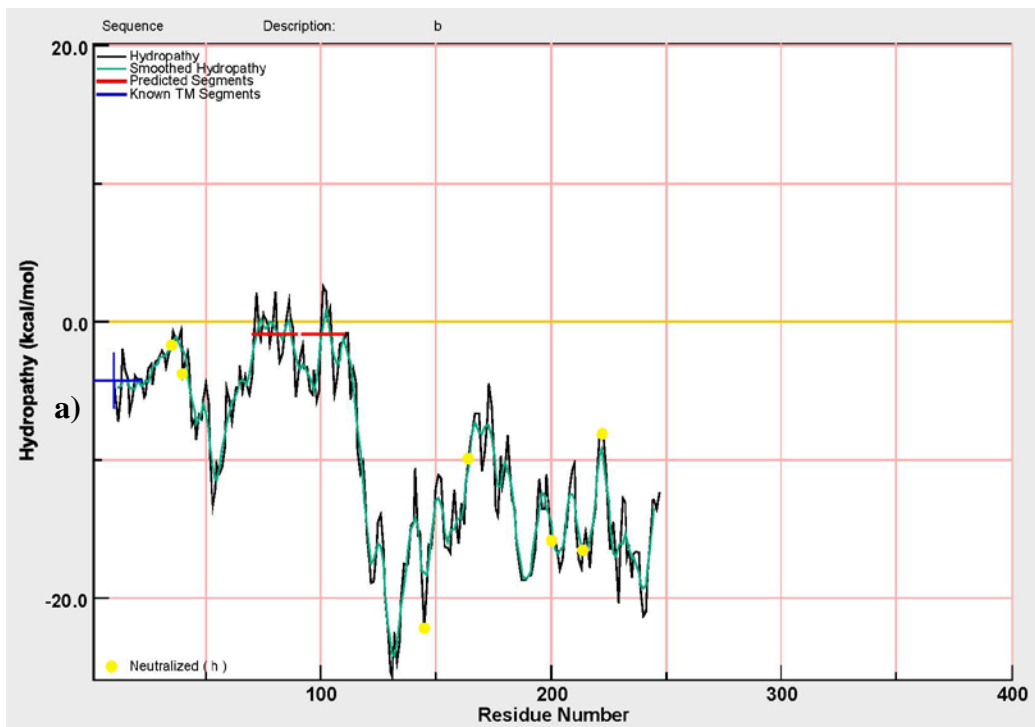
## 5.2.5) Identification of subunit b

The protein G25-1 (XP\_001015517.2, TTHERM\_00382330) was also predicted to be targeted to the mitochondrion. This protein was identified following cross-linking and a pull down purification using the inhibitor protein. It is a protein of 328 amino acids, and encodes a hypothetical protein of 39 kDa. Hydropathy plot analysis show that G25-1 has a similar profile to other eukaryotic b subunits, as shown in Figure 5.15, with a very hydrophobic N-terminus containing two or three predicted transmembrane domains, and a more hydrophilic C-terminus. An alignment with maize, human and *E. coli* b subunits is shown in Figure 5.16. Although G25-1 is larger than the b subunits from the other species which are compared, there is a significant degree of sequence similarity. The stator components, including the b-subunits are high in  $\alpha$ -helical structure (Walker and Dickson 2006). Analysis of the predicted protein secondary structure (Figure 5.17) indicates that G-25-1 is likely to contain many  $\alpha$ -helices, consistent with its potential role as a b subunit homologue. This protein was also identified in the proteomics study conducted by Smith *et al.* (2007), further supporting its mitochondrial location and potential as a homologue of the b subunit.

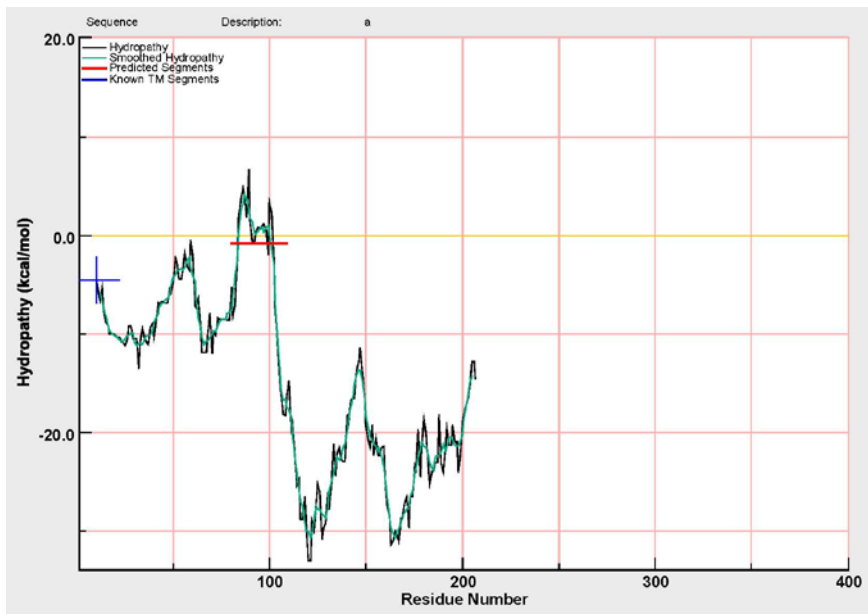
**Figure 5.15 (overleaf) Hydropathy plots of mitochondrial ATP synthase b subunit from a) *E. coli* (b) *Homo sapiens* (c) *Zea mays* d) *T. thermophila* sample G25-1.** Hydropathy, plots were generated with MPEx (Snider *et al.*, 2009). The red line indicates putative trans-membrane segments whilst the blue line indicates known trans-membrane segments identified from the MPtopo database (Jayasinghe *et al.*, 2001).



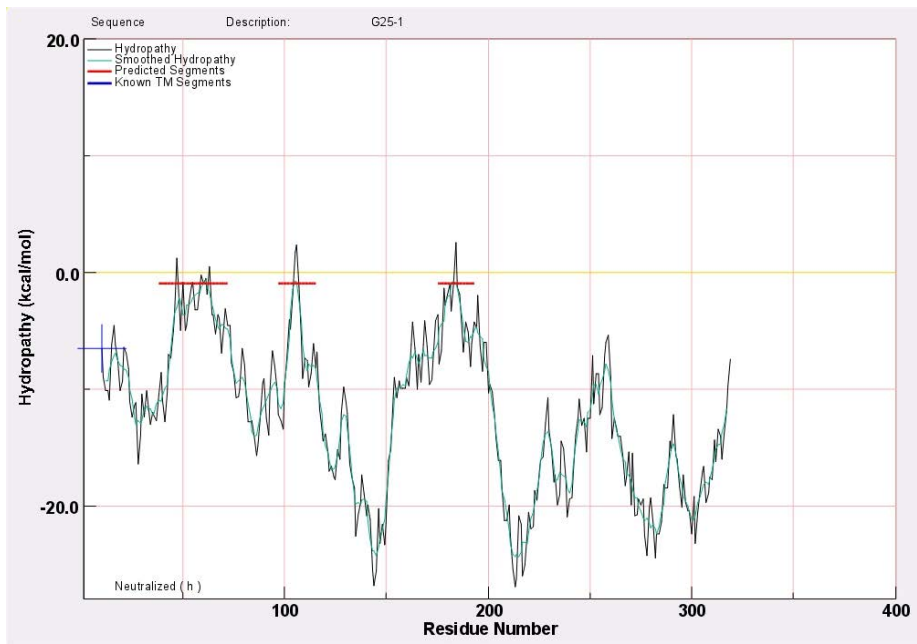
A



B



C



D

```

Maize_b : MATALMVAATTSCSPG-RAAPRLKPVASSSSSSSSSSARRRRPLAQQLPR : 49
E_coli_b : ----MNLNATILG----QAIAFVLFVLFC----MKYVWFP----- : 28
Human_b : MLSRVVLSAAATAAPSLKNAAFLGPGVLQATR-TFHTGQPHLVVPPLPE : 49
146165634 : MVRLEKILWEQLVN----VRAFSRQRVIGAPSKWYNENRTEWFKVAQHNA : 46
          m      a      af      p

Maize_b : -----LLATAA---AAAAVAAAPLPALAEQMEKAALFD-----FN : 81
E_coli_b : -----IMAAIE-----KRQKEIADG----- : 43
Human_b : YGGKVRYGIPEEF-----FQFLYPKTGVTGPVYLGTGLILYA--LSKE : 91
146165634 : FNTGFSGVILRALEPLLAKFIYRWRLDIAHQRGLTLEDSLLFMDRELRRC : 96
          1

Maize_b : LTIPAIATEFL----LIMVALDKIYFTPLGK----FMDERDAKIRG--- : 119
E_coli_b : --LASAER-----AHKDLDLAKAS-----ATIQLKKAKA--- : 70
Human_b : IYVISAETF-----TALSVLGVMVYGIKKYGPFVADFADLNEQKL : 132
146165634 : YFFETVARQNLHPYTVLFMKRRRARYYKVERGLRGFYVPLWVRREAEEERQ : 146
          a      l      d      K

Maize_b : -----ELGDVKGASEEVKCLEDQAAAIMKAARAEIAAALNK---- : 155
E_coli_b : -----EAQVIECANKRRSQILDEAKAEAEQ----- : 96
Human_b : A-----QLEEAKQASICHIQNAIDTEKSQQALVQKRHYLFDV- : 169
146165634 : LSETVDNIFNWENFVYREYMSDMTPIGRWTSLSKITPLDMFQYYGLFRENE : 196
          a      q      k      a

Maize_b : -----MKKETTAELEAKLDEGRSRVEAELVEAL : 183
E_coli_b : -----ERTKIVAQAQAEIEAERKRAREELRKQV : 124
Human_b : -----QRNNIAMALEVTYRERLYRVYKEVKNRL : 197
146165634 : AWDRFFYNEAFYESYSEKEKQEANGNPFGKFNLQTADGRAQFEKEVNTFI : 246
          r      r      E

Maize_b : ANLEAQK-----EEAVKALDAQIASLS-DEIVKKVLPSA---- : 216
E_coli_b : AILAVAG-----AEKIIERSVDEAANSDIVDKLVAEI---- : 156
Human_b : DYHISVQNMMRRKEQEHMINWVEKHVVQSISTQQEKETIAKCIADIKLLA : 247
146165634 : ERYPFAVTKPGQKFDFTRFYALEDLANKRDTSKYDPALLESVKNELKQSA : 296
          ek      k      l

Maize_b : ----- : -
E_coli_b : ----- : -
Human_b : KKAQAQPVM----- : 256
146165634 : ALPADNGANKTKKSKPILPDWLQPKFGKAFQA : 328
          *      320      *

```

**Figure 5.16 Alignment of b subunits with the proposed *T. thermophila* subunit b**  
The proposed *T. thermophila* subunit is labelled 146165634. Green residues are conserved across three species; blue residues are conserved across all four.



## 5.3) Discussion

Various subunits of the mitochondrial ATP synthase subunit appear to be missing from the ciliate *T. thermophila*, as well as other alveolate species such as dinoflagellate algae and apicomplexans (Mogi and Kita, 2010; Vaidya, 2009; Nina, 2011; Butterfield, 2013; Strum, 2015). The research carried out in this chapter was focused on this protein complex in order to identify the missing subunits in *T. thermophila*. Firstly, the mitochondria of *T. thermophila* were isolated. This was followed by a pull down of the ATP synthase complex via three different techniques. The use of the bovine inhibitor protein to pull down the ciliate ATP synthase complex is particularly interesting as there are no previous reports of the use of the inhibitor protein to pull down ATP synthase from species that do not contain the inhibitor protein (Bason, 2011; Runswick, 2013). The successful pull down of ATP synthase was shown by the appearance of bands of expected size in western blots of *T. thermophila* total protein when the anti- $\beta$  subunit antibody was applied. In order to identify the missing subunits of ATP synthase, 71 proteins were isolated and identified using mass spectrometry. Out of these proteins, five proteins were identified as the alpha, beta, delta and gamma subunits subunit of F1 domain and the c subunit of the F<sub>o</sub> domain of ATP synthase (Table 5.6). Following an extensive range of bioinformatics analyses, one protein (A2-32, XP\_001010660.1) was identified as a potential candidate for the ATP synthase a subunit, and a second protein (G25-1, XP\_001015517.2) as a candidate for the b subunit.

The a subunit was identified when the ATP synthase complex was isolated using an antibody pull down technique. Bioinformatics data search showed that A2-32 is a membrane-bound protein with a molecular weight of 37 KDa, which is predicted to be targeted to the mitochondria. The hydropathy plots of this protein showed similar structural homology with the a subunit proteins of *Z. mays*, *E.coli* and *Homo sapiens* (Figure 5.13). The multiple sequence alignment also showed that this protein has several

amino acid residues which are highly conserved across other species including the extremely important R210 residue, responsible for H<sup>+</sup> transfer to the c subunit.

The b subunit was identified using cross-linking in combination with pull-down purification using the inhibitor protein. It is annotated as a hypothetical protein, conserved across the alveolates with molecular weight 39kDa. It is predicted to be targeted to the mitochondrion, and has a similar hydropathy profile and size to other b subunits. To confirm these results, it will be necessary to do the reverse pull-down (i.e. with an anti-a and an anti-b antibody) to determine that these proteins are indeed a part of the ATP synthase complex.

The *T. thermophila* mitochondrial ATP synthase was previously investigated by Nina *et al* (2010). They identified five proteins from the ATP synthase complex including F1 subunits ( $\alpha$ ,  $\beta$ ,  $\gamma$ ,  $\delta$ ) and the c subunit of the F<sub>o</sub> domain. In addition, they found sixteen unassigned proteins. Amongst these proteins, they proposed that Ymf66 was a putative ATP synthase subunit a like protein. This protein was not identified in the analyses presented in this chapter.

There were some significant technical differences between Nina *et al* (2010) and the research presented in this chapter. Nina *et al* (2010) lysed *T. thermophila* cells with a hand-held homogenizer while in the research presented here, cells were lysed by applying a mechanical homogeniser driven with a constant gas pressure which results in the uniform breakage of the cells. Nina *et al* (2010) used mitochondria which were purified from a sucrose gradient. Sucrose may cause the shrinkage of the cellular membranes, therefore in this study a Percoll gradient was used instead. The isolation of mitochondria was later verified under transmission electron microscopy which showed intact mitochondria (Section 3.2.1.3, Figures 3.7 and 3.8). In order to isolate ATP synthase, Nina *et al* electro-eluted the ATP synthase complex using Blue-Native PAGE.

There were no confirmatory experiments carried out to confirm that the isolated complex was ATP synthase, apart from an in-gel ATP assay (Nina *et al*, 2010).

In contrast, the work presented here isolated the ATP synthase complex using three different pull-down techniques. Following the pull-down, the presence of ATP synthase was verified by western blotting with an anti- $\beta$  subunit antibody as shown in Figure 5.11.

I was unable to reproduce findings of the Nina *et al* (2010) results, and did not identify the Ymf66 protein (Figure 5.6). None of the putative ATP synthase proteins identified by Nina *et al* (2010) were identified using any of the three pull-down approaches. The potential  $\alpha$  subunit which Nina *et al* found consists of 446 amino acids, which is significantly longer than the conventional  $\alpha$  subunit (226 aa), and contains eight rather than five transmembrane helices. In contrast, the putative  $\alpha$  subunit identified in this chapter is significantly smaller, at 330 amino acids and is predicted targeted to the mitochondria and was identified in a comprehensive proteomics analysis of Purified *Tetrahymena* mitochondria (Smith *et al*, 2007). According to Blast searches, this protein resembles a mitochondrial carrier protein. The hydropathy plots of two putative  $\alpha$  subunits identified in the two studies are presented in Figure 5.13, demonstrating that the  $\alpha$  subunit identified in the research presented here more closely resembles the hydropathy plots of a plant  $\alpha$  subunit when compared to the putative protein identified by Nina *et al* (2010).

**Table 5.6 Canonical ATP synthase subunits identified through different protein purification procedures and mass spectrometry**

subunit	Inhibitor protein	Inhibitor plus crosslinker	antibody	Nina et al (2010)
$\alpha$	+			+
$\beta$	+	+		+
$\gamma$	+			+
$\delta$ (OSCP)	+			+
$\epsilon$				
a			+	yfm66
b		+		
c	+			+
d				
e				
F6				
g				

## 5.4) Conclusion

In conclusion, this chapter presents the successful pull down of mitochondrial ATP synthase of *T. thermophila*. I have potentially identified the mitochondrially-targeted a and b subunit proteins, both of which are of expected size, and the a subunits contains key conserved residues necessary for the passage of protons during ATP synthase. The identification of the first two subunits in the F<sub>0</sub> domain will allow the future identification of the remaining subunits that compose the F<sub>0</sub> domain in *Tetrahymena*.

In addition to the identification of two new subunits, this research presents for the first time the use of the ATP synthase inhibitor protein as a purification technique in a species which does not normally encode this protein. This discovery may be of great use to others studying ATP synthase in diverse species which also do not encode the inhibitor protein, for it gives the ability to carry out pull-down assays more easily than would otherwise be possible.

# Chapter 6

## Final Conclusion

The research presented in this thesis aimed to characterize the electron transport chain and oxidative phosphorylation capability of the *T. thermophila* mitochondrion. Although mitochondria had been previously been partially purified and characterized from other *Tetrahymena* species in studies conducted in the 1960s and 1970s (Kobayashi, 1965; Conklin and Chou, 1972; Kilpatrick and Erecinska, 1977), the mitochondrial electron transport chain of *T. Thermophila* has not previously been characterized using isolated mitochondria. Given that this species has become the ciliate reference species with the sequencing of its genome (Eisen *et al.*, 2006) and several proteomics studies (Smith *et al.*, 2007; Jacobs *et al.*, 2006) there was a pressing need to characterize the respiratory pathways of this species. It should be noted that even more recent respiratory studies with *T. thermophila* (Nina *et al.*, 2010), that were published after this study commenced, used detergent permeabilised cells rather than purified mitochondria. Following the identification of an active mitochondrial ATP synthase, biochemical characterization of the complex was carried out in order to identify subunits which have functionally replaced the conserved subunits which are apparently missing, as they cannot be identified by sequence homology.

Both crude and Percoll purified *T. thermophila* mitochondria were characterized. The Percoll purified mitochondria gave the highest yield of intact, morphologically correct, biochemically active mitochondria, as shown by TEM and analysis of cytochrome oxidase and malate dehydrogenase assays.

Isolated mitochondria were used in a series of experiments to characterize the respiratory chain. Experiments using an oxygen electrode revealed the presence of a functional electron transport chain that was capable of transferring electrons from the substrates succinate and to a lesser extent malate, to oxygen. These observations are similar to those of Conklin and Chou (1972) with *T. pyriformis* mitochondria where the respiratory rate with succinate was approximately 2.5 times greater than with malate. Furthermore, the substrate TMPD-Ascorbate which reduces endogenous cytochrome c, providing a substrate for cytochrome oxidase (Complex IV) resulted in high rates of oxygen consumption. This observation differs to that observed in *T. pyriformis* mitochondria where the TMPD-ascorbate respiratory rate was 70% of that with succinate as the substrate (Kobayashi, 1965).

In some species, an alternative oxidase and a non-phosphorylating NADH dehydrogenase are used by the mitochondria to bypass sections of the mitochondrial electron transport chain. Inhibitor assays revealed that *Tetrahymena* has near complete sensitivity to potassium cyanide (KCN), indicating that the mitochondria does not contain an alternative oxidase. This contrast to previous studies with isolated *T. pyriformis* mitochondria where only 70% inhibition of succinate oxidation was observed in the presence of KCN (Conklin and Chou 1972). Although the latter observation is more consistent with the observation that an mRNA sequence for a *Tetrahymena* alternative oxidase has been annotated in the genome (XM\_001025571.2). However, this protein was not identified in the proteomics analysis of Smith *et al*, 2007. Together, these results suggest that if a gene encoding an alternative oxidase is indeed present, it is likely only expressed under certain conditions, and not during standard laboratory growth conditions used in the current study.

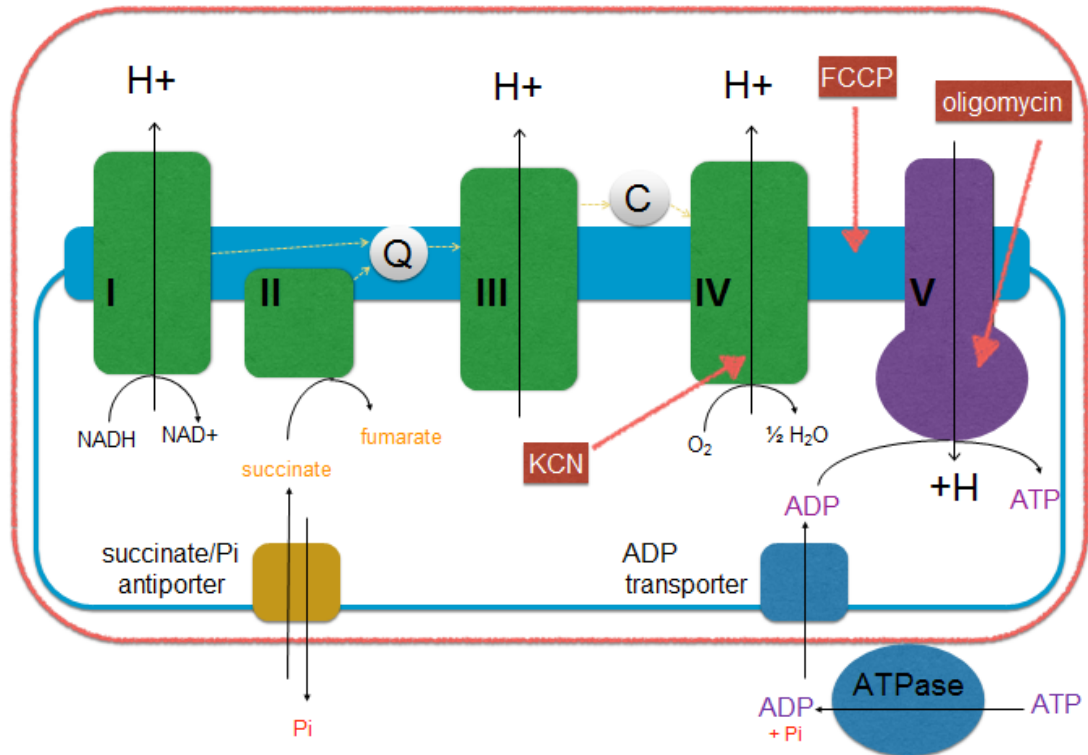


**Figure 6.1 The electron transport chain in *Tetrahymena*.** The mitochondrial outer membrane is shown in red, and the membrane-spanning succinate/Pi and ADP transporters are indicated. The inner mitochondrial membrane is shown in blue, chemical inhibitors to the electron transport chain are shown in red. Roman numerals refer to the number of the Complex. The electron transfer pathways are shown with dotted lines. The mobile electron carrying molecules Ubiquinone (Q) and cytochrome c (C) are shown.

NADH was found to be unsuitable as a substrate, as no oxygen consumption was observed. This observation is consistent with those observed for *T. pyriformis* mitochondria, where low or negligible respiratory rates were observed with NADH as a substrate (Kobayashi, 1965; Conklin and Chou, 1972). This indicates that *Tetrahymena* is unlikely contain an alternative, non-phosphorylating NADH dehydrogenase (Soole and Menz, 1995). Such enzymes are common in plant mitochondria, and can mediate rotenone-independent oxidation of NADH (i.e. independent of Complex I) (Rasmusson *et al*, 2004). This finding is consistent as BLAST searches revealed that *T. thermophila* genome does not encode any proteins with significant homology to the type II

dehydrogenases found in *Arabidopsis thaliana*, nor were they identified in the large-scale proteomic analysis of *Tetrahymena* mitochondria (Smith *et al*, 2007).

These results support the presence of a basic electron transport chain composed of Complex I (NADH-ubiquinone oxidoreductase), Complex II (succinate: ubiquinone oxidoreductase), complex III (ubiquinol: cytochrome c oxidoreductase) and Complex IV (cytochrome c oxidase) as depicted in Figure 6.1. The presences of subunits constituting all of these respiratory complexes were identified by Smith *et al*, 2007 in their proteomic analysis of *Tetrahymena thermophila* mitochondria.

The oxidation rate of isocitrate was less than a quarter of that observed with malate. This is a significant point of difference with previous studies with *T. pyriformis* where the respiratory rate with isocitrate as substrate was similar to that obtained with succinate as substrate (Conklin and Chou, 1972). The proteomic analysis has identified both NAD and NADP forms of isocitrate dehydrogenase as being present in *T. thermophila* mitochondria (Smith *et al*, 2007). The lower rates of oxidation of isocitrate compared to malate could be due to a variety of reason including enzyme abundance, enzyme kinetics, or transport of the substrates and resulting products into or out of the mitochondria.

Surprisingly, typical state 3 to state 4 transitions were not observed. This was found to be due to an exogenous ATPase activity, which hydrolyzed ATP as fast as it was synthesized. Although this phosphatase activity has not been specifically mentioned in previous studies with crude ciliate mitochondria, it is interesting to note the earlier studies with *T. pyriformis* were conducted in the presence of NaF which is a known phosphatase inhibitor (Conklin and Chou, 1972; Kilpatrick and Erecinska, 1977). A

phosphatase inhibitor was able to greatly reduce this activity and allow the detection of ATP production using the luciferase assay demonstrating that the mitochondria contain a functional ATP synthase. Finally, the rate of oxygen consumption was found to be greatly reduced if phosphate was present. This is due to the respiratory substrate succinate entering the mitochondrial matrix via a succinate/phosphate antiporter (a dicarboxylate carrier, Lancar-Benba *et al*, 1996) in the mitochondrial membrane. The increase in concentration of Pi outside the mitochondria would result in the equilibrium of the transporter changing such that Pi was transported in and succinate was transported out of the mitochondrion. This would effectively reduce the matrix concentration of succinate slowing the respiratory rate. This inhibitory effect of Pi on succinate oxidation has been previously documented in mammalian mitochondria (Johnson and Chappell, 1974).

Finally, the ATP synthase complex was examined. The presence of a mitochondrial ATP synthase was first confirmed using immuno-gold electron microscopy. It has been known for some time that several key subunits are not encoded on either the nuclear or the mitochondrial genomes (Eisen *et al*, 2006), and were not identified in a proteomic survey (Smith *et al*, 2007). The complex was therefore isolated from intact mitochondria using two different methods, in order to identify the missing subunits.

The first method involved a pull-down of the ATP synthase using the anti-beta antibody, with and without the addition of a chemical cross-linker. Secondly, a pull-down experiment was carried out using the bovine inhibitor protein which binds to F1 ATP synthase to regulate its activity. Although the successful pull-down of an ATP synthase complex using the inhibitor protein has previously been reported (Runswick *et al.*, 2013), this is the first report of the successful pull down of the ATP synthase

complex in a species which does not appear to contain an endogenous inhibitor protein. As BLAST searches of the *Tetrahymena* genome using the bovine inhibitor protein as query failed to find any significant matches. In addition, the extreme evolutionary distance between the two species (ciliate ATP synthase/bovine inhibitor protein) shows how well conserved the F1 component of this complex is.

The results obtained from these pull-down experiments allowed the identification of six proteins from ATP synthase including all the key subunits ( $\alpha$ ,  $\beta$ ,  $\gamma$ ,  $\delta$ , OSCP and c) identified by bioinformatics analysis of the genome.

This is in contrast to the ATP synthase isolated by Nina *et al.* (2010), using a sucrose gradient and a Blue-Native PAGE, who also identified five key subunits ( $\alpha$ ,  $\beta$ ,  $\gamma$ , OSCP and c). Nina *et al.* (2010) additionally identified a protein Ymf66 which they suggested encoded the missing a subunit, as it has a similar number of trans-membrane domains as the a subunit, is encoded on the mitochondrial genome and a partial alignment shows a conserved arginine residue in the correct location. However, the protein of 52 kDa is much larger than that typically observed for a subunits from a variety of species (expected size 24 kDa), and contains a large N-terminal domain. Furthermore, alignment of the full protein with the sequence of a subunits from other species reveals that the arginine identified in Ymf66 does not align with the arginine that is conserved in other species. The fact that the protein was not identified in any pull-down experiment, together with the biochemical analysis presented here, it seems likely that this protein is not the functional replacement of subunit a in *Tetrahymena*.

Instead, the gene XP\_001010660 is suggested to encode the apparently missing a subunit protein. This protein is of expected size, is targeted to the mitochondria and

contains the key conserved residues for the passage of protons during ATP synthesis. This protein was identified in the proteomics analysis of the *T. thermophila* mitochondria (Smith *et al* 2007). It has no conserved sequence with other eukaryotic a subunits, suggesting that the protein is either an analogue of the a subunit specific to ciliates, or an extremely divergent homologue.

Our original hypothesis was that the a subunit proteins in the Alveolata would have a common origin, hence our rationale for selecting candidate proteins on the basis that homologues were present in the apicomplexan and dinoflagellates. However, the recent analysis of an early-branching alveolate species, *Colponema* identified a potential a subunit which is not seen in any other lineage (Dorrell *et al*, 2013). This suggests that the a subunit in ciliates, dinoflagellates and Apicomplexa may have been replaced in independent events. This would mean that a subunits in one lineage may not be homologous but rather analogous to those in other lineages. Whether the proteins that take on the function of the a subunits in other species are homologues or analogues of a subunits from other species cannot be answered until the genes coding for these proteins can be definitively identified.

A potential b subunit was also identified (XP-001015517). The protein, of 39kDa is targeted to the mitochondrion and has a similar hydropathy profile to other b subunits. Again, the three candidate b subunit proteins identified by Nina *et al* (2010) were not identified in the data presented here. To fully confirm the identity of the proposed a and b subunits, it will now be necessary to use other experimental techniques to confirm that these proteins are part of the ATP synthase. One possible way of doing this is by developing antibodies against these potential a and b subunits and then using these antibodies in an attempt to pull-down the ATP synthase complex.

Together, the results presented in this thesis greatly expand our knowledge of the *Tetrahymena* mitochondrial electron transport chain. Further subunits of the mitochondrial ATP synthase complex have been identified. In addition, the bovine ATP synthase complex inhibitor protein has been used to pull down successfully an ATP synthase complex which does not appear to normally interact within inhibitor protein, for the very first time.

# References

- Adl SM, Simpson AGB, Farmer MA, *et al.* (2005); The new higher level classification of eukaryotes with emphasis on the taxonomy of protists. *J. Eukaryote. Microbiol*, 52; 399–451.
- Angevine CM, Herold KAG, Vincent OD, and Fillingame RH (2007). Aqueous access pathways in ATP synthase subunit A—reactivity of cysteine substituted into transmembrane helices 1, 3, and 5. *J. Biol. Chem.* 282; 9001–9007.
- Ballmoos *et al.*, (2009); Essentials for ATP synthesis by F<sub>1</sub>F<sub>0</sub> ATP synthases *Annu. Rev. Biochem.* 78; 649–672.
- Barth D, Berendonk TU (2011); The mitochondrial genome sequence of the ciliate *Paramecium caudatum* reveals a shift in nucleotide composition and codon usage within the genus *Paramecium*. *BMC Genomics.* 12:272.
- Bason JV, Runswick MJ, Fearnley IM, Walker JE (2011); Binding of the Inhibitor Protein IF<sub>1</sub> to Bovine F<sub>1</sub>-ATPase. *J Mol Biol.* 406(3); 443–453
- Boxma B, de Graaf RM, van der Staay GW, van Alen TA, Ricard G, Gabaldón T, van Hoek AH, Moon-van der Staay SY, Koopman WJ, van Hellemond JJ, Tielens AG, Friedrich T, Veenhuis M, Huynen MA, Hackstein JH (2005); An anaerobic mitochondrion that produces hydrogen. *Nature*, 3; 434(7029):74–9.
- Boyer PD (1997); The ATP synthase: A splendid molecular motor. *Annu. Rev. Biochem.* (66); 717–749.
- Brandt U, (2006); Energy converting NADH: Quinone oxidoreductase (Complex I). *Annu. Rev. Biochem.* 75; 69–92.
- Breman JG, Egan A, Keusch GT (2001); The intolerable burden of Malaria: A new look at the numbers. *American J. Trop. Med. Hyg.* 64; 4–6.
- Brunk CF, Lee LC, Tran AB, Li J (2003); Complete sequence of the mitochondrial genome of *Tetrahymena thermophila* and comparative methods for identifying highly divergent genes. *Nucleic Acids Research.* 31(6); 1673–1682.
- Bryan TM, Sperger, JM, Chapman KB, Cech, TR (1998); Telomerase reverse transcriptase genes identified in *Tetrahymena thermophila* and *Oxytricha trifallax*. *Proceedings of the National Academy of Sciences.* 95(15) 8479–8484.
- Buchan DWA, Minneci F, Nugent TCO, Bryson K, Jones DT. (2013); Scalable web services for the PSIPRED protein analysis workbench. *Nucleic Acids Research.* 41 (W1); 340–348.
- Burger G, Zhu Y, Littlejohn TG, Greenwood SJ, Schnare MN, Lang BF, Gray MW (2000); Complete sequence of the mitochondrial genome of *Tetrahymena pyriformis* and comparison with *Paramecium aurelia* mitochondrial DNA. *J Mol Biol.* 24; 297(2);365–80.
- Butterfield ER, Howe CJ, Nisbet RER (2013); An Analysis of dinoflagellate metabolism using EST data. *Protist.* 164; 218–236

- Cabezón E, Montgomery MG, Leslie AG, Walker JE (2003); The structure of bovine F1-ATPase in complex with its regulatory protein IF1. *Nat Struct Biol.* 9; 744-50.
- Carlton, JM (2002); Genome sequence and comparative analysis of the model rodent malaria parasite *Plasmodium yoelii yoelii*. *Nature.* 419; 512–519.
- Cavalier-Smith T (2003); Protist Phylogeny and the high-level classification of Protozoa. *European J. Protistology.* 39(4); 338-348.
- Collins K, Gorovsky MA (2005); *Tetrahymena thermophila*. *Current Biol.* 15; 317-318.
- Conklin KA, Chou SC (1972); Isolation and Characterization of *Tetrahymena pyriformis* GL Mitochondria. *Comparative Biochemistry and Physiology.* 41(1B); 45-54.
- Danne JC, Gornik SG, Macrae JI, McConville MJ, Waller RF (2013); Alveolate mitochondrial metabolic evolution: dinoflagellates force reassessment of the role of parasitism as a driver of change in apicomplexans. *Mol Biol Evol.* 30(1);123-39.
- de Graaf RM, Ricard G, van Alen TA, Duarte I, Dutilh BE, Burgtorf C, Kuiper JW, van der Staay GW, Tielens AG, Huynen MA, Hackstein JH (2011); The organellar genome and metabolic potential of the hydrogen-producing mitochondrion of *Nyctotherus ovalis*. *Mol Biol Evol.* 28(8); 2379-91.
- Desagher S, Martinou JC (2000); Mitochondria as the central control point of apoptosis. *Trends Cell Biol.* 10; 369-77.
- Doherty JP, Lindeman R, Trent RJ, Graham MW, Woodcock DM(1993); *Escherichia coli* host strains SURETM and SRB fail to preserve a palindrome cloned in lambda phage: improved alternate host strains. *Gene.* 124(1); 29-35.
- Dooren GV, Marti M, Tonkin CJ, Stimmler LM, Cowman AF, McFadden GI (2005); Development of the endoplasmic reticulum, mitochondrion and apicoplast during the asexual life cycle of *Plasmodium falciparum*. *Mol. Microbiol.* 57; 405-419.
- Dooren GV, Stimmler LM, McFadden GI (2006); Metabolic maps and functions of *Plasmodium* mitochondrion. *FEMS Microbiol. Rev.* 30; 596-630.
- Dorrel RG, Butterfield ER, Nisbet RER, Howe CJ (2013); Evolution: Unveiling Early Alveolates. *Current Biology.* 23; 1093–1096.
- Eisen *et al* (2006); Macronuclear Genome Sequence of the Ciliate *Tetrahymena thermophila*, a Model Eukaryote. *PLOS Biology.* 4(9); 286.
- Erik LL, Sonnhammer, Gunnar von Heijne, Anders K (1998); A hidden Markov model for predicting transmembrane helices in protein sequences. In *Proc. of Sixth Int. Conf. on Intelligent Systems for Molecular Biology.* 175-182.
- Feagin JE, Gardner MJ, Williamson DH, Wilson RJ (1991); The putative mitochondrial genome of *Plasmodium falciparum*. *J Protozool.* 38(3); 243-5.
- Feagin JE (1992); The 6-kb element of *Plasmodium falciparum* encodes mitochondrial cytochrome genes. *Mol Biochem Parasitol.* 52(1); 145-8.
- Fillingame, RH, Angevine CM, Dmitriev, OY, (2003); Mechanics of coupling proton movements to c-ring rotation in ATP synthase. *FEBS Letters.* 555(1) 29-34.

- Foth BJ, McFadden GI (2003); The apicoplast: a plastid in *Plasmodium falciparum* and other apicomplexan parasite. *Int. Rev. Cytol.* 224; 57-110.
- Fry M, Webb E, Pudney M (1990); Effect of mitochondrial inhibitors on adenosinetriphosphate levels in *Plasmodium falciparum*. *Comp Biochem Physiol B.* 96(4); 775-82.
- Futai, M, Noumi T, Maeda M (1989); ATP Synthase (H<sup>+</sup>-Atpase) - Results by combined biochemical and molecular biological approaches. *Annual Review of Biochemistry.* 58:111-136.
- Gardner *et al* (2002); Genome sequence of the human malaria parasite *P. falciparum*. *Nature.* 419; 498-509.
- Gibbons C, Montgomery MG, Leslie AGW, Walker JE (2000); The structure of resolution the central stalk in bovine F<sub>1</sub>-ATPase at 2.4 Å resolutions. *Nature Structural and Mol. Biol.* 7; 1055-1061.
- Gledhill JR, Walker JE (2006); Inhibitors of the catalytic domain of mitochondrial ATP synthase. *Biochemical Society Transactions.* 34; 989-992.
- Goodman CD, Su V, McFadden GI (2007); The effects of anti-bacterials on the malaria parasite *Plasmodium falciparum*. *Molecular & Biochemical Parasitology.* 152; 181–191
- Gornik SG, Ford KL, Mulhern TD, Bacic A, McFadden GI, Waller RF (2012); Loss of nucleosomal DNA condensation coincides with appearance of a novel nuclear protein in dinoflagellates. *Curr Biol.* 18; 22(24); 2303-12.
- Gould SB, Tham WH, Cowman AF, McFadden GI, Waller RF (2008); Alveolins, a new family of cortical proteins that define the protist infra kingdom Alveolata. *Mol.Biol.Evol.* 25(6); 1219-30.
- Gray MW (2012); Mitochondrial evolution. *Cold Spring Harb Perspect Biol.* 4(9);a011403.
- Greider CW, Blackburn EH (1985); Identification of a specific telomere terminal transferase activity in *Tetrahymena* extracts. *Cell.* 43; 405-413.
- Hill DL (1972); The biochemistry and physiology of *Tetrahymena*. Academic Press, New York.
- Hjort K, Goldberg A.V, Tsaousis A.D, Hirt R.P, Embley T.M. (2010); Diversity and reductive evolution of mitochondria among microbial eukaryotes. *Phil. Trans. R. Soc. B.* 365; 713–727.
- Hofmann K., Stoffel W. (1993); TMbase – A database of membrane spanning proteins segments. *Biol. Chem. Hoppe-Seyler.* 374;166.
- Jacobs, ME, DeSouza, LV, Samaranayake H, Pearlman R.E, Siu KM, Klobutcher LA, (2006); The *Tetrahymena thermophila* phagosome proteome. *Eukaryotic cell.* 5(12); 1990-2000.
- Jayasinghe S, Hristova K, White SH (2001); MPtopo: A database of membrane protein topology. *Protein Sci.* 10(2); 455–458.

Johnson RN, Chappell JB (1974); The inhibition of mitochondrial dicarboxylate transport by inorganic phosphate, some phosphate esters and some phosphonate compounds. *Biochem J.* 138(2);171-5.

Ke H, Lewis IA, Morrisey JM, McLean KJ, Ganesan SM, Painter HJ, Mather MW, Jacobs-Lorena M, Llinás M, Vaidya AB (2015); Genetic investigation of tricarboxylic acid metabolism during the *Plasmodium falciparum* life cycle. *Cell Rep.* 7;11(1);164-74.

Kilpatrick L, Erecińska M (1977); Mitochondrial respiratory chain of *Tetrahymena pyriformis*. The thermodynamic and spectral properties. *Biochemica et Biophysica (BBA) – Bioenergetics*, 460; 346-363.

Ko YH, Delannoy M, Hullihen J, Chiu W, Pedersen PL (2003); Mitochondrial ATP synthasome cristae-enriched membranes and a multiwell detergent screening assay yield dispersed single complexes containing the ATP synthase and carriers for P<sub>i</sub> and ADP/ATP. *The Journal of Biological Chemistry.* 278; 12305–12309.

Kobayashi S. (1965); Preparation and properties of mitochondria from the ciliated protozoan *Tetrahymena*. *The Journal of Biochemistry.* Vol (58), No.5.

Kobayashi T, Endoh H (2005); A possible role of mitochondria in the apoptotic-like programmed nuclear death of *Tetrahymena thermophila*. *FEBS J.* 272(20);5378-87.

Kolarov J, Šubík J, Kováč L (1972); Oxidative phosphorylation in yeast. 8. Osmotic and permeability properties of mitochondria isolated from wild-type yeast and from a respiration-deficient mutant. *Biochim Biophys Acta.*267; 457–464.

Krungskrai J (2004); The multiple roles of mitochondrion of the malarial parasite. *Parasitology.*129; 511-524.

Kuruma Y, Suzuki T, Ono S, Yoshida M, Ueda T (2012); Functional analysis of membranous Fo-a subunit of F1Fo-ATP synthase by in vitro protein synthesis. *Biochem J.*442; 631–8.

Lancar-Benba *et al*, (1996); Characterization, purification and properties of the yeast mitochondrial dicarboxylate carrier (*Saccharomyces cerevisiae*). *Biochimie.*78(3); 195-200.

Leander, Brian S. (2008); Alveolates. Alveolata.<http://tolweb.org/Alveolates/2379/2008.09.16> in The Tree of Life Web Project.

Lim L, McFadden GI (2010); The evolution, metabolism and functions of the apicoplast. *Biol Sci.*365; 749–763.

Lodish *et al* (2006); *Molecular Biology of the Cell.*

Mallo N, Lamas J, Leiro JM (2013); Evidence of an Alternative Oxidase Pathway for Mitochondrial Respiration in the Scuticociliate *Philasterides dicentrarchi*. *Protist.*164(6); 824–836

Maréchal E, Cesbron-Delauw MF (2001); The apicoplast: a new member of the plastid family. *Trends Plant Sci.*6(5); 200-5.

- Martin WF, Müller M (1998); The hydrogen hypothesis for the first eukaryote. *Nature*.392; 37-41.
- Martin WF, Garg S, Zimorski V (2015); Endosymbiotic theories for eukaryote origin. *Philos Trans R Soc Lond B Biol Sci*. 26;370 (1678)
- MacRae JI, Dixon MW, Dearnley MK, Chua HH, Chambers JM, Kenny S, Bottova I, Tilley L, McConville MJ (2013); Mitochondrial metabolism of sexual and asexual blood stages of the malaria parasite *Plasmodium falciparum*. *BMC Biol*.11:67.
- Menz, R.I, Griffith, M, Day, DA, Wiskich, JT (1992); Matrix NADH dehydrogenases of plant mitochondria and sites of quinone reduction by complex I. *European Journal of Biochemistry*. 208(2); 481-485.
- Minauro-Sanmiguel, F, Wilkens, S, Garcia, JJ. (2005); Structure of dimeric mitochondrial ATP synthase: Novel F<sub>0</sub> bridging features and the structural basis of mitochondrial cristae biogenesis. *PNAS* 102 (35) 12356-12358
- Miranda-Astudillo H, Cano-Estrada A, Vázquez-Acevedo M, Colina-Tenorio L, Downie-Velasco A, Cardol P, Remacle C, Domínguez-Ramírez L, González-Halphen D (2014); Interactions of subunits Asa2, Asa4 and Asa7 in the peripheral stalk of the mitochondrial ATP synthase of the chlorophycean alga *Polytomella* sp. *Biochim Biophys Acta*. 1837(1);1-13
- Mogi T, Kita K (2009); Identification of mitochondrial Complex II subunits SDH3 and SDH4 and ATP synthase subunits a and b in *Plasmodium* spp. *Mitochondrion*. 9(6); 443-453.
- Mogi T., Kita K. (2010); Diversity in mitochondrial metabolic pathways in parasitic protists *Plasmodium* and *Cryptosporidium*. *Parasitol Int*. 59(3);305-12.
- Musrati, RA, Kollarova, M, Mernik, N, Mikulasova, D, (1998); Malate dehydrogenase: distribution, function and properties. *General physiology and biophysics*.17; 193-210.
- Nanney DL, Simon EM (2000); Laboratory and evolutionary history of *T.thermophila*. *Methods Cell. Biol*.62; 3-25.
- Nash EA, Barbrook AC, Rachel K, Stuart E, Bernhardt K, Howe CJ, Ellen RER (2007); Organization of the Mitochondrial Genome in the Dinoflagellate *Amphidinium carter*. *Molecular Biology and Evolution*.24(7); 1528-1536.
- Nelson DL, Cox MM (2008); *Lehninger Principles of Biochemistry* (4th ed.). W. H. Freeman.
- Nina PB, Dudkina NV, Kane LA, Eyk JE, Boekema E, Mather MW, Vaidya AB (2010); Highly Divergent Mitochondrial ATP Synthase Complexes in *Tetrahymena thermophila*. *PLOS Biology*, Vol. (8) e1000418.
- Nina PB, Morrisey JM, Ganesan SM, Ke H, Pershing AM, Mather MW, Vaidya AB (2011); ATP synthase complex of *Plasmodium falciparum*: dimeric assembly in mitochondrial membranes and resistance to genetic disruption. *J. Biol. Chem*. 286(48); 41312-22.
- Painter HJ, Morrisey JM, Mather MW, Vaidya AB (2007); Specific role of mitochondrial electron transport in blood-stage *Plasmodium falciparum*. *Nature*. 446(7131); 88-91.

- Perkins DN, Pappin DJ, Creasy DM, Cottrell JS (1999); Probability-based protein identification by searching sequence databases using mass spectrometry data. *Electrophoresis*. **20** (18); 3551–67.
- Pomajbíková K, Oborník M, Horák A, Petrželková KJ, Grim JN, Levecke B, Todd A, Mulama M, Kiyang J, Modrý D. (2013); Novel insights into the genetic diversity of *Balantidium* and *Balantidium*-like cyst-forming ciliates. *PLoS Negl Trop Dis*. **7**(3) e2140.
- Poole RK (1983); Mitochondria of *Tetrahymena pyriformis*: enumeration and sizing of isolated organelles using a Coulter Counter and pulse-height analyser. *J Cell Sci*. **61**;437-51.
- Prikhodko EA, Brailovskaya IV, Korotkov SM, Mokhova EN (2009); Features of Mitochondrial Energetics in Living Unicellular Eukaryote *Tetrahymena pyriformis*. A Model for Study of Mammalian Intracellular Adaptation. *Biochemistry*. **74** (4); 371-376.
- Rasmusson AG, Soole KL, Elthon TE (2004); Alternative NAD(P)H dehydrogenases of plant mitochondria. *Annu Rev Plant Biol*. **55**; 23-39.
- Runswick MJ, Bason JV, Montgomery MG, Robinson GC, Fearnley IM, Walker JE (2013); The affinity purification and characterization of ATP synthase complexes from mitochondria. *Open Biol*. **3**; 120-160
- Sambrook J, Fritsch E, Maniatis T (1989); *Molecular Cloning: A laboratory manual* (2nd ed). Cold Spring Harbor Laboratory Press, Cold Spring Harbor, New York.
- Schwitzguebel JP, Siegenthaler PA (1984); Purification of peroxisomes and mitochondria from spinach leaf by Percoll gradient centrifugation. *Plant Physiology*. **75**(3); 670-674.
- Sherman IW (1998); Purine and Pyrimidine metabolism of asexual stages. In: ed. Sherman, *Malaria; parasite biology, pathogenesis and protection*. American Society for Microbiology, Washington DC, 177-184.
- Shevchenko A, Tomas H, Havliš J, Olsen JV, Mann M (2007); In-gel digestion for mass spectrometric characterization of proteins and proteomes. *Nature Protocols*. **2**: 2856 – 2860.
- Shoguchi E, Shinzato C, Hisata K, Satoh N, Mungpakdee S (2015); The Large Mitochondrial Genome of *Symbiodinium minutum* Reveals Conserved Noncoding Sequences between Dinoflagellates and Apicomplexans. *Genome Biol. Evol.* **7**(8); 2237–2244.
- Smith DGS, Gawryluk RMR, Spencer DF, Pearlman RE, Siu KWM, Gray MW (2007); Exploring the mitochondrial proteome of the ciliate protozoon *Tetrahymena thermophila*: Direct analysis by Tandem Mass Spectrometry. *J. Mol. Biol.* **374**; 837-863.
- Snider C., Jayasinghe S., Hristova K., & White S.H. (2009); MPEX: A tool for exploring membrane proteins. *Protein Sci*. **18**; 2624-2628.
- Soole KL, Menz RI (1995); Functional Molecular Aspects of the NADH Dehydrogenases of Plant Mitochondria. *Journal of Bioenergetics and Biomembranes*. **27**(4).

- Steidinger (1996); A New toxic dinoflagellate with a complex life cycle and behaviour. *J. Phycol.* 32; 157-164.
- Stey SH., Schwab D, Krebs W (1971); Electron microscopic examination of isolated mitochondria of *Tetrahymena pyriformis*. *J. Ultrastruct. Res.* 37; 82-93.
- Stock D, Leslie AGW, Walker JE (1999); Molecular architecture of the rotary motor in ATP synthase. *Science.* 286; 1700–1705.
- Strohalm M, Kavan D, Novák P, Volný M, Havlíček V (2010) mMass 3: a cross-platform software environment for precise analysis of mass spectrometric data. *Anal Chem.* 82; 4648–4651.
- Sturm A, Mollard V, Cozijnsen A, Goodman C.D., McFadden G.I (2015) ; Mitochondrial ATP synthase is dispensable in blood-stage *Plasmodium berghei* rodent malaria but essential in the mosquito phase. *PNAS.* 112(33); 10216–10223
- Symersky J, Osowski D, Walters DE, Mueller (2012); Oligomycin frames a common drug-binding site in the ATP synthase. *Proc Natl Acad Sci U S A.* 109(35); 13961–13965.
- Taylor FJR, (1987); *The Biology of Dinoflagellates*. Blackwell Scientific Publications.
- Tellis C, Pantazia D, Ioachim E, Galanic V, Lekka ME (2003); Localization of an alkyl-acetyl-glycerol-CDPcholine :cholinephosphotransferase activity in submitochondrial fractions of *Tetrahymena pyriformis*. *European Journal of Cell Biology.* 82; 573 - 578.
- Tonkin CJ., van Dooren GG, Spurck TP, Struck NS, Good RT, Handman E, Cowman AF, McFadden GI (2004); Localization of organellar proteins in *Plasmodium falciparum* using a novel set of transfection vectors and a new immunofluorescence fixation method. *Mol Biochem Parasitol.* 137(1); 13-21.
- Tsoukatos DC, Tselepis AD, Lekka ME (1993); Studies on the subcellular distribution of 1-O-alkyl-2-acetyl-sn-glycero phosphocholine (PAF) and on the enzymic activities involved in its biosynthesis within the ciliate *Tetrahymena pyriformis*. *Biochemica et Biophysica Acta.* 1170; 258-264.
- Turner G, Lloyd D, Chance B (1971); Electron transport in Phosphorylating Mitochondria from *Tetrahymena pyriformis* Strain ST. *Journal of General Microbiology.* 65; 359-374.
- Unitt MD, Lloyd D (1981); Effects of Inhibitors on Mitochondrial Adenosine Triphosphatase of *Tetrahymena pyriformis* ST. *Journal of General Microbiology.* 126; 261-266.
- Uyemura SA, Luo S, Vieira M, Moreno SN, Docampo R (2004); Oxidative phosphorylation and rotenone-insensitive malate- and NADH-quinone oxidoreductases in *Plasmodium yoelii* mitochondria in situ. *J. Biol. Chem.* 279(1); 385-93.
- Vaidya AB, Mather MW (2005); A post-genomic view of the mitochondrion in malaria parasites. *Curr. Top. Microbiol. Immunol.* 295; 233-50.
- Vaidya AB, Mather MW (2009); Mitochondrial Evolution and Functions in Malaria Parasites. *Annual Review of Microbiology.* 63; 249-267.

Waller RF, Keeling PJ, Donald RG, Striepen B, Handman E, Lang-Unnasch A, Cowman AF, Besra GS, Roos DS, McFadden GI (1998); Nuclear-encoded proteins target to the plastid in *Toxoplasma gondii* and *Plasmodium falciparum*. Proc. Natl. Acad. Sci. USA. **95**; 12352–12357.

Waller RF, Jackson CJ (2009); Dinoflagellate mitochondrial genomes: stretching the rules of molecular biology. Bioassays.31(2); 237-45.

Walker JE, Gay NJ, Powell SJ, Kostina M, Dyer MR (1987); ATP synthase from bovine mitochondria: sequences of imported precursors of oligomycin sensitivity conferral protein, factor 6, and adenosinetriphosphatase inhibitor protein. Biochemistry. 26(26); 8613-9

Walker JE, Dickson VK (2006); The peripheral stalk of the mitochondrial ATP synthase. Biochim Biophys Acta. 1757(5-6); 286-96.

Walker G, Dorrell RG, Schlacht A, Dacks JB (2011); Eukaryotic systematics: a user's guide for cell biologists and parasitologists. Parasitology. 138(13); 1638-63.

Walker JE (2013); The ATP synthase: the understood, the uncertain and the unknown. Biochem. Soc Trans. 41; 1-16.

Weatherby K, Carter D (2013); *Chromera velia*: The missing link in the evolution of parasitism. Adv. Appl. Microbiol. 85; 119-44

Wessel D, Flügge UI (1984); A method for the quantitative recovery of protein in dilute solution in the presence of detergents and lipids. Anal Biochem. 138(1);141-3.

Wheatley DN, Rasmussen L, Tiedtke A (1994); *Tetrahymena*: a model for growth, cell cycle and nutritional studies, with biotechnological potential. Bioassays. 16(5); 367-72.

Yeh E, DeRisi JL (2011); Chemical rescue of malaria parasites lacking an apicoplast defines organelle function in blood-stage *plasmodium falciparum*. PLOS Biology. 9; e1001138

Yi Z, Song W, Clamp JC, Chen Z, Gao S, Zhang Q (2009); Reconsideration of systematic relationships within the order Euplotida (Protista, Ciliophora) using new sequences of the gene coding for small-subunit rRNA and testing the use of combined data sets to construct phylogenies of the Diophrys-complex. Molecular Phylogenetics and Evolution. 50;. 599–607.

# Appendix 1







Sample	Nucleosome datasets (p)					Antibody pull-down					BAST					Deadlight data					
	Accession#	Description	Max Score	Total score	Query cover	E-value	Max identifiLinks	Accession#	Description	Max Score	Total score	Query cover	E-value	Max identifiLinks	Accession#	Description	Max Score	Total score	Query cover	E-value	Max identifiLinks
A2-32	<a href="#">F572933</a>	<a href="#">F572933:TTTCA47748 Tetrahymena Thermoph</a>	533	521	90%	0	89%	<a href="#">D018802.1</a>	<a href="#">SFAA-aaa7y02.y1 cSP1 Serine-rich tubulin cD</a>	32	32	100%	2.2	32%	<a href="#">D064936</a>	<a href="#">CAG03579 rev CAG0 Kaennin bet</a>	34.3	34.3	25%	0.22	24%
	<a href="#">F572933</a>	<a href="#">F572933:TTTCA47748 Tetrahymena Thermoph</a>	503	508	90%	3.00E-179	89%	<a href="#">D023248.1</a>	<a href="#">D023248 Phlebotomus bergeri mitogen strand q</a>	32	32	100%	2.9	30%	<a href="#">K062620.1</a>	<a href="#">Ave011011011017_x1_26_p0e01</a>	33.5	33.5	12%	0.27	42%
	<a href="#">D064936</a>	<a href="#">D064936:TTTCA67514C Tetrahymena Thermoph</a>	490	490	85%	2.00E-176	89%	<a href="#">D030892.1</a>	<a href="#">D030892 XPB Suspan cDNA library Phlebotom</a>	32	32	100%	4.3	32%	<a href="#">G544925</a>	<a href="#">UFD-GC1-aaa-h-08-0-UT.s1 UFD-G</a>	32.7	32.7	14%	0.02	33%
A4-14	<a href="#">D030892.1</a>	<a href="#">D030892.1:TTTCA47748 Tetrahymena Thermoph</a>	378	378	84%	3.00E-152	100%	<a href="#">D013760.1</a>	<a href="#">Tj15Kyy72013.y1 Tj15K Fully sequenced mcpys</a>	339	339	89%	2.00E-43	72%	<a href="#">F188032</a>	<a href="#">CA027-C. rubra pAgpaca-3 Library</a>	47	47	30%	3.00E-11	62%
	<a href="#">F572933</a>	<a href="#">F572933:TTTCA47748 Tetrahymena Thermoph</a>	378	378	84%	5.00E-152	100%	<a href="#">D023248.1</a>	<a href="#">Tct01D0101E.y1 D013015 cDNA library, Erem</a>	337	337	89%	4.00E-43	72%	<a href="#">G579826</a>	<a href="#">UFD-GC1-aaa-y-20-0-UT.s1 UFD-G</a>	27.3	27.3	33%	4.00E-04	33%
	<a href="#">D064936</a>	<a href="#">D064936:TTT00030311 Max unannotated beta</a>	375	375	84%	8.00E-152	100%	<a href="#">D030892.1</a>	<a href="#">Tj15Kyy61012.y1 Tj15K #1 R2 Tetrahymena cDNA 1</a>	337	337	89%	5.00E-43	72%	<a href="#">G0779701</a>	<a href="#">Ave011011011010 P0C10.y_p0e013</a>	26.9	26.9	40%	5.00E-04	31%
A5-24	<a href="#">G038939</a>	<a href="#">G038939:TTT000233119 Amphioxus Express - C</a>	333	331	40%	1.00E-103	89%	<a href="#">G546044.1</a>	<a href="#">Tj15Kyy610015.y2 Tj15K CDUG Tetrahymena cDNA Lib</a>	308	308	100%	0.007	30%	No significant similarity found						
	<a href="#">G038939</a>	<a href="#">G038939:TTT000292048 Amphioxus Express - C</a>	222	293	45%	8.00E-69	50%	<a href="#">D077225.1</a>	<a href="#">D077225 Phlebotomus bergeri mitochd Phlebot</a>	27.3	27.3	9%	0.01	40%	<a href="#">G579826</a>	<a href="#">UFD-GC1-aaa-y-20-0-UT.s1 UFD-G</a>	27.3	27.3	33%	4.00E-04	33%
	<a href="#">G038939</a>	<a href="#">G038939:TTT00011116 Amphioxus Express - C</a>	193	191	30%	2.00E-152	89%	<a href="#">D0674023.1</a>	<a href="#">PTE5kua94012.y1 Phlebotomus falciparum 3D7 g</a>	26.6	26.6	2%	1.1	44%	<a href="#">G574675</a>	<a href="#">D064936:TTT00010740E Oxytricha muscaea No</a>	33.5	33.5	8%	1.1	29%
A7-38	<a href="#">D064936</a>	<a href="#">D064936:5008-0-23-ADM.1.1 Chlamydomonas</a>	43.9	43.9	9%	3.00E-04	31%	<a href="#">A021403.1</a>	<a href="#">A021403 Kn206 Thelema maritima cDNA clone f</a>	46.6	46.6	20%	4.00E-04	25%	<a href="#">G579826</a>	<a href="#">UFD-GC1-aaa-y-20-0-UT.s1 UFD-G</a>	35	35	9%	0.42	30%
	<a href="#">D064936</a>	<a href="#">D064936:TTT00010740E Tetrahymena Thermoph</a>	42.7	414	16%	0.001	33%	<a href="#">D023248.1</a>	<a href="#">D023248 Phlebotomus bergeri cytochrome c-oh</a>	40.8	40.8	10%	0.00	25%	<a href="#">E023332</a>	<a href="#">D064936:TTT00010740E Oxytricha muscaea No</a>	33.5	33.5	8%	1	29%
	<a href="#">D067793</a>	<a href="#">D067793:TTT00010740E Tetrahymena Thermoph</a>	42.4	26.6	8%	0.001	36%	<a href="#">F524426.1</a>	<a href="#">F524426 Thelema maritima plasmid full-length</a>	36.6	36.6	15%	0.5	29%	<a href="#">E023332</a>	<a href="#">D064936:TTT00010740E Oxytricha muscaea No</a>	33.5	33.5	8%	1.1	29%
A9-10	<a href="#">D067777</a>	<a href="#">D067777:TTT00010740E Tetrahymena Thermoph</a>	59.3	59.3	9%	8.00E-11	81%	<a href="#">D001227.1</a>	<a href="#">D001227 XPB Suspan cDNA library Phlebotom</a>	31.2	31.2	10%	0.7	34%	No significant similarity found						
	No significant similarity found					No significant similarity found					No significant similarity found										
	<a href="#">F087034</a>	<a href="#">F087034:TTT00010740E Tetrahymena Thermoph</a>	95.5	322	51%	3.00E-21	36%	No significant similarity found					<a href="#">D064936</a>	<a href="#">CAG04171 rev CAG0 Kaennin bet</a>	42.4	28.6	43%	0.001	22%		
A9-21	<a href="#">F087034</a>	<a href="#">F087034:TTT00010740E Tetrahymena Thermoph</a>	67.6	308	52%	5.00E-12	42%	No significant similarity found					<a href="#">D000369</a>	<a href="#">ank_K_Brevia1445 Kaennin Brevia E</a>	40.6	22.9	36%	0.002	31%		
	<a href="#">G038939</a>	<a href="#">G038939:TTT00027311 Amphioxus Express - C</a>	58	117	41%	7.00E-07	34%	No significant similarity found					<a href="#">D064936</a>	<a href="#">CAG04171 rev CAG0 Kaennin bet</a>	37	37	30%	0.001	24%		
	<a href="#">G038939</a>	<a href="#">G038939:TTT00010740E Tetrahymena Thermoph</a>	482	483	30%	7.00E-113	81%	No significant similarity found					<a href="#">D064936</a>	<a href="#">ALAO2045 rev ALAO Kaennin bet</a>	32.3	32.3	2%	3.1	34%		
J2-38	<a href="#">D064936</a>	<a href="#">D064936:TTT00010740E Tetrahymena Thermoph</a>	273	271	10%	2.00E-03	52%	No significant similarity found					<a href="#">D064936</a>	<a href="#">ALAO2045 full ALAO Kaennin bet</a>	32.3	32.3	2%	3.1	34%		
	<a href="#">G038939</a>	<a href="#">G038939:TTT00010740E Tetrahymena Thermoph</a>	326	326	100%	2.00E-40	99%	<a href="#">F236161.1</a>	<a href="#">Tj15Kyy30103.y1 Tj15K Tetrahymena cDNA Libr</a>	29.6	29.6	20%	0.07	33%	<a href="#">E023332</a>	<a href="#">D064936:TTT00010740E Oxytricha muscaea No</a>	33.5	33.5	8%	1.1	29%
	<a href="#">G038939</a>	<a href="#">G038939:TTT00027311 Amphioxus Express - C</a>	326	326	100%	4.00E-40	99%	<a href="#">D000875.1</a>	<a href="#">D000875 XPB Suspan cDNA library Phlebotom</a>	29.3	29.3	100%	1.1	30%	<a href="#">E023332</a>	<a href="#">D064936:TTT00010740E Oxytricha muscaea No</a>	33.5	33.5	8%	1.1	29%
J4-13	<a href="#">F087034</a>	<a href="#">F087034:TTT00010740E Tetrahymena Thermoph</a>	326	326	100%	6.00E-40	99%	<a href="#">D000875.1</a>	<a href="#">D000875 XPB Suspan cDNA library Phlebotom</a>	29.3	29.3	100%	1.1	30%	<a href="#">E023332</a>	<a href="#">D064936:TTT00010740E Oxytricha muscaea No</a>	33.5	33.5	8%	1.1	29%
	<a href="#">G038939</a>	<a href="#">G038939:TTT00027311 Amphioxus Express - C</a>	326	326	100%	6.00E-40	99%	<a href="#">D000875.1</a>	<a href="#">D000875 XPB Suspan cDNA library Phlebotom</a>	29.3	29.3	100%	1.1	30%	<a href="#">E023332</a>	<a href="#">D064936:TTT00010740E Oxytricha muscaea No</a>	33.5	33.5	8%	1.1	29%
	<a href="#">F087034</a>	<a href="#">F087034:TTT00010740E Tetrahymena Thermoph</a>	326	326	100%	6.00E-40	99%	<a href="#">D000875.1</a>	<a href="#">D000875 XPB Suspan cDNA library Phlebotom</a>	29.3	29.3	100%	1.1	30%	<a href="#">E023332</a>	<a href="#">D064936:TTT00010740E Oxytricha muscaea No</a>	33.5	33.5	8%	1.1	29%
J4-15	<a href="#">F573442</a>	<a href="#">F573442:TTT00010740E Tetrahymena Thermoph</a>	373	373	27%	3.00E-129	79%	No significant similarity found					No significant similarity found								
	<a href="#">G038939</a>	<a href="#">G038939:TTT000231121 Amphioxus Express - C</a>	304	304	21%	5.00E-16	27%	No significant similarity found					No significant similarity found								
	<a href="#">D064936</a>	<a href="#">D064936:TTT00010740E Tetrahymena Thermoph</a>	277	277	19%	8.00E-05	63%	No significant similarity found					No significant similarity found								
J5-16	<a href="#">D064936</a>	<a href="#">D064936:TTT00010740E Tetrahymena Thermoph</a>	309	309	100%	1.00E-14	99%	<a href="#">D077236.1</a>	<a href="#">Tj15Kyy61010.y1 Tj15K #9 3 day invasin bodyless</a>	29.3	29.3	20%	2.7	50%	<a href="#">E023332</a>	<a href="#">D064936:TTT00010740E Oxytricha muscaea No</a>	33.5	33.5	8%	1.1	29%
	<a href="#">G038939</a>	<a href="#">G038939:TTT00010740E Tetrahymena Thermoph</a>	309	309	100%	1.00E-14	99%	No significant similarity found					<a href="#">G000876</a>	<a href="#">Ave023045.1 Acanthamoeba sp. Ka</a>	29.3	29.3	100%	3.00E-04	27%		
	<a href="#">F087034</a>	<a href="#">F087034:TTT00010740E Tetrahymena Thermoph</a>	353	353	26%	6.00E-48	52%	<a href="#">D000875.1</a>	<a href="#">D000875 XPB Suspan cDNA library Phlebotom</a>	29.3	29.3	20%	1.1	30%	<a href="#">G079834</a>	<a href="#">UFD-GC1-aaa-y-22-0-UT.s1 UFD-G</a>	28.1	28.1	42%	0.001	22%
J6-A	<a href="#">F573164</a>	<a href="#">F573164:TTT00010740E Tetrahymena Thermoph</a>	479	479	25%	2.00E-160	94%	<a href="#">D000875.1</a>	<a href="#">Tj15Kyy21012.y1 Tj15K Tetrahymena Mann 5 cDNA</a>	32	32	4%	0.6	29%	No significant similarity found						
	<a href="#">G038939</a>	<a href="#">G038939:TTT00020743 Amphioxus Express - C</a>	476	476	25%	3.00E-159	94%	No significant similarity found					No significant similarity found								
	<a href="#">F573063</a>	<a href="#">F573063:TTT00010740E Tetrahymena Thermoph</a>	462	459	27%	3.00E-153	94%	No significant similarity found					No significant similarity found								